A thesis submitted to

Université Louis Pasteur
Ecole et Observatoire des Science de la Terre
UMR 7517
Strasbourg, France

and

Charles University
Institute of Petrology and Structural Geology
Prague, Czech Republic

of the requirement for the degree of

Doctor of Philosophy in Earth Sciences

by

Jan Franěk

From microstructures to large-scale crustal deformations in collisional orogen: multidisciplinary approach

Jury — Prague, 2007

Prof. Shah Wali Faryad	Charles University, Prague	External reviewer
Dr. Holger Stünitz	University Basel, Switzerland	External reviewer
Prof. Hubert Whitechurch	Université Louis Pasteur, Strasbourg	Internal reviewer
Prof. Hrouda František	Charles University, Prague	Member of the jury
Pitra Pavel, Ph.D.	Université Rennes 1	Member of the jury
Konopásek Jiří, Ph.D.	Charles University, Prague	Member of the jury
Prof. Karel Schulmann	Université Louis Pasteur, Strasbourg	Supervisor
Ondrej Lexa, Ph.D.	Charles University, Prague	Co-supervisor

Science... never solves a problem without creating ten more.

George Bernard Shaw

I approve that in the presented Ph.D. thesis I used only data acquired from my own research or from sources mentioned in the list of used literature.

I also approve that I didn't present this work, or even its significant part, to acquire another academic title, except the Ph.D. title from the Université Louis Pasteur Strasbourg in frame of the co-tutelle scholarship.

In Prague, 1.7.2007

Jan Franěk

……

Abstract

The thesis aims to compile response of deep-seated rocks to continental collision in the root zone of Variscan orogen exposed in Bohemian Massif. It treats the orogenic processes from the scale of microscopic grains constituting rocks through scale of individual outcrops to an overall view of ~4000 km^2 large domain of the high-grade rocks.

The thesis is divided into three chapters. The first represents an article summarizing study of structurally most complex area - Blanský les granulite massif - published in the Mineralogy and Petrology journal (2006). The second chapter unravels regional evolution of the south Bohemian Moldanubian domain and correlates the presented results with suitable studies from other orogenic regions or with numerical models of continental collisions. The related article will be submitted to Tectonics journal in June 2007. The last section focuses on the mechanisms of deformation in the felsic granulites and extrapolates the results to rheology of the Variscan lower crust and behavior of common felsic rocks under HT HP conditions. The corresponding paper will be submitted to Journal of Metamorphic Geology in the autumn 2007.

The Bohemian massif represents the easternmost exposure of Variscan orogen in Europe. During the 380-300 Ma complex subduction - collision a ~300km wide orogenic chain has developed, showing tectonic zonation comparable to other European Variscan fragments. From the NW to the SE following tectonic sequence is developed: undeformed Paleozoic Saxothuringian sediments to high-grade Saxothuringian crystalline, suture zone and lower-grade Teplá-Barrandian unit. Further to the SE the arc-related granitoid plutons separate the Teplá-Barrandian folded Paleozoic sediments from high-grade Moldanubian unit, which shows widespread anatexis and contains slices of lower-crustal and mantle rocks. Further to the E follows Brunia microplate, which is almost unaffected by Variscan tectonometamorphic processes.

The studied Moldanubian domain has been pervasively deformed between ~350-335 Ma by NW-SE oriented shortening and subsequently during ~330-310 Ma suffered a perpendicular NE-SW transpression. It exhibits intimate mixing of mantle, lower- and mid-crustal rocks with polyphase deformation history, which requires combination of various research approaches to unravel its evolution. We focus on evolution in the W part of the Moldanubian root domain to reveal the mechanical behavior of the mid- and lower-crustal rocks in the collisional setting and to outline possible exhumation mechanisms of lower crust into shallow

levels. The studied region covers 130x30 km area of Southern Bohemia, roughly following the 9HR reflection seismic line. The basis for our interpretations is built on detailed field research focused on structural evolution. The acquired attitudes of foliations, lineations and small-scale structures were generalized and combined with existing geological maps to reveal regional trends of orogenic fabrics. Field structural data are supported by microstructural investigations and available petrology. The rock fabrics could have been extrapolated only to ~3-5 km depth based on the field geology, but a seismic reflection line passing through majority of our study area allowed for much deeper extrapolation and let us consider our results in a frame of the whole continental crust. Simple 3D gravity modeling was also employed to support our structural and seismic interpretations. To develop a dynamic scenario from the observed relative succession of deformation events, we have built a database of published radiometric ages for majority of Bohemian massif containing ~550 ages. The results are embedded into overall geotectonic setting of the Bohemian Massif.

Structural pattern of the South Bohemian Moldanubian domain comprises evidence of five significant deformational episodes, being dominated by pervasive NW dipping amphibolite facies foliations, particularly steep S_3 and gently dipping S_4. They indicate intensive NW-SE shortening followed by subhorizontal flow of the partially molten rocks. These fabrics parallel strike of the Brunian and Saxothuringian margins and their attitude can be correlated to the steep and flat lying amphibolite facies foliations dominating the eastern Moldanubian. In the vicinity of the granulite massifs the S_4 is being disturbed to form irregular patterns passively adjusting a fold-like shape of rheologically stronger granulite bodies.

In the SW, this fabric is overprinted by a younger crenulation cleavage with mesoscopic structures indicating dextral transpressive strain. It documents a late-Variscan NE-directed shortening that was induced at the SW boundary of the Moldanubian, nevertheless a hypothetical continental block that caused such shortening remains unknown. Syntectonic magmatism plus anatexis and presumably deformation culminates here at ~320 Ma, about 15 Ma after previous Moldanubian deformations. Due to the distinct orientation and timing, this shortening must be treated as a late isolated episode at the end of the Variscan collision in the Bohemian Massif.

In the centre of the studied region crop out several large massifs of rheologically stronger felsic granulites, which cause the disturbation of the above described fabrics. Inside the massifs the older Variscan structures have been well preserved, documenting two-stage exhumation history (D_2 and D_3) of these HP HT rocks. The gravity modeling with structural interpretations indicates that individual South Bohemian granulite massifs reach depth of

more kilometers. Reflection seismics additionally depicts region of probable steep fabrics across the whole crust below granulites, which is interpreted as a possible continuation of the granulite-dominated mélange exposed on the surface. This vertical region of low reflectivity would then represent a trace of the deformed granulite ascent channel. Complex geometry of retrograde amphibolite facies S_3 fabric in granulites indicates a large-scale fold-like structure, which is interpreted to be a result of crustal-scale F_3 buckling of an already exhumed granulite sheet in kinematical continuity with the regional amphibolite facies D_3 deformation.

A large-scale relict domain of granulite facies deformation fabrics has been identified within the Blanský les granulite body, where the granulite facies mylonitic S_2 bears scarce remnants of S_1 compositional banding. The S_2 fabrics allow for a reconstruction of the early exhumation mechanism because the subsequent cooling history froze these fabrics enabling us to observe them continuously in ~8x2 km area. They contain ~70° angle to the dominant amphibolite facies structures of the surrounding retrograde granulite. The cylindrical geometry of S_2 restored by unfolding suggests that the partially molten granulites from the lower crust were in this phase emplaced in form of a syn-compressional viscous extrusion. Such a new mechanism can explain presence of relatively small portions (X000 km^3) of HP HT rocks inside much shallower units in the internal parts of orogens. Once emplaced, the granulites deformed coherently with the surrounding middle crust.

The unfolded S_2 fabrics run sub-perpendicularly to the NE-SW orogen trend, as well as the youngest S_5. The observed regional variations of principal strain orientation up to 70° resemble magnitude of strain switches known from recent orogenic areas, e.g. the Alps.

From the ~850 outcrops studied in southern Bohemia, the most representative ones were sampled to perform basic petrographical observations. In case of felsic granulites the more detailed petrological study was linked with microstructural analysis of exhumational fabrics in order to define deformational mechanisms and estimate their rheology during exhumation. During detailed studies of granulite-facies fabrics have been found relict samples of granulite precursor on several outcrops. These allow to describe a process of granulitization and help to constrain a pre-granulitic history of the rocks.

Answering the mentioned questions again requires combination of various approaches, from which lattice preferred orientation (LPO) measurements using the electron back-scattered diffraction (EBSD) method with fore scatter imaging are the most important ones. Essential was also quantification of various microstructural parameters from manually digitalized thin sections. The chemical changes during recrystalization were additionally studied on a

scanning electron microscope with attached EDX analyzer, where compositional maps were acquired and complemented by spot or areal analyses of representative places.

The relict samples of granulite precursor contain up to 1.7cm large grains of perthite that bear numerous inclusions of quartz, garnet and kyanite accompanied by less frequent biotite, rutile, ilmenite, zircon, monazite, apatite and Fe-sulphide crystals. Except perthites, the samples consist of granulitic fine-grained matrix and quartz bands dismembered into ribbons. The inclusions of garnet, biotite and partially kyanite exhibit euhedral crystal shapes inconsistent with solid-state deformation during their growth and encapsulation into perthites. Additionally the quartz inclusions show drop-like or euhedral forms characteristic for crystallization at solid - melt boundary. For these features we suggest that the precursor of the felsic granulites was a coarse grained hypersolvus orthogneiss bearing alkali feldspar – quartz – garnet – biotite - kyanite association.

Some of the perthites preserve in their strain shadows an excellent evidence of granulitization process, in which the perthites recrystalize into fine grained K-feldspar – plagioclase granulitic matrix. Such a matrix shielded by surrounding perthite exhibits ± same lattice orientation as its parental perthite grain, pointing to almost static disintegration of the original large perthites into a granulitic matrix of uniform and small grain size. Back-scattered electron images suggest that the new grains developed on a sharp recrystalization front that gradually advanced into the intact perthite grain. The isochemical and almost static recrystalization of large perthites was driven probably by chemical disequilibrium due to change of PT conditions combined with subtle strain. The matrix started to flow due to D_2 deformation to develop penetrative S_2 mylonitic foliation. On majority of the outcrops the granulitization affected the whole volume of the felsic rock, forming framework of interconnected weak layers (IWL) which bear more or less isolated quartz ribbons.

Analysis of the corresponding microstructure reveals very high plastic strain of the quartz while the prevailing fine-grained feldspar dominated matrix shows only limited signs of plastic deformation. Together with the presence of syn-deformational intergranular partial melt this implies highly ductile behavior attaining characteristics of pseudoplastic flow, presumably facilitated by grain boundary sliding deformation mechanism and grain boundary diffusion. Despite low shape-preferred orientation of matrix feldspars, the EBSD study reveals strong LPO of both K-feldspar and plagioclase, which suggests also important component of dislocation creep. The combination of dislocation creep with grain-size sensitive flow enhanced by the presence of silicate melts offered an efficient way to transport the relatively small portions of lower crust rapidly upwards through the orogenic root.

Younger deformation episode is expressed by development of amphibolite facies fabrics at middle crustal levels. After cooling and crystallization of the partial melt along grain boundaries the granulites deformed only by less efficient dislocation creep similarly to common orthogneisses, where the eventual partial melt segregates from solid matrix into discontinuous pockets or bands. Significant hardening of the retrograde granulite indicated by the distinct microstructures increased strength of the granulites and allowed for active buckling of the granulite sheets, which acted as strong elongated boudins inside the weaker metasediments.

The described inversion of rheology of the rock-forming feldspars and consequently of the whole felsic rock (weakening under the lower crustal HT HP conditions and hardening in mid-crustal levels) should change the present geotectonic rheological considerations based purely on the Byerlee and Weertmann laws.

First of all let me thank to the ladies and gentlemen who directly or indirectly contributed to progress of my scientific work.

I am very grateful to my supervisors, prof. Karel Schulmann and Ondrej Lexa, for giving the support and direction to my research activities, crucial help with fieldwork and also numerous advices and discussions. Not less important was help of my consultant, prof. Gianreto Manatschal who always found time to discuss tectonic topics and opened to me a new view on links between field data and plate tectonic processes. My results wouldn't reach the present quality without help of prof. Čestmír Tomek, Jean-Bernard Edel, Pavla Štípská, Stano Ulrich and Jiří Konopásek who helped me either in the field or by discussing my interpretations. Last but not least let me thank to prof. Shah Wali Faryad, Dr Stanislav Vrána, Vojtěch Janoušek and doc. František Holub for inspiring discussions concerning my results and Jakub Haloda with Patricie Týcová for support by laboratory work. The smooth solution of related bureaucracy wouldn't be possible without help of Ms Miloslava Wontrobová and Dr Vladimír Tolar.

I highly appreciate the financial support given by the French government, which allowed me to spend almost half of my PhD studies at the Université Louis Pasteur in Strasbourg in frame of the co-tutelle scholarship.

Big thanks go to my parents and sister who always patiently supported my activities, creating me a base for successful realization of my plans.

Probably it is not possible to mention all the friends who made better my time in Prague, Strasbourg or at any other time during the studies and please don't be angry with me if your name is not mentioned here… Just randomwise these were Lenka, Prokop, Pavlína, Monika, Lůca, Kryštof, Zůza, Pinďa, Lukáš, Aleš & Kačka, Jarda, Petr, Jana, Ondřej, Franta, Emilka, Jeremie, Julia, Nicolas, Geoffroy, Mohammed, Francis and many others.

Extraordinary thanks belong to Jaroslav Cícha for borrowing a robust geological compass in the period of lack of such equipment. The Army of the Czech Republic is greatly acknowledged for access permission to the Boletice military area and tank shooting ranges where part of the fieldwork was held. I am also grateful to the staff of sport centre at the ULP in Strasbourg for organizing various sport activities that didn't allow my body to decay during most stressful stages of the thesis development.

Without all of you the thesis would pass much harder.

Table of contents

Introduction

Continental collision represents one of the most exciting processes studied by geological disciplines, which achieves coalescence of independent lithospheric plates into larger blocks. Nevertheless the question how do the lower- and mid- crustal rocks respond to collisional forces on a large scale remains broadly unresolved. Ambiguity of interpretations cause mainly the different mechanical behavior of the brittle upper crust compared to ductile modes of deformation operating in lower levels. Study of recent orogenic areas doesn't then sufficiently improve our knowledge, because the distinct deformational behavior makes extrapolations of upper crustal structures into deeper levels hardly possible. The main tool for unraveling the orogenic processes in deeper crust remains study of exhumed fragments of deep crust in ancient orogens, which represents also the scope of the presented work.

My thesis aims to compile response of deep-seated rocks to continental collision in the root zone of Variscan orogen exposed in the Bohemian Massif in central Europe. It treats the orogenic processes from the scale of microscopic grains constituting rocks through scale of individual outcrops to an overall view of ~4000 km^2 large domain of the high-grade rocks.

The thesis is divided into three chapters. The first one represents an article *(Kinematic and rheological model of exhumation of high pressure granulites in the Variscan orogenic root: example of the Blanský les granulite, Bohemian Massif, Czech Republic)* summarizing study of structurally most complex area - Blanský les granulite massif - published in the Mineralogy and Petrology journal in 2006. The second chapter unravels regional evolution of the south Bohemian Moldanubian domain and correlates the presented results with suitable studies from other orogenic regions or with numerical models of continental collisions. The related article will be submitted to Tectonics journal in June 2007. The last section focuses on the mechanisms of deformation in the felsic granulites and extrapolates the results to rheology of the Variscan lower crust and behavior of common felsic rocks under HT HP conditions. The corresponding manuscript will be submitted to Journal of Metamorphic Geology.

The studied Moldanubian domain has been pervasively deformed between ~350-335 Ma by NW-SE oriented shortening and subsequently during ~330-310 Ma suffered a perpendicular NE-SW transpression. It exhibits intimate mixing of mantle, lower- and mid-crustal rocks with polyphase deformation history, which requires combination of various research approaches to unravel its evolution. We focus on evolution in the western part of the Moldanubian root domain to reveal the mechanical behavior of the mid- and lower-crustal rocks in the collisional setting and to outline possible exhumation mechanisms of lower crust

into shallow levels. The studied region covers 130x30 km area of Southern Bohemia, roughly following the 9HR reflection seismic line. The basis for our interpretations is built on detailed field research focused on structural evolution. The acquired attitudes of foliations, lineations and small-scale structures were generalized and combined with existing geological maps to reveal regional trends of orogenic fabrics. The rock fabrics could have been extrapolated only to ~3-5 km depth based on the field geology, but a seismic reflection line passing through majority of our study area allowed for much deeper extrapolation and let us consider our results in a frame of the whole continental crust. Simple 3D gravity modeling was also employed to support our structural and seismic interpretations. To develop a dynamic scenario from the observed relative succession of deformation events, we have built a database of published radiometric ages for majority of the Bohemian Massif containing ~550 ages. Final conclusions are embedded into overall geotectonic setting of the Bohemian Massif.

From the ~850 outcrops studied in southern Bohemia, the most representative ones were sampled to perform basic petrographical observations. In case of felsic granulites the more detailed petrological study was linked with microstructural analysis of exhumational fabrics in order to define deformational mechanisms and estimate their rheology during exhumation. During detailed studies of granulite-facies fabrics, relict samples of granulite precursor have been found on several outcrops. They allow to describe a process of granulitization and help to constrain a pre-granulitic history of these mysterious rocks.

The individual geological disciplines mentioned above cannot resolve the large-scale orogenic processes alone. Despite difficulties they must be rather combined to create a coherent scheme of evolution that is in accord with various data available. Such an approach I have chosen to create the presented thesis, which puts together structural, petrological, microstructural, geochronological, seismic, gravimetric and numerical/analogue modeling results acquired either by my own research or by study of literature. The Variscan orogen exposed in Bohemian Massif represents a well described and sufficiently exposed collisional domain, from which the examined mid- and lower-crustal processes can be extrapolated to other orogenic areas.

Kinematic and rheological model of exhumation of high pressure granulites in the Variscan orogenic root : example of the Blanský les granulite, Bohemian Massif, Czech Republic

J. Franěk, K. Schulmann, O. Lexa

Mineralogy and Petrology, 2006, Vol. 86, N° 3-4, Pages 253–276

Exhumation of HP HT lower-crustal rocks in frame of multiple deformations in the centre of Variscan collisional orogen, South Bohemian Moldanubian domain of the Bohemian Massif

Jan Franěk[1,2], Karel Schulmann[1], Ondrej Lexa[1,2], Čestmír Tomek[3], Jean-Bernard Edel[1]

1 Université Louis Pasteur, EOST, UMR 7517, 1 Rue Blessig, Strasbourg 67084, France
2 Institute of Petrology and Structural Geology, Albertov 6, Prague 2, 128 43, Czech Republic
3 Institut für Geographie und Geologie, Hellbrunnerstrasse 34, 5020 Salzburg, Austria

1 Abstract

We focus on structural evolution of the western part of the Moldanubian root domain in the Bohemian Massif to reveal mechanical behavior of mid- and lower-crustal rocks in the collisional setting and to outline possible exhumation mechanisms of lower crust into shallow levels. Studied region covers 130x30 km area of Southern Bohemia, roughly following the 9HR reflection seismic line. Field structural data supported by microstructural investigations are correlated with reflection seismics, available petrology and geochronology, and discussed in terms of geotectonic model of the Bohemian Massif. Structural pattern of the studied part of the Moldanubian domain is dominated by pervasive NW dipping amphibolite facies foliations developed between ~350-337 Ma, which strike parallel to the Brunian and Saxothuringian plate margins. Their attitudes suggest intensive NW-SE horizontal shortening related to exhumation of lower crustal rocks in form of ~20 km wide subvertical ascent channel, immediately followed by subhorizontal spreading in mid-crustal levels. In the SW, these fabrics are overprinted by a younger crenulation cleavage with mesoscopic structures indicating a dextral transpressive strain. It documents a late-Variscan NE-directed shortening that was induced at the SW boundary of the Moldanubian, nevertheless a hypothetical continental block that caused such shortening remains unknown. Syntectonic magmatism, anatexis and presumably deformation culminates here at ~320 Ma, about 17 Ma after previous Moldanubian deformations. Due to the distinct orientation and timing, this shortening must be treated as a late isolated episode at the end of the Variscan collision in the Bohemian Massif. In the centre of the studied region several large massifs of rheologically stronger felsic granulites crop out, causing disturbation of all the above mentioned fabrics. Inside them the older Variscan structures have been well preserved, documenting two-stage exhumation history of these HP HT rocks. Based on the kinematic model of granulite exhumation history we use these fabrics to point out additional stress changes in space and time during the Variscan collision. The observed double switching of principal shortening direction points out complex architecture of natural orogens and restricts usage of numerical or analogue 2D models only to individual stages of an orogeny.

Keywords: Exhumation, Orogenic lower crust, Granulites, Moldanubian domain, Bohemian Massif, Variscan belt

2 Acknowledgments

The work was supported by a grant of Czech Science Foundation (GACR 205/05/2187). Prof. Gianreto Manatschal is greatly acknowledged for inspiring discussions.

3 Introduction

Deformational behavior of the orogenic lower crust in convergent domains remains for decades a matter of debate. In general the different mechanical response of brittle upper and ductile lower crust (supra- and infra- structure) to deformations makes direct investigation of deep processes almost impossible. The large scale field-based, analogue or numerical models often assume cylindricity of the simulated processes and reduce the considerations to a 2D view despite many of preserved orogens exhibit 3D architecture accounting for higher complexity of the collision-related deformations.

Various mechanisms have been proposed for synorogenic exhumation of deep-seated rocks as well as for spreading of the thickened continental crust. Majority of the published exhumation models focus on processes along suture zones that offer a pre-existing discontinuity along which deep-seated rocks can be transported upwards. These comprise a classical concept of buoyant serpentinized subduction channel created by [*Chemenda, et al.*, 1995], simulated numerically e.g. by [*Gerya and Stockhert*, 2006] and indirectly proved by discovery of serpentinite mélanges carrying eclogite fragments in the present-day Mariana trench. [*Beaumont, et al.*, 2001; *Beaumont, et al.*, 2004] present a collisional alternative to this idea by numerical modeling of viscous lower-crustal channel that flows upwards along predisposed inclined crustal-scale weak zones in the thickened continental crust. Such a model driven by gravity potential energy is favored e.g. by [*Hodges, et al.*, 2001] or [*Klemperer*, 2006] for exhumation along the MCT in the Himalayas. Similar suture-related exhumation models pull up the light continental crust via buoyancy during the continent-continent collision stage as described from the southern Tibet [e.g., *de Sigoyer, et al.*, 2004] or recently also from the Bohemian Massif [*Konopásek and Schulmann*, 2005].

The other family of models examines the exhumation inside a collisional zone, apart from the suture. [*Platt*, 1993] proposes a corner flow regime operating on a crustal scale between subduction zone and rigid buttress of the overriding plate which evokes rise of lower-crustal material along its edge. Numerical models of [*Stockhert and Gerya*, 2005] develop the corner flow scheme and combine it with exhumation along subductional channel. [*Burg and Podladchikov*, 1999] offer numerical models of lithospheric-scale buckling, where the buckled crust may undergo fragmentation via thrust zones, which uplift particular blocks in the order of >10 km vertically [*Sokoutis, et al.*, 2005]. Other models deal with syn-orogenic localized extension that triggers more or less passive doming of a weak lower crust [e.g., *Beaumont, et al.*, 2004]. Alternatively [*Talbot and Koyi*, 1995] proposes diapiric exhumation of the orogenic root driven purely by buoyancy at the end of the collisional episode, which he applies to large regions of high-grade rocks like Proterozoics in the Kiruna area in Sweden.

The distinct exhumation processes inside strike-slip zones have been studied only on few examples so far (e.g. San Andreas in California, [*Spotila, et al.*, 2001]. Nevertheless such faults may also achieve significant localized exhumation when the movements are slightly oblique in part of their tectonic history.

At the end of an orogeny the thickened crust in many cases undergoes a rapid tectonic thinning rather than slow erosion-related decrease of crustal thickness [e.g., *Dewey, et al.*, 1993]. [*Dewey, et al.*, 1993] or [*Andersen, et al.*, 1993] interpreted the responsible tectonic processes as extensional collapse causing development of pervasive flat crustal fabrics observed e.g. in the Norwegian Caledonides. Alternatively the heat redistribution leading to weakening of the deep crustal rocks via partial melting may trigger a sort of channel flow [e.g., *Beaumont, et al.*, 2006], where anastomosing subhorizontal fabrics develop throughout ductile lower crust.

In the new generation of models coming from Bohemian Massif we propose a description of localized exhumation of lower crust in the centre of the thickened orogenic root during compression in frame of Variscan orogeny, ca 340 Ma ago. The ascent is multistage but very

rapid on a time scale of several Ma. The exhumation doesn't follow any preexisting ascent structure cutting the crust but rather creates new subvertical ascent channel by rapid amplification of some initial instabilities in a non-linear viscous material of the orogenic root. Such a process, described in nature e.g. by [*Kisters, et al.*, 1996] on a km scale, would be enabled by extremely low viscosity of the Variscan root due to it's unusually hot thermal structure [e.g., *Schulmann, et al.*, 2005; *Štípská and Powell*, 2005; *Tajčmanová, et al.*, 2006] combined with felsic composition [*Hrubcová, et al.*, 2005]. The resulting exhumation path is complex both geometrically and kinematically, with complex evolving rheology. Uplift is highly localized and juxtaposes contrasting crustal levels instead of creating a smooth metamorphic gradient. There's no exhumation observed in similar geotectonic settings in recent orogens. Subsequent pervasive development of flat-lying amphibolite facies fabrics throughout whole studied region provides direct evidence on mid-crustal processes operating during later stages of an orogeny. Last recognized tectonic events refer to rearrangement of far-field forces that drive crustal deformations. Our interpretations are based on extensive field structural data supported by crustal-scale seismic reflection profile, local gravity modeling and large collection of published geochronological with petrological data.

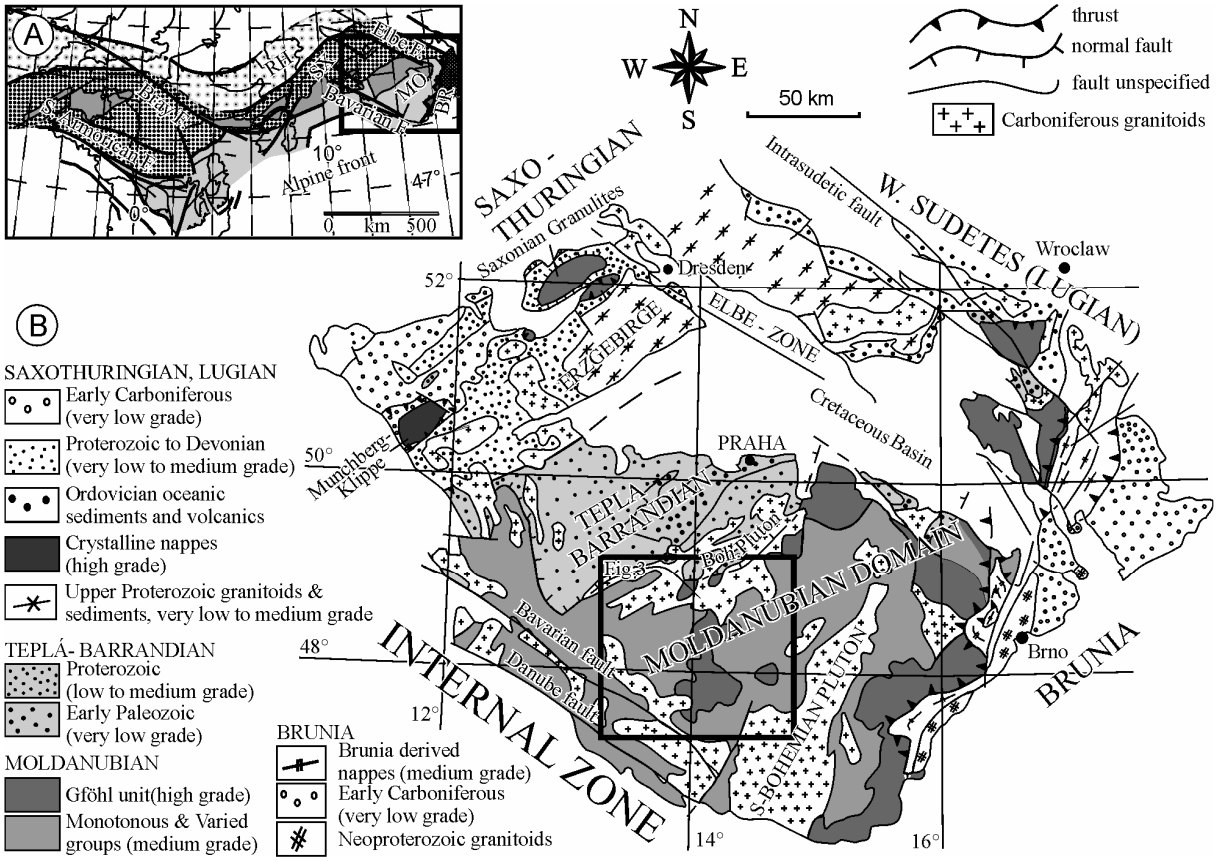

Figure 1. a) Principal division of the Variscan chain. b) Simplified geological map of the Bohemian Massif modified after [*Franke*, 2000].

4 Geological setting

4.1 Overall frame of the Variscides, timing and microplate setting

The Variscan orogenic belt in Europe developed during Paleozoic collision of Laurentia, Gondwana and north-Gondwana derived microplates [*Franke*, 2000]. Presently it outcrops as isolated massifs from Iberia in the south-west through western Europe and central Europe to the Carpathians in the East, being dismembered by a number of syn-orogenic strike-slip dextral faults, e.g. the Elbe or the Bray fault [*Edel, et al.*, 2003; 1995] (Figure 1a). The Bohemian Massif occurs at the eastern extremity of European Variscan belt representing its largest exposure (Figure 1b). This massif is traditionally divided into the Saxothuringian Zone to the West, the Teplá-Barrandian (TBU) and Moldanubian domains in the central part of the orogenic belt *[Kossmat, 1927]* and the Brunia Neoproterozoic continent to the east *[Dudek, 1980]*. The paleontological record of lower Paleozoic sediments of the Saxothuringian and Teplá-Barrandian show affinities to the Gondwana faunas implying that all these blocks were derived from the northern Gondwana margin [e.g., *Chlupáč*, 1994].

[*Babuška and Plomerová*, 2001; *Plomerová, et al.*, 2005] shown that the P-wave anisotropy and shear-wave splitting patterns of the sub-crustal lithosphere of the Saxothuringian domain exhibit uniform NW plunging fabrics and suggested that this domain represent originally one pre-Variscan microplate. On the other hand Moldanubian domain reveals S dipping sub-crustal mantle fabrics suggesting different microplate provenience. The Teplá-Barrandian and Brunia show also distinct mantle fabrics, but the published data are not sufficiently constrained to provide idea about their independent lithospheric origin. Differences in mantle fabrics revealed by this seismological study imply that the lithospheric mantle underneath the Bohemian Massif did not suffer pervasive ductile deformation since the last stages of the Variscan collision.

According to [*Schulmann, et al.*, 2005] the Bohemian Massif can be treated as a single collisional domain characterized by: 1) relics of the south-east directed subduction of the Saxothuringian lithosphere underneath the Teplá-Barrandian, 2) the magmatic arc represented by the Central Bohemian Plutonic Complex (CBPC) in the centre, and 3) the rigid foreland represented by the Brunia microplate in the SE. In this concept, the Teplá-Barrandian between the suture zone and magmatic arc represents the fore-arc domain and the Moldanubian domain between the magmatic arc and the Brunia constitutes shortened and thickened intracontinental back-arc spreading region. The Variscan strike-slip zones, particularly the Bavarian-Pfahl shear zone, Elbe fault zone and other parallel fault zones further to the NE (Figure 1a,b) strike NW-SE parallel to the Teyssier-Tornquist line and dismember the NNE trending Variscan structure of the Bohemian Massif [*Edel and Weber*, 1995]. These lithospheric fault zones accommodate dextral movements since ~340 Ma [e.g., *Aleksandrowski, et al.*, 1997; *Edel, et al.*, 2003; *Mattern*, 2001].

Since 345 till 300 Ma a 7.5 km thick Variscan flysch (Culm facies) sedimented onto the Brunia foreland, marking beginning of massive exhumation in the neighboring Moldanubian domain [*Hartley and Otava*, 2001]. However, already since 370 Ma, deepening of foreland sedimentary environment occurred, being accompanied by extensional faulting induced possibly by flexural subsidence of the Brunia margin due to overburden by the thickened Moldanubian root to the west [*Mazur, et al.*, 2006]. Low-grade source rocks between c.345-330 Ma gradually pass to high-grade metamorphics from c. 330Ma [*Hartley and Otava*, 2001], with first HP felsic granulites occurring in 325 Ma old strata [*Vrána and Novák*, 2000]. Since 330 Ma begins also lateral shortening of the flysch basin and deformation front progressively migrates from west to east in conjunction with decreasing intensity of deformation [*Hrouda*, 1993]. This evolution expresses progressive thrusting of the Moldanubian domain to the east over the Brunia (e.g. [*Kumpera and Martinec*, 1995; *Synek,*

et al., 1990]. The flysch deformation was finished at c. 300 Ma as indicated by Ar-Ar cooling ages of [*Maluski, et al.*, 1995] of the western metamorphic Culm and the deformation of Variscan molasse sediments in the east [*Čížek and Tomek*, 1991].

Despite relatively well established time constraints, the exact microplate setting of lithospheric segments located between colliding Gondwana and Laurentia remains unresolved [*von Raumer, et al.*, 2003; *Winchester, et al.*, 2002]. Amount of rotations of microplates and movements along transcurrent faults is difficult to asses by paleomagnetism [e.g., *Edel, et al.*, 2003] but the structural analysis combined with geochronology can provide important constraints.

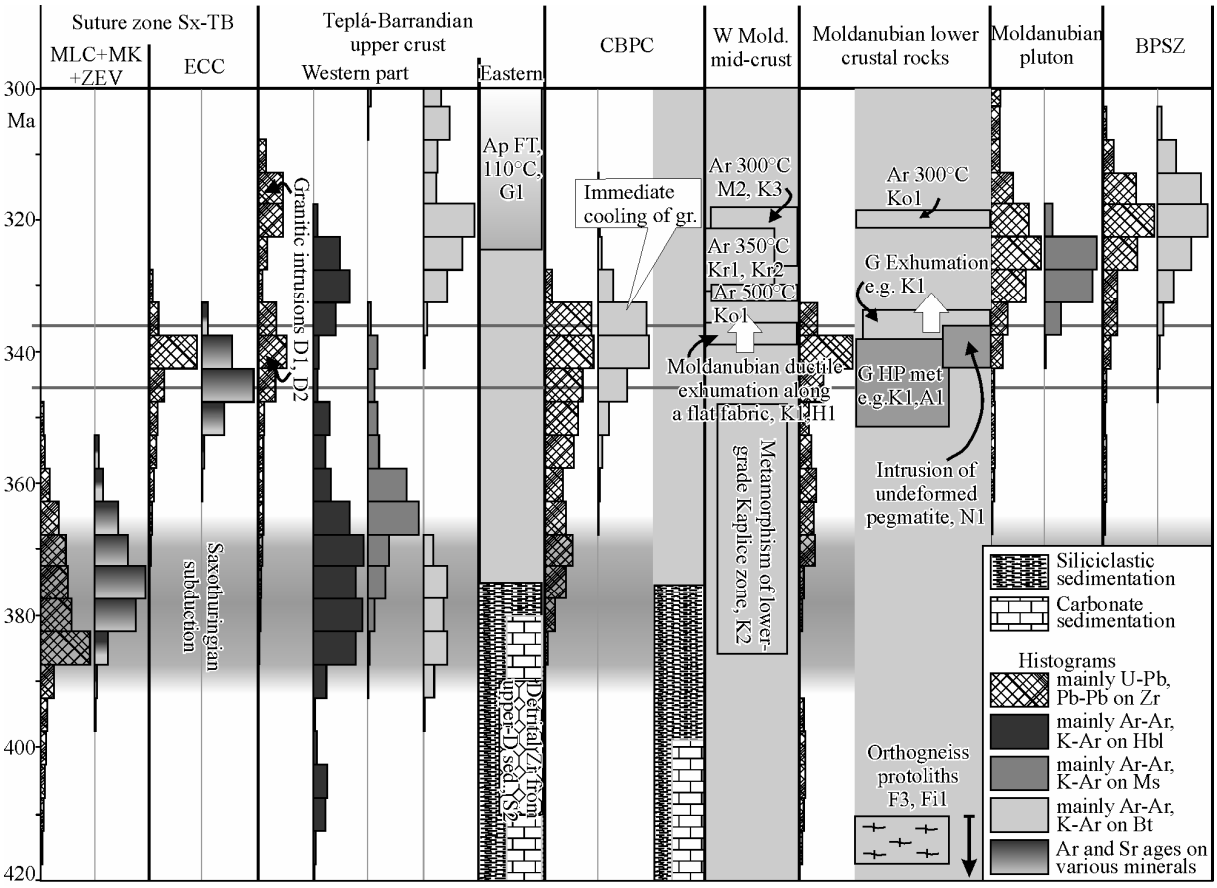

Figure 2. Summary of geochronology for the individual units in majority of Moldanubian + Teplá-Barrandian. Histograms of larger datasets are mixed with shaded columns that contain individual geochronological data combined with stratigraphy of neighboring Paleozoic sediments. Histograms represent sum of Gaussian probability curves for each involved radiometric age. Citations for the 211 plotted ages are given in electronical supplementary materials as Appendix 1. BPSZ – Bavarian Moldanubicum with Bavarian-Pfahl shear zone.

4.2 Geology of the Moldanubian and Teplá-Barrandian domains

The Moldanubian domain is considered as the internal zone of the Variscan orogen, being surrounded by rigid and less metamorphosed blocks to the NW and SE *[Suess, 1926]*. This intensively reworked "orogenic root zone" consists of high-grade rocks including eclogites, granulites and mantle fragments, and it is intruded by numerous Variscan plutons *[Finger and Steyer, 1995; Suess, 1926]* of I-type melasyenites (durbachites) and I to S-type granitoids [e.g., *Janoušek, et al.*, 2000; *Liew, et al.*, 1989; *Žák, et al.*, 2005a]. From geodynamic point of

view the Moldanubian rocks have been originally formed in the previous back arc spreading region [*Schulmann, et al.*, 2005]. To the east the Moldanubian grades to Brunia through a several kilometers thick zone of highly deformed mélange derived from both the Brunia and Moldanubian domain rocks [*Konopásek, et al.*, 2002; *Suess*, 1912],

Tectonic subdivision of the Moldanubian domain is traditionally based on geological structure of high grade rocks in lower Austria [*Fuchs*, 1976]. Three main groups are distinguished there according to structural position, metamorphic grade and prevailing lithology: (1) the structurally deepest medium-grade Monotonous group is overlain by (2) the medium-grade Varied group and (3) the structurally highest high-grade Gföhl unit *[Fuchs, 1986; Matte, et al., 1990]*. The Monotonous group consists of biotite-plagioclase paragneiss with minor orthogneiss, quartzite, amphibolite and locally preserved eclogite bodies [*Medaris, et al.*, 1995; *O'Brien and Vrána*, 1995]. The Varied group differs from the underlying Monotonous group by more pelitic protoliths of metasediments and abundance of amphibolite, quartzite, marble and calc-silicate intercalations. The Gföhl unit consists of anatectic orthogneiss, kyanite-bearing felsic granulite, peridotite, and eclogite. Based on petrological arguments, [*Tollmann*, 1982] combined the Monotonous and Varied groups into a single Drosendorf unit.

Because of complex structural and metamorphic relations among these units in the studied southern Bohemian Moldanubian domain, we distinguish the Varied from the Monotonous group purely on the basis of lithological arguments. The protolith of varied metasediments is supposed to be at least partly Early Paleozoic in age, based e.g. on the 509±27 Ma Nd model age of the amphibolite layers [*Janoušek, et al.*, 1997] or on the abundance of marbles that are not known in such an extent from pre-Paleozoic sequences in the Gondwana realm. The Monotonous group sometimes contains metagranitoids of early Paleozoic age (see Figure 2) suggesting even older sedimentary protolith of the surrounding paragneisses.

Conversely the neighboring Teplá-Barrandian block suffered significantly weaker reworking during the Variscan orogeny. Its SE half constitutes of Neo-Proterozoic to mid-Devonian non-metamorphosed sedimentary sequences, whereas to the W the Variscan metamorphism of Neo-Proterozoic rocks increases up to the Ky isograde [*Zulauf*, 2001; *Žáček and Cháb*, 1993]. Overall structure arises from interference of Variscan ductile deformation and metamorphic zonality with older Cadomian imprint, both separated by Cambro-Ordovician intra-continental rift related intrusions of granitoid plutons [*Dorr, et al.*, 1998; *Zulauf, et al.*, 1997]. Boundary with the easterly migmatites of the Moldanubian domain is marked by intense strike slip deformation along so called Central Bohemian Shear Zone [*Rajlich*, 1988], however, the true contact is in many places masked by the CBPC intrusions [*Žák, et al.*, 2005a]. Along the SW margin of the TBU the two units are separated by the so-called West-Bohemian shear zone [*Zulauf, et al.*, 2002a] and in the NW the TBU is bounded by the Saxothuringian suture zone [*Konopásek and Schulmann*, 2005; *Zulauf, et al.*, 2002b].

4.3 Distribution and significance of HP granulites and eclogites in the Variscan chain

In the Bohemian Massif the HP lower crustal rocks appear to be distributed throughout the whole Saxothuringian and Moldanubian domain, comprising eclogites, mafic and felsic granulites [*O'Brien and Carswell*, 1993]. Some eclogites are spatially related to previous sutures as for example between Saxothuringian and Teplá-Barrandian domain [*Klápová, et al.*, 1998; *Konopásek and Schulmann*, 2005], or in the micaschist rich mélange marking thrust of Moldanubian domain onto Brunia [*Konopásek, et al.*, 2002; *O'Brien*, 1993; *Štípská, et al.*, 2006]. Additionally these rocks occur in allochtonous napes as in the Műnchberg massif [*O'Brien*, 1993] or in relation to deep-seated intra-Moldanubian thrusts, like in the Světlík eclogite zone between the Monotonous and the Varied groups in southern Bohemia [*Faryad,*

et al., 2006]. However, structural position of many eclogite occurrences, particularly inside the Moldanubian domain, remains unresolved because of their limited size, rarely exceeding 1 km, combined with incomplete structural and petrological record.

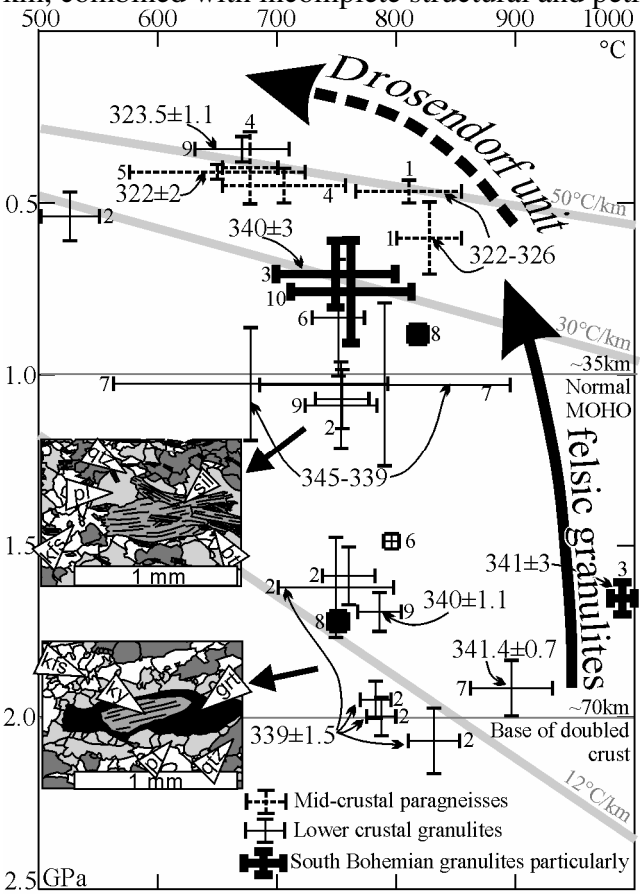

Figure 3. Relevant PT data from Bohemian granulites and Drosendorf metasediments. Abbreviated citations for PT data: 1 - [*Kalt, et al.*, 1999] 2 - [*Kotková*, 1993] 3 - [*Kröner, et al.*, 2000] 4 - [*Linner*, 1996] 5 - [*Pitra, et al.*, 1999] 6 - [*Racek, et al.*, 2006] 7 - [*Štípská, et al.*, 2004a] 8 - [*Štípská and Powell*, 2005] 9 -[*Tajčmanová, et al.*, 2006] 10 - [*Verner, et al.*, 2007]. Abbreviated citations for geochronology: 1 - [*Kalt, et al.*, 1997] 2 - [*Kotkova, et al.*, 1996] 3 - [*Kröner, et al.*, 2000] 5 - [*Gebauer, et al.*, 1989] 7 - [*Štípská, et al.*, 2004b] 9 - [*Schulmann, et al.*, 2005] 10 - [*Verner, et al.*, 2007].

The felsic granulites occur mainly in form of large bodies (X0-X00 km^2) as Saxonian Granulitgebirge dome emerging through metasediments and gneisses of the Saxothuringian domain [*Franke*, 2000] or in form of thin allochtonous sheets thrust over Saxothuringian basement [*Konopásek and Schulmann*, 2005]. Large granulite bodies that are studied in this paper occur in south Bohemia in the central part of the Moldanubian domain. There is another large belt of HP granulites rimming the Moldanubian domain and Brunia continent boundary where the lower crustal rocks rise along the Moldanubian thrust [*Schulmann, et al.*, 2005]. Felsic granulites outcrops are also known in the equivalents of Moldanubian zone in the Vosges Mts., Schwarzwald and French Massif Central [*Pin and Vielzeuf*, 1983]. Some of the felsic granulite massifs enclose mafic granulites ranging from small boudins up to bodies several cubic kilometers in size [*Fiala, et al.*, 1987; *Janoušek, et al.*, 2006; *Kodym*, 1972]. In general the felsic granulites represent the far most abundant deep crustal material known in the Variscides. Therefore, it is argued that a felsic material of comparable properties formed a significant constituent of the deep Variscan orogenic root.

4.4 Relevant PT estimates

We compile PT data from the whole Moldanubian (Figure 3), because the granulite bodies and surrounding metasediments provide fairly similar PT records throughout the whole root system [*O'Brien*, 2006; *Schulmann, et al.*, 2005] , and because there are only a few reliable petrological PT estimates available from the studied region.

The petrological studies of granulites in the Bohemian Massif focus traditionally on their peak metamorphism and amphibolite facies retrogression pointing out almost isothermal decompression followed by near isobaric cooling ([e.g., *O'Brien and Rotzler*, 2003; *Vrána, et al.*, 1995], Figure 3). The PT estimates depend on the composition of analyzed minerals and calculation method used more, than on the chosen sampling locality. Conventional thermobarometry yields approximately 1000 ºC / 1.6 GPa for metamorphic peak, followed by

retrogression at 800 – 900 ºC / 0.8 – 1.2 GPa [*Carswell and O´Brien*, 1993; *Cooke, et al.*, 2000; *O'Brien and Seifert*, 1992; *Vrána*, 1989] and 700-800 ºC / 0.5-0.8 GPa [*Cooke, et al.*, 2000; *O'Brien and Carswell*, 1993; *Vrána*, 1997]. The ultrahigh temperature estimates at peak pressures are based on an assumption of metamorphic origin of relict ternary feldspars. [*Štípská and Powell*, 2005] challenged this model and proposed 750-850 ºC at 1.6-1.8 GPa for the peak metamorphic event followed by retrogression at 700-800 ºC and 0.5-0.7 GPa. Subsequently, [*Tajčmanová, et al.*, 2006] and [*Racek, et al.*, 2006] found similar results for peak conditions in other parts of the Bohemian Massif applying the Thermocalc or Vertex software (Figure 3). The pre-granulitic origin of ternary feldspar has been discussed by [*Štípská and Powell*, 2005], who have studied relict ternary feldspars and assemblages preserved in low-Ca garnets from Opx-bearing granulite lens inside the Blanský les granulite massif (BLGM), which is a subject of this study. These authors concluded that the protolith of the intermediate granulite was a magmatic rock crystallizing at HT-MP conditions. PT estimates for the Drosendorf unit define the peak conditions of 750 °C / 0.7-1.2 GPa for the Varied group [*Petrakakis*, 1997; *Racek, et al.*, 2006] and 650 °C / 0.6-0.7 GPa for the Monotonous group , with retrogression at 650 °C / 0.4-0.5 GPa suffered by the whole Drosendorf unit [*Pitra, et al.*, 1999; *Racek, et al.*, 2006].

4.5 Regional geochronology

Regardless the geotectonic position of granulites in the frame of the Bohemian Massif , most of the existing U-Pb zircon ages cluster around 340 Ma (Figure 2, for review see e.g., [*Janoušek and Holub*, 2007]). The older ages, widely scattered between 350 and 400 Ma, are interpreted usually as protolith ages [e.g., *Friedl, et al.*, 2003; *Kröner, et al.*, 2000; *Wendt, et al.*, 1994]. Sm-Nd garnet data reveal slightly older ages than the 340 Ma [e.g., *Lange, et al.*, 2005; *Prince, et al.*, 2000]. [*Janoušek, et al.*, 2004] suggest an Ordovician granitic protolith with model age around 450 Ma for the Variscan felsic granulites, supported also by radiometric U-Pb zircon ages of [*Kröner, et al.*, 2000] or [*Friedl, et al.*, 2003]. In contrary [*Schulmann, et al.*, 2005] proposed a Devonian age of the granulite protolith (around 370 - 400 Ma), which originated by melting of continental crust in the back arc region of the Saxothuringian subduction. However, recent Lu-Hf dating of garnets from intermediate granulites shows Devonian (390 Ma) age of garnet growth which may indicate a Devonian granulite facies metamorphism [*Anczkiewicz, et al.*, 2007].

The short time span around 340 Ma, dominating in U-Pb ages of the south Bohemian granulites, is considered to date the exhumation from the peak metamorphic conditions (U-Pb zircon ages of 338±2 Ma by [*Aftalion, et al.*, 1989], 341±3.3 by [*Kröner, et al.*, 2000] or 346±5 from [*Wendt, et al.*, 1994]), through amphibolite facies retrogression to the mid-crustal hydration and partial melting ([*Kröner, et al.*, 2000], zircons from Crd-bearing melt patches from the Prachatice granulite at 340.4±2.9 Ma). The Rb-Sr biotite and muscovite cooling ages span between ~330 and 310 Ma [*Svojtka*, 2001; *Van Breemen, et al.*, 1982] similarly to ^{40}Ar - ^{39}Ar ages on amphibole, muscovite and biotite [*Košler, et al.*, 1999], marking cooling through 500 – 350 – 300 °C blocking temperatures. The youngest numbers of 194±5 and 180±5 Ma acquired by [*Svojtka*, 2001] from the apatite fission tracks express the subsurface residence.

There is very poor U-Pb zircon age database from the surrounding Drosendorf unit suggesting a metamorphic event at 355±2 Ma for the Světlík orthogneiss [*Wendt, et al.*, 1993] or the 367±19 Ma for Kaplice Mu-paragneiss [*Kröner, et al.*, 1988]. The age of ductile deformation restrict also 331±5 Ma old syndeformational pegmatites from the Bechyně orthogneiss ca 40 km to the NNE of the BLGM (Rb-Sr on muscovite, [*Van Breemen, et al.*, 1982]).

The independent time limits define neighboring syn- to post-tectonic granitoids. According to overview of [*Žák, et al.*, 2005a] and references therein the CBPC in the NW records

regional transpression from at least 354 Ma to ~346 Ma. Following exhumation of adjacent Moldanubian orogenic root lasted until ~337 Ma when a post-tectonic body of Tábor syenite was emplaced. The Moldanubian pluton to the SE consists mostly of post-tectonic granitoids, which intruded the Monotonous group in a wide time span between 338 to 314 Ma.

The Moldanubian rocks in northern Bavaria exhibit younger metamorphism associated with widespread migmatitization dated by U-Pb on monazite at 326 [*Kalt, et al.*, 1997] or 315 Ma [*Schulzschmalschlager*, 1984]. The Bavarian granitoids (335-322 Ma, e.g. [*Siebel, et al.*, 2005]) yield ages comparable to the Moldanubian pluton but here the intrusions are interpreted as syntectonic.

5 Geology and Structural geology of South Bohemian Moldanubian domain

The studied region covered with ~850 documentation points forms 130x30 km traverse through the whole south Bohemian Moldanubian domain from the Moldanubian batolith in the SE to the CBPC in the NW following the 9HR seismic line (Figure 4a). The SE part is characterized by occurrence of three large neighboring bodies of felsic granulites (Blanský les granulite - BLGM, Křišťanov granulite - KGM and Prachatice granulite massif – PGM in Figure 4b). Discontinuous stripes of the Grt or Spl peridotites and mantle eclogites are systematically found along margins of all the granulite massifs, the BLGM contains large bodies of mantle-derived rocks also in its interior. The adjacent Moldanubian domain consists of the Varied group to the SE and the Monotonous group to the NW. The individual massifs are separated by narrows zones of medium-grade paragneisses with affinity to Monotonous group (NW-SE trending Libín zone) or Varied group (N-S trending Lhenice zone). The north-eastern margin of the BLGM is marked by a complex association of medium- and high-grade rocks of the Drosendorf and Gföhl units (Figure 4a). Farther to the east all units become parallel to major thrust zone marked by the occurrence of eclogite bodies [*Rajlich, et al.*, 1986; *Vrána and Šrámek*, 1999] marking the ductile thrust of the Varied group over the underlying Monotonous group. A zone of lower grade muscovite-biotite paragneiss (the Kaplice zone) intruded by granitoids of the Moldanubian batolith occurs in the eastern most extremity of the studied area. The Monotonous group in the northwestern part of the studied area is intercalated with several large NE-SW elongated bodies of Varied group and Gföhl orthogneiss (Figure 4a).

The detailed structural field study revealed complex polyphase evolution and identified five distinct ductile deformation events responsible for development of individual fabrics in the studied area. The structural classification is based on outcrop-scale crosscutting relations and mutual transpositions accompanied with petrological and microstructural characteristics of individual fabrics [*Turner and Weiss*, 1963]. The geometrical criteria and fabrics continuity are used for large-scale regional fabric correlations. The two oldest ones (S1, S2) are preserved only inside granulite massifs and bear high-grade metamorphic assemblages [*Franěk, et al.*, 2006]. The third and fourth fabrics (S3, S4) were developed throughout the whole region and the fifth heterogeneously affects studied area except granulites.

The deformational history and structural evolution of all three granulite massifs is described together due to similarity of the structural record and microstructural and petrological features preserved in all the granulite massifs. Similarly, the adjacent Drosendorf and Gföhl units share common structural record and therefore their structural characterization is also described together.

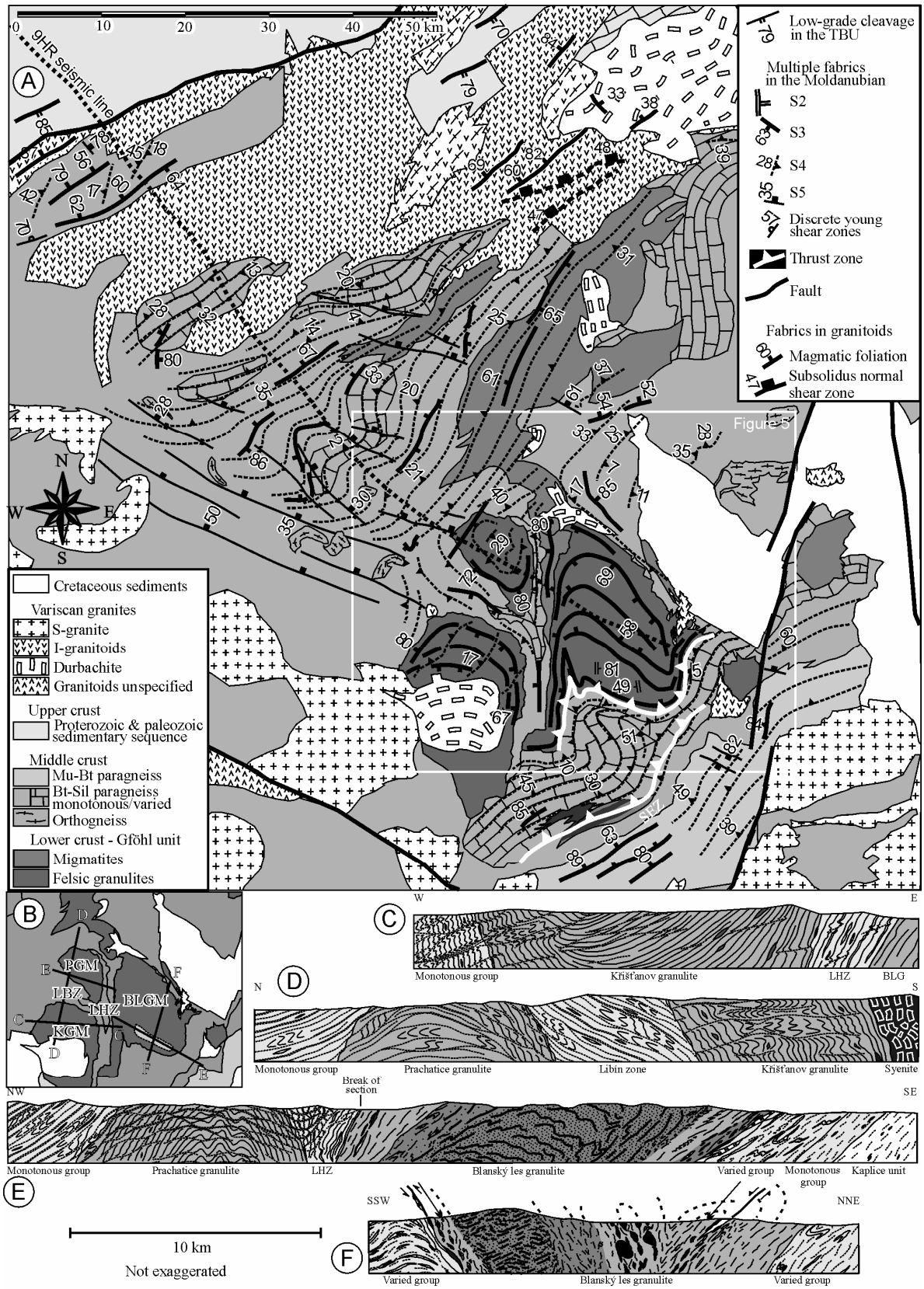

Figure 4. a) Structural map of the whole studied area. Structural data from granitoids adopted from [*Žák, et al.*, 2005a]. b) Location of geological profiles across the granulites. All profiles have the same scale and are not exaggerated. c) W-E view of KGM. d) N-S profile across PGM, Libín Zone and KGM. e) NW-SE Section of PGM and BLGM, roughly following the seismic reflection line. f) N-S section of BLGM. Part of profile e) and profile f) are adopted from [*Franěk, et al.*, 2006].

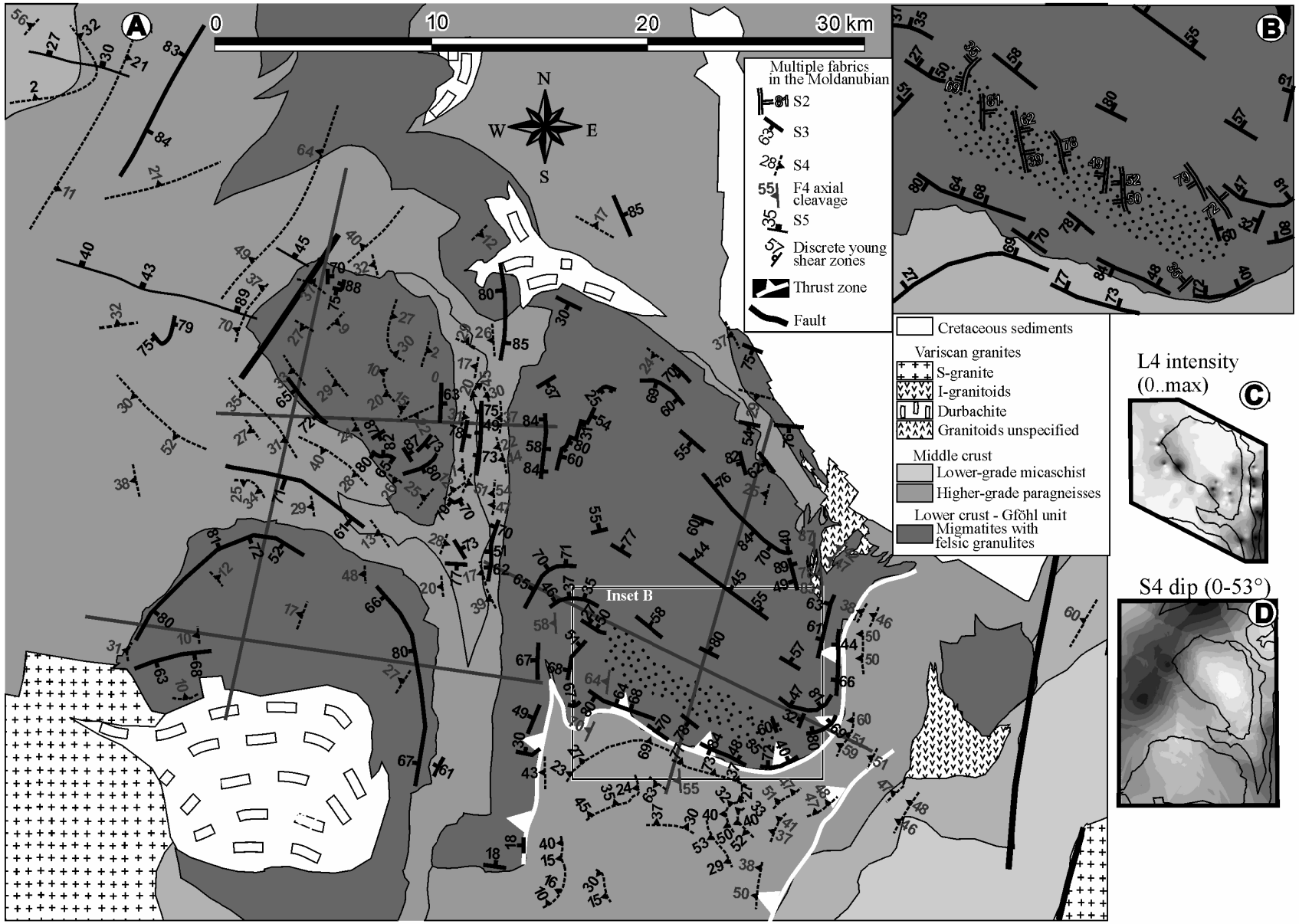

Figure 5. a) Structural map of the SE part of studied region dominated by granulites. The S2 fabrics are depicted in the inset b) in a detail of the relict granulitic domain inside the BLGM. c) Intensity of L4 lineations in the PGM surroundings (dark = intensive, white = none). d) Steepness of the S4 foliation in the PGM surroundings (darker = steeper).

5.1 Earliest granulite facies fabrics

The oldest identified fabrics (S1, S2) are exceptionally preserved in an 8.4 x 2.5 kilometers wide elliptical domain in the southern part of the BLGM (Figure 5a, b). Small relicts are further present throughout the BLGM and scarcely also in the PGM, but they were never found inside the KGM. In particular, in the BLGM elliptical area, the granulites exhibit penetrative mylonitic foliation S2 which contains relicts of S1 compositional banding (Figure 5b), both bearing a stable granulite facies mineral assemblage of Qtz + Kfs + Pl + Grt + Ky + Bt [*Franěk, et al.*, 2006].

5.1.1 Compositional banding S1

The S1 fabrics are preserved in small-scale low strain domains being marked by a ~1 cm scale Q-Fsp compositional banding resembling to common Q and Kfs domains of anatectic augen orthogneisses. [*Franěk, et al.*, in prep.] shows that such hypersolvus augen orthogneisses represent protolith of the felsic granulites. Quartz bands alternate with coarse-grained perthitic alkaline feldspar bands that are usually decomposed to a fine-grained mixture dominated by cryptoperthitic K-feldspar, with subordinate plagioclase and tiny quartz. The S1 is preserved only in short limbs of close to isoclinal F2 folds ([*Franěk, et al.*, 2006]; Figure 6a) and the relicts are too rare to allow any structural interpretations.

Similar microstructure has been reported from the Saxonian Granulitgebirge where some occurrences of S1 (Figure 9a,b in [*Behr*, 1961]) exhibit the Qtz-Kfs compositional banding up to ~ 1 cm scale. Comparable microstructure was not described in all other Variscan felsic granulites, probably due to extensive reworking by younger events.

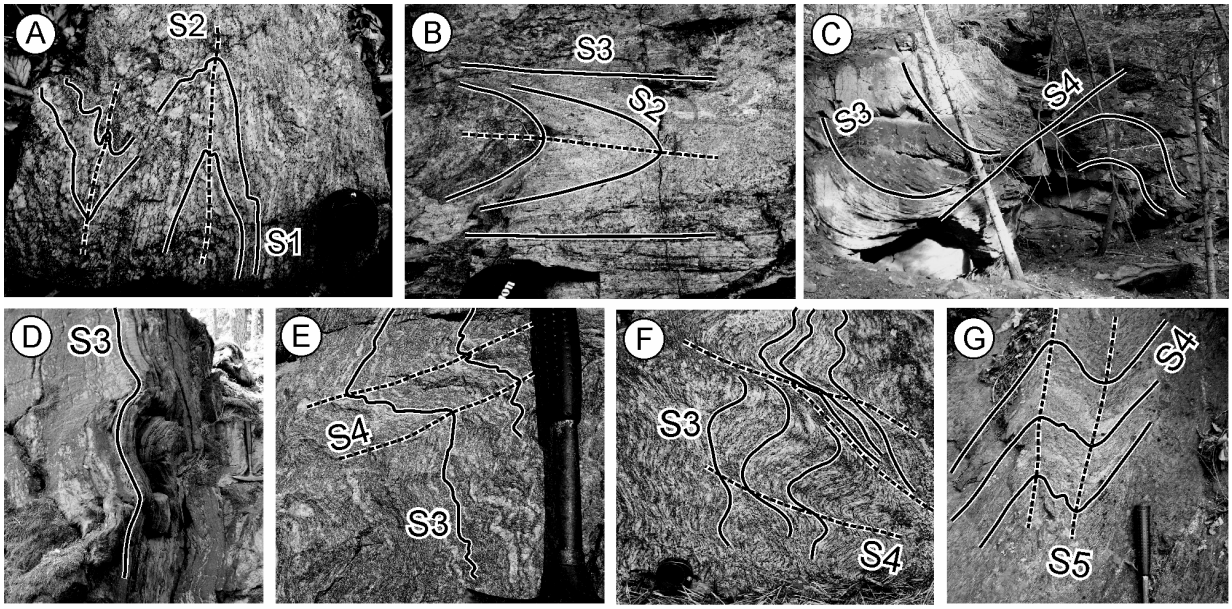

Figure 6. Field photos of structures in granulites. a) Development of S2 axial cleavage during F2 passive folding. b) Transposition of S2 to S3 via mesoscopic similar folds. c) Initial S4 in discrete shear zones affecting S3 in the PGM. d) Steep S3 only weakly affected by D4, Kaplice unit in the SE. e) S4 crenulation cleavage in a migmatized paragneiss. Varied unit in the NW. f) S3 transposed into S4 via crenulations and shear bands. The latter are often filled with granitic partial melt. Orthogneiss in NW part of the studied region. g) S5 crenulation cleavage in monotonous migmatitic paragneisses in the SW, at the edge of region reworked by D5.

5.1.2 Granulite mylonitic fabric S2

The onset of S2 fabric development is characterized by pervasive static recrystalization of the former coarse grained orthogneiss into a fine-grained mosaic of Pl, Kfs and Qtz containing low amount of partial melt distributed along the Kfs and Pl boundaries [*Franěk, et al.*, in prep.]. The subsequent folding of S1 is accompanied with progressive development of S2 axial plane cleavage and penetrative reworking of D1 fabric into fine-grained Kfs dominated matrix (see Figure 3e in [*Franěk, et al.*, 2006]) containing large Q ribbons and Bt flakes oriented parallel to stretching direction. Pl coronas commonly elongated parallel to D2 stretching are developed around matrix Ky and Grt implying syn-D2 origin. These coronas were interpreted as a product of decompressional reaction of Ky or high-grosular Grt by [*Tajčmanová, et al.*, 2007]. The S2 foliation from the ~8x2 km relict domain inside the BLGM strikes uniformly N-S showing variable dip of 50-90° to the W or less commonly to the E (Figure 4e and 5b). Poles to S2 foliation planes concentrate along a great circle suggesting a sub-cylindrical geometry in 3D. Pervasive N-S L2 stretching lineation lies at the pole of this great circle, i.e. parallel to the axis of the cylindrical structure [*Franěk, et al.*, 2006]. Other S2 relicts in the granulites show the same microstructural and petrological features but because of small extent and significant later reworking the regional structural correlations are precluded.

Similar features related to transition of S1 banding to S2 granulite mylonitic foliation are found also in the Saxonian granulite massif (Figure 9a,b in [*Behr*, 1961]). In other Bohemian granulites, the steep granulite-facies mylonitic fabrics marked by typical Qtz ribbons and Pl decompressional coronas around Grt and/or Ky represent the oldest fabrics [*Kotková*, 1993; *Racek, et al.*, 2006; *Štípská, et al.*, 2004a; *Tajčmanová, et al.*, 2006].

5.2 Mid-crustal orogenic fabrics

Mid-crustal fabrics correspond to amphibolite facies deformations that occurred at three distinct events: 1) Large scale folding of granulite bodies and surrounding host rocks after their emplacement in mid-crustal levels, 2) subsurface horizontal flow affecting all lithologies, 3) N-S shortening resulting in development of steep WNW-ESE trending cleavage affecting all previous fabrics in southern part of the studied area.

5.2.1 Amphibolite facies fabrics S3 – crustal scale folding

In the Drosendorf and Gföhl units excluding granulites, the first well-defined metamorphic fabric is steep and NE-SW trending foliation carrying metamorphic assemblages indicative for amphibolite facies conditions. Based on structural correlation with granulite bodies, where this deformation affects granulite facies fabrics S1 and S2, this fabric is assigned as S3. The S3 cleavage generally shows stable orientation but it is modified in the vicinity of regionally folded granulite sheets thanks to large wave-length of F3 folds.

Despite of strong later reworking, the S3 fabrics are usually well-preserved in competent lithologies forming low-strain domains preserved from dominant D4 deformation. The NW dipping S3 fabric is well preserved in the SW part of Kaplice unit and at the boundary of the Moldanubian with the Teplá-Barrandian domain. The S3 foliation occasionally bears weak mineral lineations or corrugations, both shallowly plunging NE and SW.

The S3 is defined by preferred orientation of micas and flattened Q-Fsp aggregates. Paragneisses from both the Monotonous and Varied groups bear mineral assemblage of Bt + Qtz + Pl + Kfs ± Sil, complemented locally by Grt in the Varied group or Ms in the Monotonous group. Paragneisses often contain Qtz-Fsp aggregates, which represent segregated partial melts forming oftalmitic to stromatitic textures. Degree of migmatitization does not systematically vary between the Monotonous and Varied group. The exceptions represent two regions of dominant S3 fabric, which exhibit lower metamorphic grade: 1) In

the Kaplice zone where the S3 is defined by preferred orientation of Mu and Bt crystals and segregation of quartz lenses with Crd or And [*Vrána and Bártek*, 2005; *Vrána, et al.*, 1995]. 2) Towards the boundary of Moldanubian and Teplá-Barrandian domains the S3 bears higher amount of Mu in conjunction with decreasing intensity of partial melting. The Gföhl gneisses consist of Bt + Qtz + Pl + Kfs ± Sil ± Grt and exhibit stromatitic to often nebulitic textures indicating higher degree of migmatitization than the Drosendorf unit. Here, the S3 fabric is represented by typical migmatitic layering.

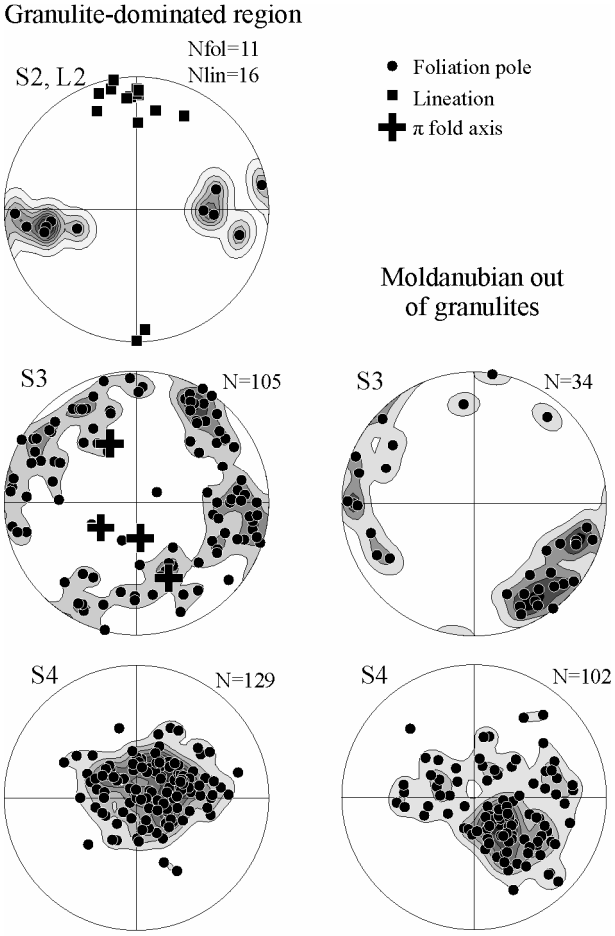

Figure 7. Equal area lower hemisphere polar projections of S2, S3 and S4 fabrics in the granulite dominated region contrasted against the same fabrics developed in the Moldanubian devoid of granulites.

In the granulites, the S3 represents dominant planar fabric in the BLGM and KGM while in the PGM it is preserved only along its southern and eastern margins. The S3 results from transposition of S2 via outcrop-scale folding accompanied by development of S3 axial cleavage. The stable assemblage of Qtz + Kfs + Pl + Bt ± Sil ± Grt indicates syndeformational retrogression at amphibolite facies conditions combined with hydration. Additional syn-D3 partial melting occurred in the outer parts of the BLGM and to some extent in the KGM. In general, the alignment of Bt and elongation of Q with Fsp define the S3 planes, being occasionally emphasized by cm to dm - scale compositional banding [*Franěk, et al.*, 2006]. At the transition from S2 to S3 the microstructures of S3 still partly resemble the granulitic ribbon Qtz mixed with fine-grained Fsp matrix. These features reflect HT conditions at the onset of the D3, possibly at the granulite-amphibolite facies transition. With progressive reworking the S3 microstructure rapidly evolves to coarser grain size associated with important alignment of felsic phases [*Franěk, et al.*, 2006].

In granulites the S3 exhibits arcuate geometry (Figure 5a) with moderate to steep dips. The regional scale fold-like geometry of the S3 in the BLGM was mapped in detail by [*Kodym*, 1972] and later on by [*Franěk, et al.*, 2006]. The poles of S3 in each of studied granulite massifs plot around a great circle suggesting a sub-cylindrical fold geometry of this fabric. At the E and W limits of the BLGM this fabric dips to the W. However, in the central portion of the BLGM the S3 attitude is more complex and dips towards NE in the southern half and to the SW in the northern half of the granulite body. In the PGM the S3 strikes N-S along the E margin and NW-SE at the SW edge of the massif, dipping outwards from the granulite body thus forming an antiformal structure. In contrast, within the KGM body the S3 trends N-S

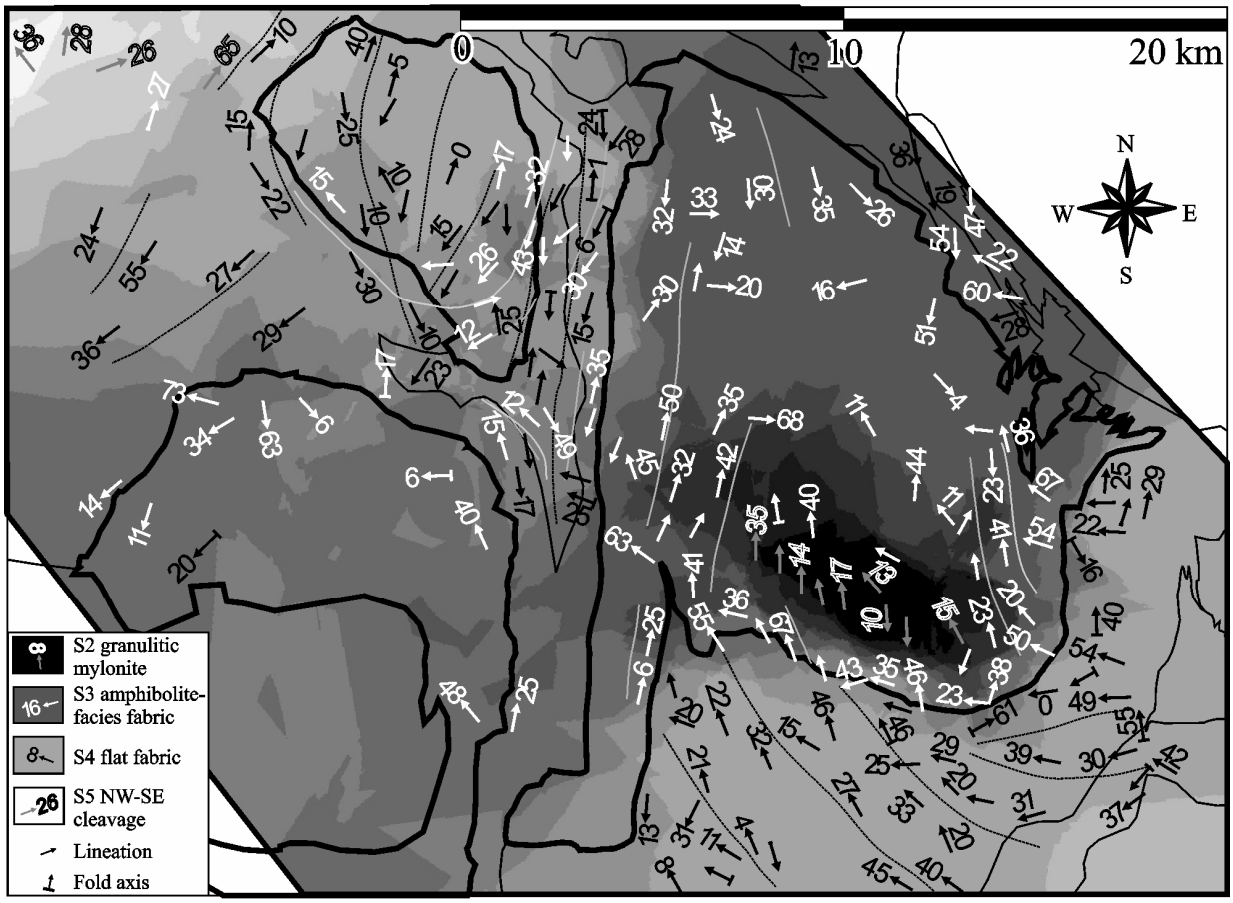

Figure 8. Krigging interpolation of the S2 – S5 fabrics prevalence inferred from field study of individual outcrops. Grey levels then visualize extent of reworking by particular deformation phases (darkest=S2, lightest=S5). 4 generations of corresponding lineations are depicted.

along the western and eastern margins while in the central part and northern margin it strikes WNW-ESE. Here, the S3 foliation dips steeply inwards the granulite body developing a synformal structure. Changes in attitude of S3 in all of the granulite bodies appear as km-scale smooth flexures, or rarely as several km wide sequence of outcrop-scale parasitic folds.

The axes and axial planes of F3 folds in the PGM, KGM and BLGM reveal similar orientation in all the granulitic bodies. (Figure 5a, 7). For the tight flexure of PGM we have used the π fold axis [e.g., *Price and Cosgrove*, 1990] and surface trace of the S3 hinges to construct a subvertical NNW-SSE trending axial surface, comparable to the 262/87 (dip direction/dip in degrees) and 246/89 axial planes of large scale folds defined previously in the BLGM by [*Franěk, et al.*, 2006]. The wide arcuate geometry of S3 in the KGM allows only to estimate a steep axial plane dipping roughly to the W. The π fold axes plunge 235/63 in the KGM and 174/68 in the PGM, similar to orientation of fold hinge (157/38) in the NW of the BLGM.

The L3 mineral lineations in granulites are usually defined by elongated biotite aggregates or less commonly by alignment of sillimanite crystals. In the BLGM predominate north to north-west moderately plunging lineations sub-parallel to hinges of F3 folds. Only in the northern and structurally most complex part of the BLGM the azimuths of moderately dipping lineations vary from south to east. The well developed L3 lineations in the PGM plunge at shallow angles sub-parallel to strike of the S3. In the contrary, L3 lineations in the KGM are poorly developed except the NW corner where they broadly scatter around SW direction (Figure 8).

In the Qtz + Kfs + Pl + Bt ± Sil ± Grt bearing metasediments separating the individual granulite massifs the S3 fabrics are well preserved only in the south, while towards the north and west, only rare outcrop scale S3 relicts are preserved. The S3 foliations are defined by preferred orientation of biotite as well as by oblate shape of quartz-feldspar aggregates. Ubiquitous syn-deformational partial melting of paragneisses resulted in stromatitic migmatitic banding parallel to S3 schistosity. The S3 in these metasediments strikes parallel to the S3 in neighboring granulites: in the Lhenice zone the S3 forms tight vertical N-S elongated fan-like pattern (Figure 4e) while in the Libín Zone it steeply dips to the southwest below the KGM (Figure 4d). Lhenice zone rocks exhibit intensive N-S shallowly plunging lineations defined by biotite alignment, while in the Libín Zone the L3 lineations are not developed. Scarce remnants of an older fabric in form of closed dm-scale folds suggest important shortening during D3.

5.2.2 Subhorizontal amphibolite facies fabric S4 – result of subsurface horizontal flow

The most prominent fabric of the studied region is S4 transposition foliation that generally dips at gentle angles to the NW and strikes sub-parallel to the Moldanubian – Teplá-Barrandian boundary. SE of the granulite massifs the S4 attains slightly curved and steeper geometry still dipping generally to the NW at moderate angles. However, along the southern edge of the CBPC and ~10 km north-west of the PGM the S4 fabric dips to the SE forming large-scale open fold-like structures in the Drosendorf unit. The S4 fabric commonly bears N-S to NE-SW stretching lineations sub-parallel to hinges of these folds. The intensity of S4 development significantly decreases towards boundary of Moldanubian and Teplá-Barrandian domains. Similarly to S3, in the vicinity of granulite massifs the S4 fabric exhibits significant perturbations and locally attains steep attitude almost parallel to the S3 fabrics. The S4 fabrics in Q + Ksp + Pl + Bt ± Sil ± Grt bearing metasediments exhibit significantly lower degree of syn-deformational partial melting compared to the S3. In the granulites the S4 is marked by destruction of the typical dm-scale compositional banding and replacement of garnet by biotite which is consistent with Q + Ksp + Pl + Bt ± Sill assemblage. In granulites the transition from S3 to S4 proceeds via development of shallowly dipping S4-parallel shear-zones, often accompanied by various scales active folding of S3 without development of observable axial cleavage.

Whilst the NW half of the PGM is strongly reworked by subhorizontal S4 foliation bearing weak N-S lineation (Figure 5c,d, 8), the KGM exhibits moderate reworking by WNW shallowly dipping S4 foliation without macroscopically observable lineation and the BLGM is almost unaffected by D4. In the Lhenice zone the S4 forms an open synform with horizontal N-S axis, bearing strong N-S shallowly plunging stretching lineation. Inside the Libín zone the S4 fabric dips moderately to the SW below the KGM, bearing weak lineations of variable attitude. North of the BLGM the S4 dips shallowly to the SSW and its further continuation in the north is obscured by cretaceous sediments. In general, the geometry of the S4 fabric tends to match the shape of stiffer granulite massifs similarly to foliation development along strong boudins within deformed weaker matrix.

Occasional cm-dm scale pinch and swell structures with locally developed steep E-W trending tensional cracks filled by undeformed granitic melt pockets in neck zones develop in both the granulites and surrounding Drosendorf unit. These structures testify that very intense vertical shortening and N-S oriented stretching operated at temperatures about the 650°C corresponding to minimum granite crystallization temperature. [*Kröner, et al.*, 2000] convincingly dates the D4 fabric development along the W margin of the PGM at 340.4±2.9 and 339.6±3.1 Ma using the U-Pb method on zircons from the granitic melt pockets and granodioritic dyke syntectonic with D4 .

5.2.3 NW-SE trending steep cleavage front - result of NE-SW compression

The SW part of the studied region is affected by late D5 deformation event resulting in development of crenulation cleavage, which locally passes to new penetrative NW-SE trending foliation moderately to steeply dipping to the NE. The intensity of this fabric generally increases southwestward and it becomes dominant fabric in so-called Bavarian Moldanubicum and Bavarian - Pfahl shear zone [e.g., *Behrmann and Tanner*, 1997; *Siebel, et al.*, 2006]. In the studied area, this deformation is also expressed in map pattern by km scale open folds developed mainly north-west of the PGM and south of the BLGM. Towards the NE across a 20 km wide zone the intensity of D5 deformation progressively decreases and only rare mesoscopic crenulations and dextral shear zones are locally developed (Figure 4). There is no expression of D5 related structures inside the granulite massifs and it is assumed that the geometry and internal structure of granulites is not affected by this late deformational event.

The metamorphic conditions associated with D5 fabrics correspond to upper greenschist facies as indicated by brittle-ductile character of S5 cleavage and growth of muscovite on foliation planes. However, in the SW part of the Varied and Monotonous groups the S5 is defined by alignment of biotite and flattening of Q-Fsp aggregates, bearing occasionally biotite or sillimanite dip parallel lineation. The mineral assemblage is marked by newly grown sillimanite and muscovite in the paragneisses indicating temperatures higher than those of first sillimanite isograde close to 600°C [*Yardley*, 1989]. In the Bavarian Moldanubicum SW of the studied area the S5 fabrics exhibit widespread anatexis indicative for higher metamorphic temperatures compared to our studied area [*Behrmann and Tanner*, 1997]. These fabrics are intruded by numerous syntectonic granitoids with zircon U-Pb or Pb-Pb crystallization ages ranging from 338 to 309 Ma (Figure 2, [e.g., *Dorr, et al.*, 1998; *Siebel, et al.*, 2003]). To sum it up, the S5 fabric shows increase of metamorphic grade from amphibolite-greenschist facies transition in the north to partial anatexis in the south in conjunction with the increasing intensity of deformation.

6 Reflection seismics

Most of our study area is aligned parallel to a deep seismic reflection profile 9HR which was shot in a NW-SE direction through western half of the Bohemian Massif using explosive sources. Partly published [*Tomek, et al.*, 1997] and also unpublished seismic data presented here (Figure 9,10,11) comprise region between TBU-CBPC boundary in the NW and eastern edge of BLGM in the SE. These data offer good quality record from ~2 km below the Earth surface to the MOHO at ~40 km depth, exhibiting in places also reflections in upper mantle.

6.1 Characterization of reflection seismic data

There are several restrictions in correlation of seismic reflection image with geological features. The single seismic line in our case offers just apparent dips of reflectors which make correlation with geological structures more difficult. Nevertheless in majority of the studied area the profile runs perpendicular to strike of rock fabrics which suggests that the reflection dips approximate true dips of depicted reflectors at least in the upper crust. The reflection seismics is also blind to reflectors that dip steeper than ~45° and an additional difficulty arises from the fact that the reflections are assembled from the conical 3D space below each shot rather from a plane of the seismic section. It implies that in regions of more complex 3D

architecture must be considered also the possible aside origin of reflections. According to P-wave velocities of the Moldanubian crystalline reaching ~6.1 km/s for upper and ~6.8 km/s for lower crust [*Hrubcová, et al.*, 2005] the two-way travel times (TWT) of seismic measurements were approximately recalculated to kilometric depths. Line drawing (Figure 11) based on migrated seismic record reveals striking difference between seismic properties of the TBU and the Moldanubian crust. Whilst the Moldanubian crust itself exhibits several seismically different domains, the highly reflective TBU upper crust shows one single set of parallel and very strong reflection packages (B1-B6) dipping to the SE. These packages are interrupted at depth along a NW dipping virtual line, below which the TBU lower crust shows very poor reflectivity being constrained by subhorizontal discontinuous MOHO reflections (M1) at 11s TWT. The TBU-Moldanubian boundary is masked by CBPC granitoids on the surface and shows sudden decrease of the reflectivity of the whole crustal pile in a ~10km wide column with only rare reflections present.

The Moldanubian upper crust shows contrasting seismic image in the eastern part dominated by granulites and in western part devoid of these rocks. The latter is characterized by anastomosing reflections down to 5s TWT, which resemble pinch and swell structures of ~20 km wavelengths. Stronger reflection packages in this region (V1-V4, K1+K2) are irregularly distributed throughout the region, concentrating at the western edge of the Moldanubian domain. The upper crust in the east of the seismic profile is crosscut by a strong and unusually straight reflection package G2 dipping moderately to the SE. The package terminates abruptly at 2 km depth below the W edge of the PGM, probably on the N-S fault passing along W margin of this granulite massif. The strongest reflections on its 29 km length appear below the PGM, while it diminishes at ~18 km depth in the SE, below the centre of the BLGM. A parallel weaker package G1 of ca 12 km length appears attached to the top of this package. Except these packages the whole crust below granulites exhibits almost no reflectivity and weakly defined MOHO (M4) at 12-13s TWT. The reflections along whole SE edge of the seismic profile are probably just artifacts of a migration procedure. The lack of reflections contrasts with underlying strong NW dipping mantle reflection package below ~12s TWT that is shown in non-migrated line drawing (Figure 9).

The western part of the Moldanubian middle crust exhibits uniformly distributed horizontal reflections designated as MC, which appear in a lens-shaped domain ~60x15 km in size. The underlying lower crust bears several packages of strong reflections (S1-S4) that dip 30-40º to the SE and continue through discontinuous MOHO reflections (M2, M3) into the uppermost mantle.

6.2 Interpretation of reflection seismics data

Interpretation of seismic reflections in the high-grade Moldanubian domain that exhibits polyphase deformation meets significant difficulties. The reflection events may be induced either by lithological layering, penetrative foliation, faults or boundaries of intrusive bodies. We try to overcome this ambiguity by careful comparison with the surface extent of major lithological units and with our structural interpretations depicted from detailed structural analysis presented above.

The TBU upper crustal reflection packages (B1-B6) correspond to Proterozoic low-grade sequence of siltstones interlayered with basalts, which is exposed on the surface. Their termination located at the margin of the TBU may document sideward intrusions of granitoid bodies related to the CBPC, or reworking of the SE dipping structures by later Variscan deformations. The low reflectivity in the whole crustal column directly below the TBU-Moldanubian boundary can be best explained by presence of the CBPC granitoid intrusions.

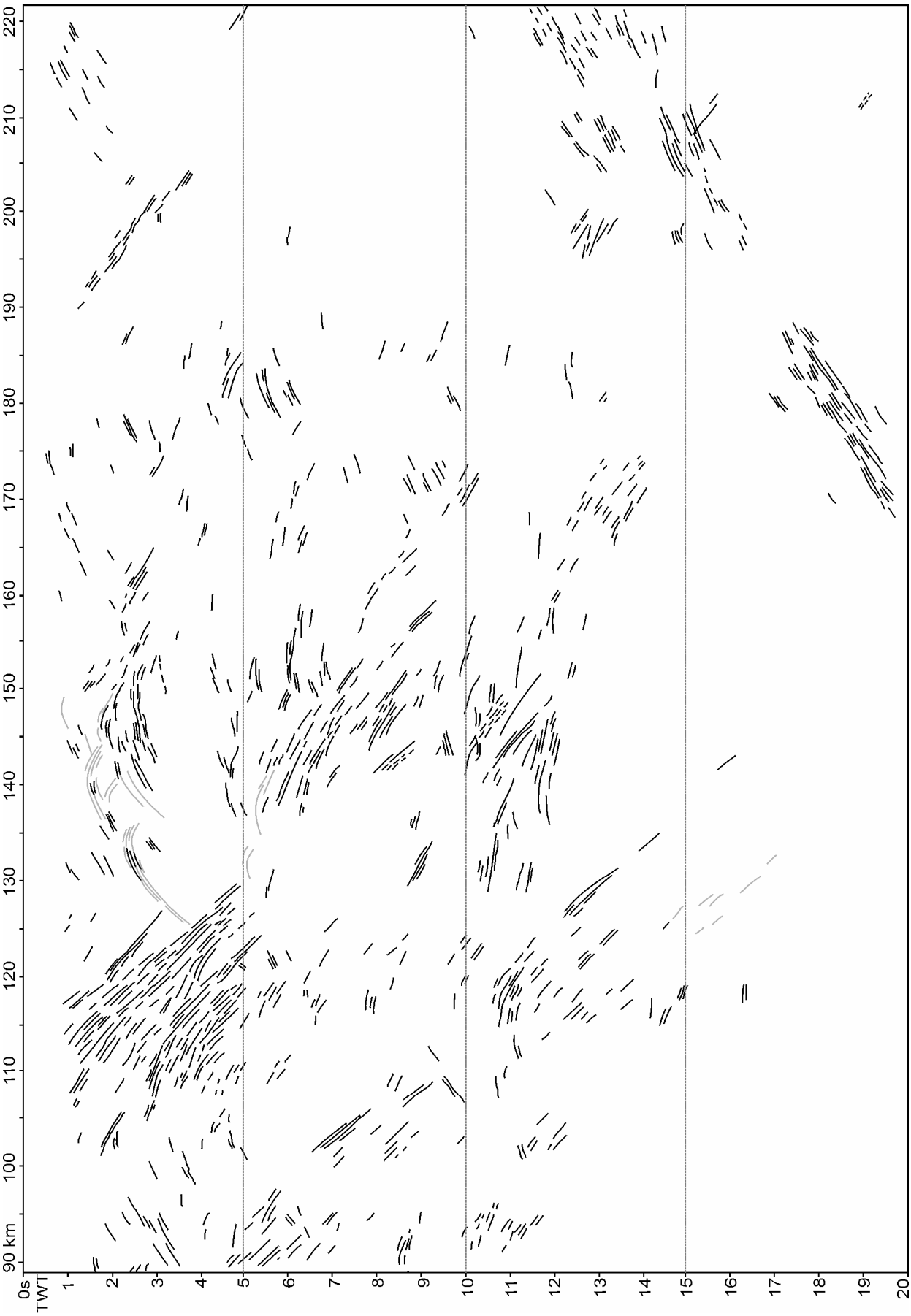

Figure 9. 9HR seismic profile, line drawing of nonmigrated reflection data. Black lines refer to reflections, grey ones depict several major diffractions. Vertical scale approximately equals the horizontal.

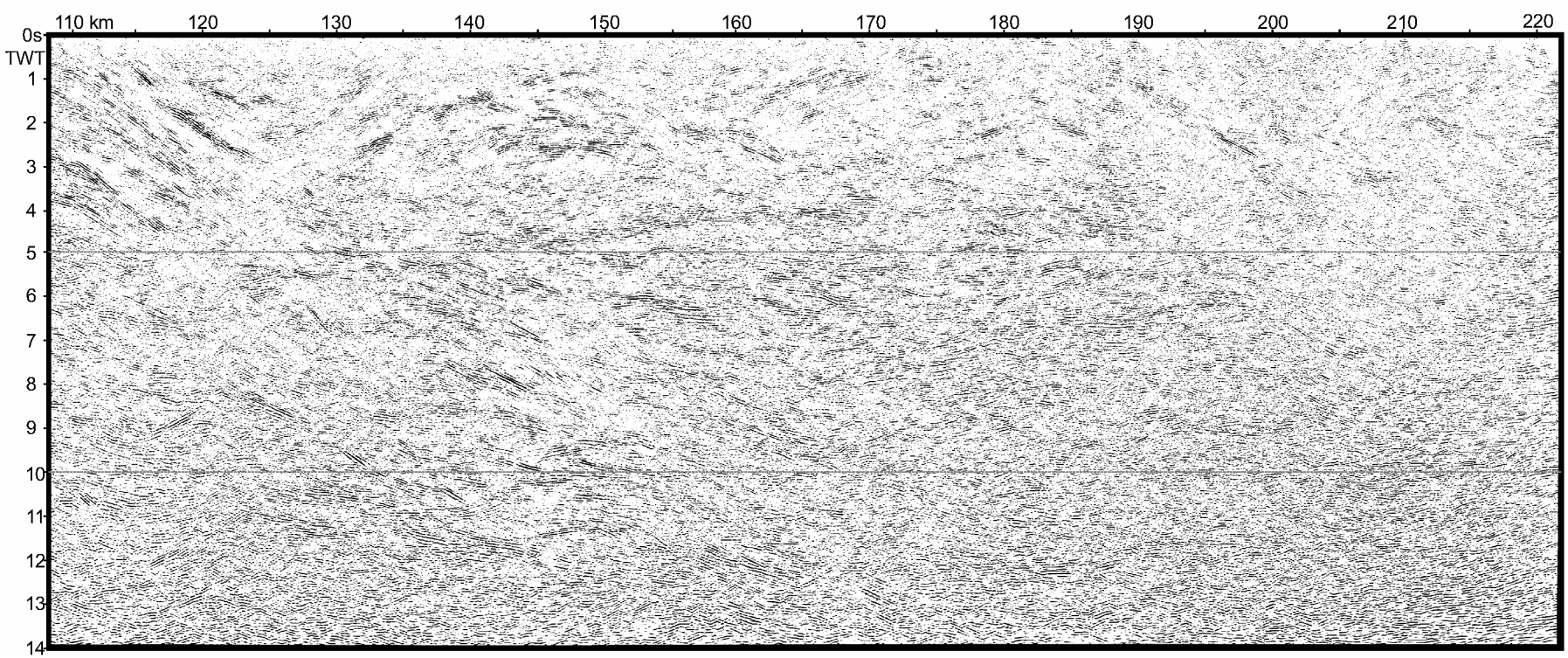

Figure 10. 9HR seismic profile, migrated raw data. Vertical scale approximately equals the horizontal.

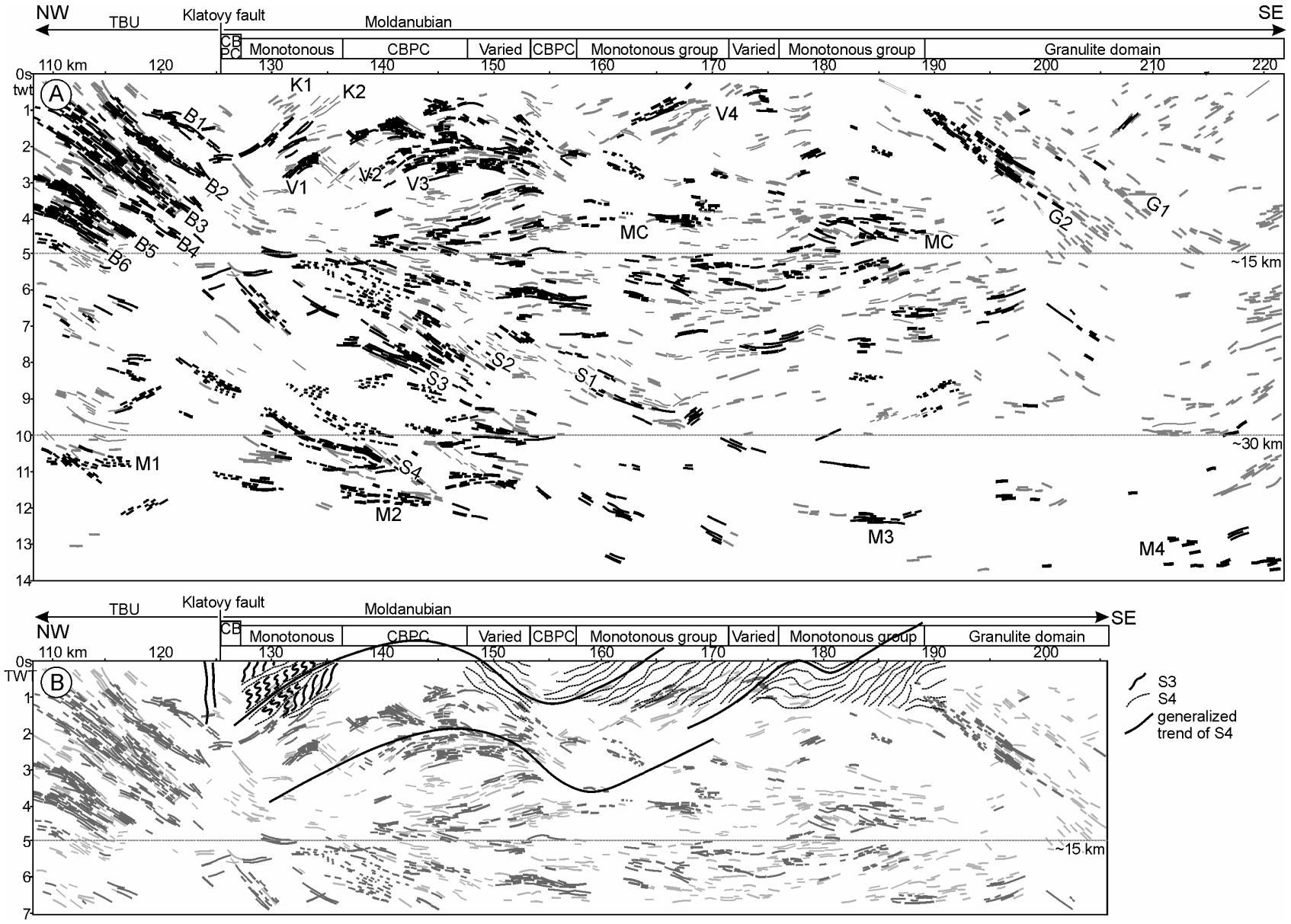

Figure 11. 9HR seismic profile, line drawing of migrated reflections. Thickness and darkness of lines expresses intensity of reflections. a) With package description. b) Upper part with geological profile that is based on field structural study. Solid black lines represent S3, dashed ones express S4. Wide fold-like lines point out regional trend of S4 inferred from field structures. The reflections west of the granulites fit very well to our independent geological interpretation down to ~5 km depth. Vertical scale approximately equals the horizontal.

The anastomosing reflections in the upper crust of the western Moldanubian correlate perfectly with S4 geometry determined by our field research (Figure 11b) suggesting that all the anastomosing reflections can be related to the subsurface continuation of S4 fabrics. Concretely the V4 reflection package spatially correlates with surface exposure of km-scale lens of Varied group suggesting that the reflectors are in this case represented by interlayering of paragneisses with marbles, amphibolites and other varied intercalations parallelized with S4 fabric. Similarly can be explained the V1-V3 packages which also extend below the surface exposure of larger volume of varied rocks. The K1 and K2 packages in this context document subsurface presence of varied intercalations at the western edge of the Moldanubian domain, which is a geologically meaningful possibility. The perfect fit of geometry of seismic structures with ductile rock fabrics poses an important precedent for further interpretation of reflections in the Moldanubian deeper crust.

The nature of straight reflection package G2 dipping below granulite massifs remains ambiguous, because the observed high intensity and length of reflections may be caused either by lithological layering similar to the Varied group or by a thick zone of intensive mylonitization. The more pronounced shallower half of the package possibly coincides with the bottom of the PGM granulite body. Based on the single seismic section the orientation of the G2 reflector can vary between steeper dip to the NE through medium dips to the SE to steeper dip to the SW. Such orientations do not fit to the NW dip of S3 and S4 fabrics prevailing in the surroundings and the G2 package cannot be correlated to any structure mapped on the surface. Its perfectly straight geometry then suggests that the corresponding reflectors weren't affected by the pervasive D4 deformation.

The low reflectivity in the whole crustal column below granulite massifs may be caused either by lack of reflection inducing inhomogeneities or extreme steepness of reflectors which wouldn't be detectable by seismic survey. Low energy of shots cannot be responsible for the lack of crustal reflections, because the much deeper mantle reflections have been recorded below this seismically transparent zone (Figure 9). All the rest of the examined Moldanubian crystalline exhibits significant reflectivity suggesting that the Moldanubian crust in general contains abundant reflectors that would be recorded if having suitable attitude. We argue that this crustal pile devoid of reflections contains reflectors similarly to the rest of the Moldanubian, but their attitude is too steep to be detected by seismics. Concerning previous precedents, if the shallowly dipping foliations would be present, they should evoke reflections. In turn, the lack of reflections serves as an indirect prove for dominance of steep foliations in the seismically transparent vertical zone throughout the whole crust below granulite massifs. The prevalence of steep fabrics in the exposed granulites together with lack of shallow reflections below the massifs accounts also for such an explanation.

The homogenously distributed reflections in middle crust, designated as MC in Figure 11a, do not reach surface along the 9HR line making their interpretation much harder. Assuming again that they at least partially depict traces of ductile fabrics we can constrain the attitude of corresponding foliations to be horizontal or striking NW-SE with shallow to moderate dip either to the SW or to the NE. Such span of orientations fits only with the attitude of S5 foliation developed penetratively ca 8-15 km to the SW of the seismic line. Here the S5 dips moderately to the NE and D5 parallelized the lithological intercalations with the S5 fabric to provide suitable reflectors. When the front of penetrative S5 is projected along dip to depth, it intersects the vertical plane of seismic section at ~8-15 km below surface, a value comparable with ~3-5s TWT depth of top of the MC reflections. The alternative explanation for the reflections is that they depict deeper continuation of S4 fabric which would loose the anastomosing character and attain parallel subhorizontal attitude. Nevertheless there are two

arguments against this possibility. At first, the S4 on surface exposures in general dips shallowly or moderately to the NW, and also the median line of anastomosing S4-related reflections dips shallowly to the NW instead of lying horizontally. At second, the transition zone between the anastomosing upper crustal reflections and MC mid-crustal ones is defined sharply, which is unexpected in gradual changes in frame of a single fabric. The MC reflections cannot represent a fabric older than S4, because the D3 phase of horizontal shortening lead to penetrative development of steep NE-SW trending fabrics in the whole studied area suggesting that also the deeper crust was reworked to similar steep ductile fabrics.

The lower-crustal reflections S1-S4, that are concentrated in a triangular domain in the NW part of the Moldanubian domain dip moderately to the SE and cut through the MOHO into the uppermost mantle. Such characteristics are best comparable with seismic images of subduction zones, suggesting that the observed seismic structure may represent remnant of a suture zone between an unknown plate and the overlying Moldanubian domain. Such a speculation is just poorly constrained due to the fact that the continuation of the structure in the NW is crosscut by the fault zone separating Moldanubian domain from TBU.

The MOHO reflections (M1-M4) below all the imaged Moldanubian crust are discontinuous and only poorly defined, documenting systematic deepening of MOHO from ~35 km in the NW to ~42 km in the SE. The observed deepening is in agreement with MOHO geometry defined by refraction study of [*Hrubcová, et al.*, 2005] or by passive seismology experiments of [*Plomerová, et al.*, 2003].

7 Gravity modeling and vertical extent of the felsic granulites

Geological unit	DM g/cm³	Note
Syenites	2.760	
Drosendorf unit		
bulk Monotonous group	2.740	
bulk Varied group from the whole Moldanubian	2.750	weighted average
Varied group from the deep borehole S of BLG	2.854	
Varied group in surface exposure S of BLG	2.804	weighted average
Amphibolite from the Varied group	3.043	
LHZ- Varied group	2.740	weighted average
LHZ- Monotonous group	2.685	weighted average
LBZ- Monotonous group	2.767	weighted average
Gföhl unit		
Gföhl felsic gneisses of the Podolsko complex	2.630	
bulk granulite massifs	2.710	approximated by orthogneisses
Felsic granulite from BLG - S2 fabrics	2.635	average
Felsic granulite from BLG - S3 fabrics	2.670	average
Felsic granulite from PG	2.697	weighted average
BLG domain rich in ultrabasites	2.705	
serpentinites from the deep borehole in BLG	2.820	

Table 1. Mineralogical densities used as starting values in 3D gravity modeling.

To decipher information dealing with vertical extents of granulite massifs, we have examined an interpolated grid of Bouguer anomalies provided by Švancara (unpublished) covering majority of the studied region (Figure 12). The area is dominated by large gravity lows related to granitoids of the Moldanubian batolith in the SE or to unknown sources in the centre and NW part of the studied region. Positive anomalies are only of smaller scale and appear in S part of the studied area. The anomalies involved in our gravity model have small areal extent and exhibit high gradients at their edges, implying that all of them are caused by upper-crustal heterogeneities. Removal of regional long-wavelength gravity components caused by deeper heterogeneities is then unnecessary and the original values of Bouguer anomalies have been used for the modeling. For the same reason the model concerns only upper crustal bodies down to 10 km depth.

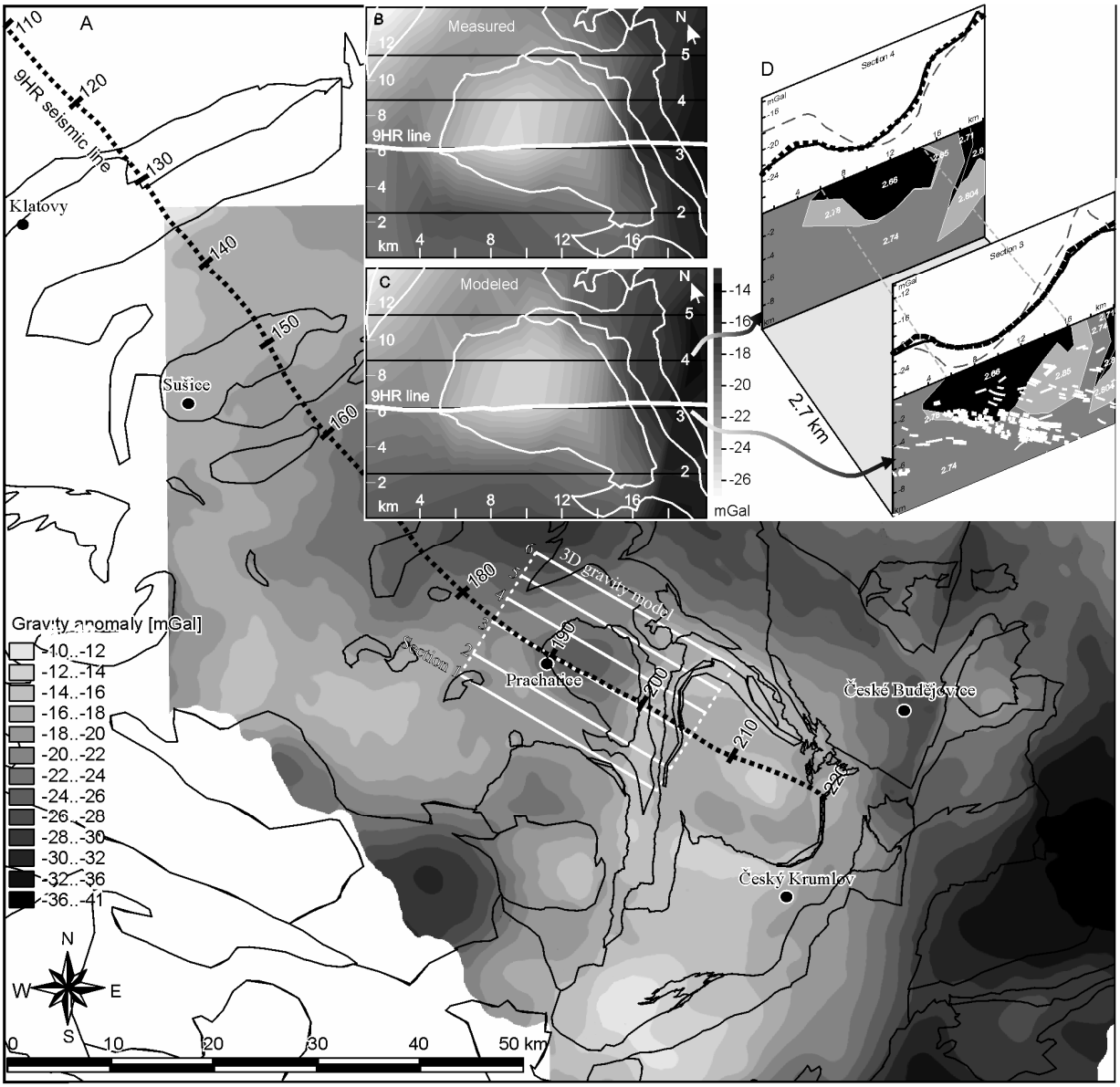

Figure 12. a) Map of Bouguer gravity anomalies with contours of geological units, location of gravity model profiles and 9HR seismic line. b-c) 3D gravity model of the PGM massif, comparison of measured with modeled gravity field. d) Two most significant model sections through the granulite body. Curves above depict the values of Bouguer anomalies measured (thick solid) and modeled in 3D (thin solid). The dashed line shows 2D gravity effect of the individual sections. Plane 3 which coincides with the reflection seismic profile contains line drawing of corresponding reflections. Only first 20 km of the horizontal extent of the profile relevant to the PGM are presented.

We performed a forward gravity modeling in 3D to constrain depth of granulite massifs and their approximate shape. The only body suitable for such approach is the PGM which forms pronounced circular negative anomaly that correlates with the surface extent of the granulite massif. The KGM induces only weak negative anomaly possibly affected by neighboring intrusion of denser durbachites, which makes this body unsuitable for modeling. The BLGM partially correlates with the extent of a positive anomaly, despite the density of felsic granulites is lower than the surrounding metasediments. This paradox may be caused by different bulk composition of the BLGM granulites compared to the PGM and KGM or, more probably, by abundance of ultrabasic bodies inside the BLGM combined with significant

thickness of the underlying dense Varied group. In conclusion, the BLGM with surroundings has too ambiguous lithology and complex geometry to be modeled in 3D.

The modeling was performed in the IGMAS software [*Schmidt and Gotze*, 1999], where the 3D geological bodies are represented by polyhedrons triangulated between manually drawn sections. The situation of the PGM has been approximated in 6 vertical sections 40 km long and 10 km deep, trending NW-SE parallel to the seismic reflection line 9HR (Figure 12). We chose the 3D approach because the PGM with surroundings exhibit a complex non-cylindrical geometry of structures on the scale of our model and circular shape of anomalies which is not suitable for 2D approach.

The model is constrained by surface extent of the geological units and structural data extrapolated to ~1 km depth. The reflection seismic line that crosscuts the PGM in the centre of its negative anomaly helped to constrain deeper levels of the model, where the strongest SE dipping reflection package probably represents interlayered stack of lithologies with different acoustic impedances. Database of corresponding rock densities used in the models (Table 1) comes from *Hanák et al.* [unpublished reports], *Chlupáčová et al.* [unpublished reports] and *Bližkovský et al.* [unpublished reports]. The mineralogical densities served as starting guesses for the modeling, being adjusted when the above mentioned constraints disabled changes of geometry of modeled bodies to fit model effect with measured gravity values. This is a common technique, because rock densities are never constants on larger scale, but they vary in space. This is particularly a problem of the Varied group, which in surface section exhibits significant gradual lithological changes on scale of first kilometers.

The model was designed as simple as possible to avoid ambiguous solutions, but its simplicity causes divergence of measured with modeled gravity at the model edges. Rather than introducing artificial bodies without good geological control on them, we decided to keep a simple model comprising these edge misfits. Most pronounced example represents the positive anomaly at the NW edge of the model, which cannot be related to any geological body at the surface.

The PGM in our model reaches maximum depth of 5.7 km, having a thick lensoidal shape. It cannot extend below the strong reflection package, because this could not arise in lithologically homogenous PGM. It also cannot form thinner lens, because then an unreasonably low density value of felsic granulite would be needed to produce the measured gravity effect. A spectacular detail represents a cusp of high-density varied rocks introduced into the granulite body from below in the hinge region of F3 large fold (e.g. on km 15 in section 3, Figure 12d). Creating this structure is the only reasonable way to produce the observed cranked gravity curves. It is probably structure analogous to a cusp at the SW edge of the BLGM, where a sheet of amphibolites with ultrabasites penetrates deeply inside the granulite massif. Our results differ from the 2D gravity model of the PGM published by [*Vrána and Šrámek*, 1999] who expect rectangular rather than lensoidal shape of the massif, reaching 9 km depth. The discrepancy is caused partially by different rock densities used and partially by a 2D approach. We argue that our model approximates better the reality due to calculation in 3D as well as better structural constraints on the near-surface geology.

8 Magnetic anomalies

The magnetic anomaly map (Figure 13) offers a supplemental and independent tool in unraveling the near-surface geology. Anomalies with high gradients may reflect large-scale faults or dikes, but in case of Moldanubian unit rich in km-scale amphibolite bodies, they often indicate extent of these bodies. In the study area such magnetic anomalies, particularly the positive ones, are often highly elongated, which allows to correlate their preferred

orientation with trends of geological structures. We use such correlation to support our division of the studied area into three regions with contrasting structural pattern.

In the SE in region of granulite massifs the curved geometry of strong magnetic anomalies follows trends of folded S3 or S4 foliations, according to a fabric which is more dominant in particular places. The area NW of granulites exhibits weaker anomalies that trend NE-SW, parallel to the strike of both S3 and S4 in this area. The SW region bears strong anomalies elongated in a NW-SE direction, parallel to the S5 fabric that overprints here older foliations. The transition between the two mentioned perpendicular directions is very abrupt and coincides with the extent of penetrative S5 fabrics mapped out during the fieldwork (Figure 4). In general the trends of small-wavelength magnetic anomalies largely parallel strikes of dominant foliations and help to define their regional trends in badly exposed areas.

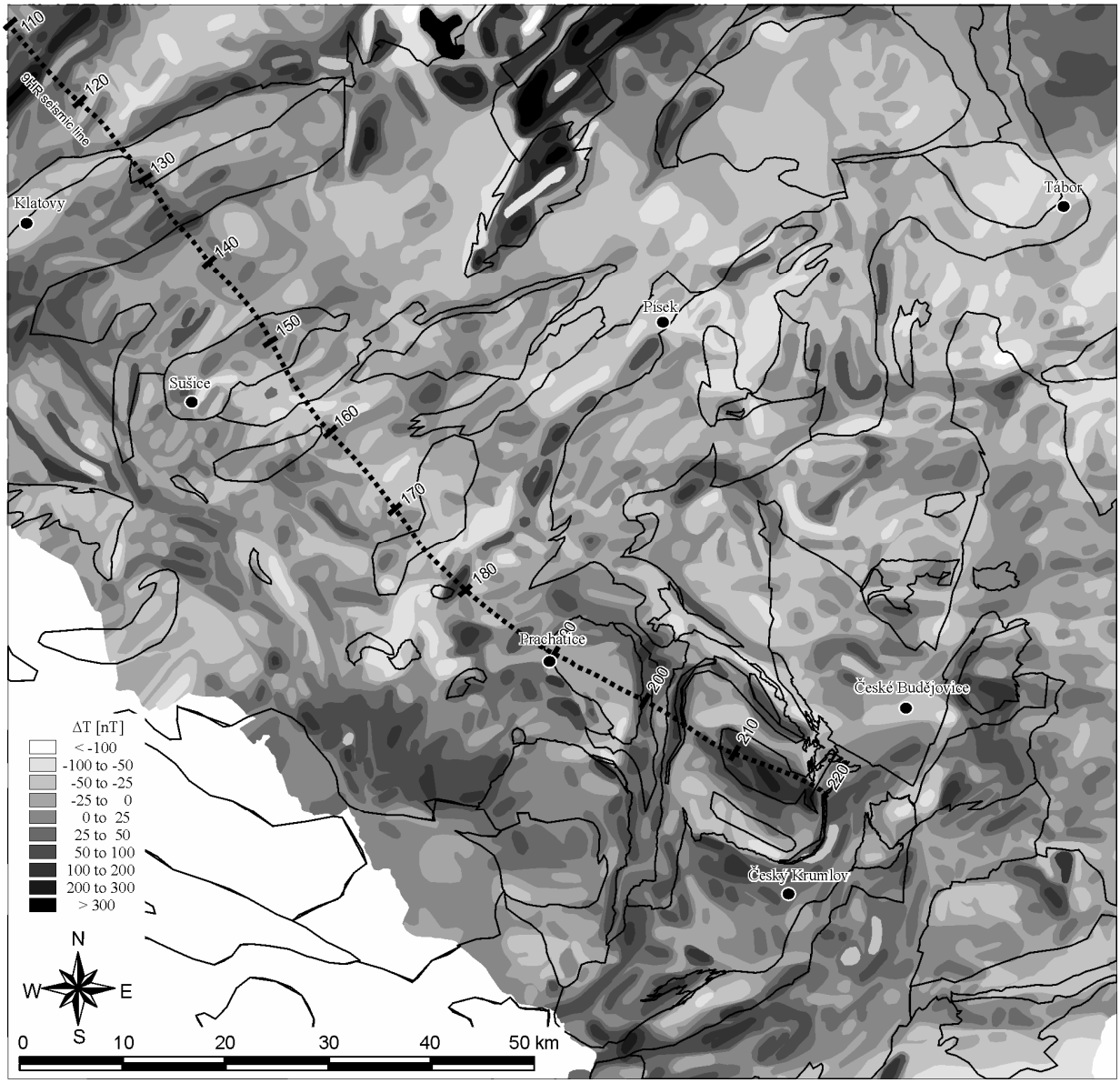

Figure 13. Map of magnetic anomalies, adopted from [*Šalanský*, 1995], with contours of geological units and location of 9HR seismic line.

9 Kinematic and mechanical significance of deformation fabrics

The described structural succession documents an evolution of different levels of orogenic crust during ~ 40 Ma of Upper Paleozoic continental collisions. The patterns of extensively preserved amphibolite facies fabrics D3 – D5 may be directly correlated with conceptual, numerical or analogue models of collisional domains [*England*, 1987; *Jamieson, et al.*, 2002; *Ježek, et al.*, 2002; *Koyi, et al.*, 1999; *Platt*, 1993], while granulite facies fabrics D1 – D2 cannot be interpreted within proposed kinematic framework of Carboniferous subduction and collision (Figure 14).

9.1 D5 vertical cleavage – indentation front

The granulite massifs separate the studied area into two domains with contrasting intensity of the youngest ductile deformation D5. The eastern part of the studied area is characterized by low intensity of D5 deformation marked by spatially heterogeneous development of cleavage zones. In the western part the D5 deformation exhibits systematic decrease of intensity and metamorphic conditions to the NE across ~ 20 km wide irregular deformation front. Towards SE the S5 fabric abruptly terminates along western and southern margins of granulite massifs (Figure 4a, 11). This structural pattern is compatible with a deformation gradient developed in front of rigid indenter moving in NE-SW direction [*England*, 1987; *Ježek, et al.*, 2002]. However, southerly hypothetical continental block responsible for indentation tectonics remains unknown and it is probably hidden below sediments of Alpine foreland basin in Bavaria. The syntectonic emplacement of granitoids associated with regional anatexis along the axis of the indentation zone culminates at ~320 Ma. Therefore, the NE-SW compressive regime is 17 Ma younger than previous Moldanubian deformation events that also developed in different kinematic framework. We suggest that the distinct orientation and timing of this event has to be considered as a late, isolated episode at the end of the Variscan collision in the frame of the Bohemian Massif and European Variscides in general.

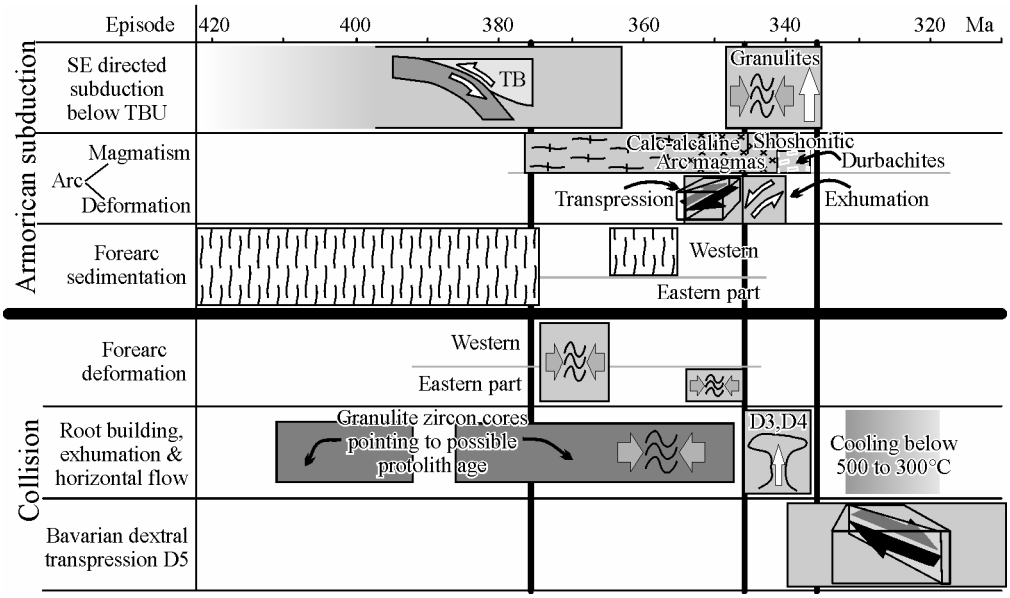

Figure 14. Interpretative geochronological sketch of Variscan evolution in the Bohemian Massif that is related to the studied region.

9.2 D4 subsurface horizontal flow – lateral spreading of orogenic crust

The structural analysis of S4 fabric exhibits good correlation between surface geometry and orientations of subsurface seismic reflections especially in the NW part of the studied area (Figure 11b) implying that S4 extends at least ca 10 km below surface along the seismic line. Based on relation between surface fabric trajectories and anastomosing pattern of seismic reflections in the vertical section, the large-scale geometry could be interpreted as a set of 10-20 km wide pinch and swell structures with subhorizontal NE-SW axes and shallowly NW dipping median planes. L4 stretching lineations, when developed, plunge sub-parallel to these NE-SW axes and parallel to intersection of S4 and subvertical NE-SW trending S3 fabrics.

The D4 fabric is characterized by important deformation and metamorphic gradient from west to the east. The degree of D4 fabric intensity systematically increases from east to west towards the CBPC. Here, the deformation culminates by highly non-coaxial shearing manifested by several kilometers wide shear zone associated with emplacement of Mg rich syenites and late shoshonitic intrusions [*Žák, et al.*, 2005a] dated at ~342 - 337 Ma. In the hanging-wall, at the Moldanubian – Teplá-Barrandian boundary, the D4 imprint rapidly ceases documenting lower-grade block sank between the two contrasting terranes. Going to the east, the D4 deformation intensity gradually decreases so that only westernmost margin of granulites shows relatively strong reworking by flat S4 fabrics at amphibolite facies conditions. The D4 deformation is vanishing quickly to the east so that the central part of granulites is unaffected by this deformation event and the D4 is relatively weakly expressed in the east medium grade schists (the Kaplice Unit).

Classically, this deformation pattern can be interpreted as a result of large scale detachment zone along which the supra-crustal Teplá-Barrandian Unit slid down to the west [*Pitra, et al.*, 1999]. The amount of vertical movement is estimated to about 12 km, which is consistent with thickness of the Teplá-Barrandian upper crust estimated on the basis of the 9HR seismic line. The western part of detachment zone characterized by almost complete reworking of previous steep S3 fabric is compatible with several models emphasizing the horizontal flow in thickened orogens [*Koyi, et al.*, 1999; *Ring and Brandon*, 1999]. It has been shown in diagrams of S4 dip, L4 lineation intensity and degree of D4 reworking (Figure 5c,d and 8) that the granulite bodies represent low strain domains preserved from large scale D4 subhorizontal overprint. These maps show that rheologically weaker host schists of Monotonous and Varied groups show structural pattern consistent with viscous flow around rigid ellipsoidal objects. This phenomenon is exemplified by S4 dip angle distribution in the PGM, which shows flat attitude in the central part of the granulite body that is interpreted as an apical part of the boudin and steeper fabrics at margins of this body interpreted as neck zones. The size of dip perturbation in the vicinity of the PGM (~2 km) and estimated 5km thickness of the granulite derived from seismics and gravity modeling are in good agreement with theoretically derived width of deflection zones around rigid ellipsoidal objects [*Ježek, et al.*, 2002; *Kidan and Cosgrove*, 1996]. In conclusion, the D4 fabric corresponds to zone of vertical shortening which is coaxial in the most of studied area with exception of highly non-coaxial narrow zone at the Moldanubian - CBPC margin in the NW.

There are two major types of kinematical models which account for such an intensive vertical shortening in central parts of orogenic root systems: 1) ductile thinning of continental accretionary wedges, where the horizontal flow originates due to so called thinning flow underneath rigid lid. 2) Horizontal flow generated by the eduction of orogenic root following advective removal of dense eclogitic lower crust and mantle lithosphere [*Andersen, et al.*, 1993; *Dewey, et al.*, 1993] or gravity rebound of thickened orogenic roots [*Koyi, et al.*, 1999; *Milnes and Koyi*, 2000; *Rey, et al.*, 2001]. We can exclude the common model of orogenic collapse [*Lister and Davis*, 1989; *Wernicke*, 1981] driven by far field extension stresses

because of lack of extensional structures in the hanging wall Teplá-Barrandian unit above the major detachment zone.

The amount of exhumation related to this event is relatively limited because of pre-D4 juxtaposition of HP granulites with Varied group metasediments that experienced only MP peak metamorphic conditions [*Racek, et al.*, 2006]. This means, that unlike in other orogenic root systems, the HP boudins do not represent relics of HP metamorphism in completely retrogressed matrix of originally coherent HP unit as shown in Caledonides by e.g. [*Dewey, et al.*, 1993; *Krabbendam and Dewey*, 1998] where HP rocks are exhumed by extensional/transtensional event. In contrast, in the Bohemian Massif the horizontal flow is responsible for relatively small amount of vertical exhumation from 0.7 – 0.8 GPa of peak metamorphic conditions within Varied group rocks to 0.3 – 0.4 GPa reflected by HT-LP metamorphism related to intrusion of post-tectonic granites. Existing geochronological data from granulites and syntectonic granitoids indicate that the horizontal mid-crustal flow occurred in relatively short time scale of the ~342 – 337 Ma.

9.3 D3 horizontal shortening and development of regional vertical fabric – juxtaposition of granulites and middle crust

The S3 fabric shows constant attitude in both Varied and Monotonous groups, in the NW part of studied area close to the boundary between the Moldanubian and Teplá-Barrandian domains and in the SE extremity of the described area. This fabric always steeply dips to the NW and it is more or less uniformly distributed in form of relics throughout the studied area indicating that the D3 affected pervasively weak, partially molten middle crust under amphibolite facies conditions.

In contrast to middle-crustal units, the distribution of S3 foliations in granulite bodies shows important variations, which can be interpreted as a result of large scale folding of granulite sheets [*Franěk, et al.*, 2006]. The distribution of S3 fabrics in all three granulite massifs implies vertical N-S trending axial planes of large scale folds. Important question arises, as whether the folded amphibolite facies foliations in granulites correspond genetically to S3 fabrics in mid-crustal host rocks that exhibit constant NE-SW trend. If the folding of amphibolite-facies fabrics represents an event of regional scale due to application of E-W far field shortening than weaker metasediments would be entirely reworked into new metamorphic fabric of N-S direction. Alternatively, if the S3 fabrics represent a finite strain orientation than the axial planes of folded granulites represent intermediate stage of fabric transposition in low strain domain, providing D3 deformation is non-coaxial dextral shear. We suggest, that the second model is more likely and that the whole region was affected by crustal scale dextral shearing which is responsible for development of steep NE-SW trending amphibolite facies fabric in both middle and lower crustal units. Because the granulite bodies were more competent than surrounding metasediments they were buckled producing asymmetrical folds with axial plane close to maximum flattening plane of instantaneous strain.

Another problem is the original attitude of S3 fabrics within granulites and architecture of granulite massifs before folding. When the Z-shaped BLGM, symmetrical KGM and V-shaped PGM are unfolded to the original NE-SW strike, than the S3 generally dips to the W in the BLGM, subvertically in the KGM and to the E in the PGM. Such spatial variations in dip of S3 fabric may be interpreted as a ~20 km wide positive vertical fan-like structure (Figure 15d). Additionally the distribution of serpentinite stripes inside the BLGM accompanied sometimes by Varied group metasediments was interpreted by [*Franěk, et al.*, 2006] as a result of isoclinal folding of granulite sheets and host rocks accompanied by imbrications during D3. This detailed observation is consistent with overall isoclinal folding of lower and middle crustal units during D3.

Unfolding of granulite massifs allows us to interpret the kinematic significance of D3 deformation in the regional scale. Regional distribution of HP granulites along NE-SW trending positive fan as well as the eclogite belt along Varied and Monotonous group boundary can be interpreted as a central part of elevated lower crust. In general, the belt of granulites and eclogites can be seen as a core of crustal scale vertical extrusion of orogenic lower crust over medium grade rocks to the east and to the west. The fan like structure is more or less symmetrical with well preserved extrusion related features to the east, whilst in the west the original thrust related structures between granulites and monotonous group are obliterated by D4 horizontal flow. The existence of fan like geometry of HP rocks can be regarded as the beginning of ductile thinning process progressively developing into D4 horizontal flow. The D3 vertical fabric is geometrically and kinematically consistent with the fabrics that are developed in the magmatic arc plutons (the CBPC) as well as in the supracrustal Teplá-Barrandian domain. The vertical NE-SW trending fabrics preserved in slates and volcanics of Neo-Proterozoic rocks as well as in syntectonic calc-alkaline (~350 Ma) and shoshonitic (~340 Ma) intrusions are consistent with dextral transpression [*Žák, et al.*, 2005a; *Žák, et al.*, 2005b]. In conclusion, the D3 deformation reflects mechanical coupling between both upper and middle crustal levels, while the D4 deformation is responsible for decoupling of Neo-Proterozoic upper-crustal lid from the middle crust.

The distribution of structural fabrics and metamorphic rocks related to D3 deformation reflects major exhumation event of HP rocks from granulite-amphibolite facies boundary up to the depth level of ~0.7 GPa. The exhumation path is reflected by seismic structure underneath the granulite – eclogite belt indicating possible existence of steep fabrics down to Moho. This means, that present structure of the crust preserve the geometry of extrusion channel related to flow of HP rocks from the crustal bottom. Existence of granulite steep structures in the depth is indirectly supported by gravity modeling suggesting significant thickness of dismembered individual granulite bodies around 5 km (Figure 12d).

9.4 Tectonic significance of granulite facies fabrics

The granulite facies S1-S2 fabrics described by [*Franěk, et al.*, 2006] represent a unique example of earliest lower crustal fabrics in the frame of the Bohemian Massif. The field and microstructural observations indicate that the S1 fabric originated during a magmatic event associated with granulite-facies deformation. This concept is supported by several recent petrological and geochemical studies [*Janoušek, et al.*, 2006; *Štípská and Powell*, 2005]. Syntectonic decompressional features indicate that the S2 fabric originated during exhumational part of metamorphic path. Despite poorly preserved structural record the fabrics provide information about deformation mechanisms and general characteristics of early stages of lower crustal ascent. These fabrics may be studied in a relic elliptical domain located in the southern part of the BLGM.

The discordant relationship between S2 granulitic fabric and S3 foliations is the most important observation from South Bohemian granulites. [*Franěk, et al.*, 2006] made an attempt to restore the original position of S2 fabric and they found that it could have been a cylindrical dome dipping steeply to the NE. However, the primary orientation of this fabric is highly speculative because of complex reworking during D3 ascent, folding and subsequent reworking by D4 subhorizontal flow. Despite the general lack of information, it is evident that the HP granulites show early deformations which are not shared neither by middle nor the upper crustal structural record. Therefore, there is a possibility that this kind of granulite facies mylonitization occurred in geographically remote position and probably also in different time compared to Lower Carboniferous structural D3 – D5 history. Zircon ages suggesting the ~340 Ma age of both the granulite-facies metamorphism and amphibolite-

facies retrogression may point to the onset of D3 episode rather than to timing of the D2 event.

10 Discussion – tectonic model

10.1 Devonian subduction

There is a following line of arguments that the D1-D2 fabrics discordant to overall NE-SW Moldanubian trend originated during independent tectonic regime in Devonian times: 1) relics of mid-Devonian oceanic subduction zone occur in hangingwall of main continental Saxothuringian subduction zone [*Konopásek and Schulmann*, 2005] 2) Devonian felsic granulites with granulite facies banding are reported from several places of the Bohemian Massif (e.g. Sowie Gory, [*O'Brien, et al.*, 1997]) and more importantly Lu-Hf dating of garnets within granulites with Carboniferous zircon ages reveals mid-Devonian age of their origin [*Anczkiewicz, et al.*, 2007]. Additionally there is a range of zircon U-Pb and Pb-Pb ages from granulites which reveal Devonian ages and which are interpreted to correspond to parent rock crystallization [*Schulmann, et al.*, 2005; *Wendt, et al.*, 1994].

Based on these indications, it can be suggested that the granulite facies rocks originated already during subduction event prior to Carboniferous collision, possibly in relation to early arc history. This model is strongly advocated by [*Gerya and Stockhert*, 2006] who proposed an origin of HP granulites in a lithosphere-scale subduction wedge. In this model the continental rocks scraped from upper lithospheric plate are dragged to depths corresponding to 2.0 – 2.5 GPa and accreted to the base of the hanging wall crust by a return flow (Figure 15a). It is likely, that rocks which passed through such a polyphase tectonic evolution can also reveal complex metamorphic history [*Štípská and Powell*, 2005] and fabrics documenting large displacements similar to the mylonitic S2. In this scenario, the granulite facies rocks can show completely discordant deformation pattern with regards to subsequent continental Saxothuringian subduction culminating in the Carboniferous collisional event. This model can explain the Devonian ages more and more often reported by the Sm-Nd and Lu-Hf studies from granulite and eclogite garnets [*Anczkiewicz, et al.*, 2007; *Beard, et al.*, 1992; *Brueckner, et al.*, 1991] because it supposes a residence of granulites at the Moho, from where the rocks would be exhumed during Carboniferous collisional event. We presume that during the D2 granulites have been vertically transported from the peak 1.8-2.0 to ~1.5 GPa, because the following D3 commenced still at granulite facies conditions (Figure 3).

10.2 Carboniferous continental subduction

The S3 with S4 foliations strike sub-parallel to the two main sutures in the Bohemian Massif – the Saxothuringian subduction zone in the NW and the Moldanubian-Brunia boundary in the SE (Figure 1b). Such a coincidence indicates that at least one of these collisional zones generated horizontal stress inducing the D3 + D4 events. Geochronological arguments ([e.g., *Schmadicke, et al.*, 1995], Figure 2) indicate activity of the Saxothuringian continental subduction and collision between ~360 and 335 Ma, a time range contemporaneous with the radiometric ages of Moldanubian deformations. The easterly Brunia margin documents prolonged thrusting from ~330 to 300 Ma [e.g., *Mazur, et al.*, 2006], which is too young to cause the above mentioned Moldanubian shortening, but we cannot exclude existence of a hypothetic continental block bounding the back-arc Moldanubian domain from the east before its juxtaposition to the present Brunia microplate.

The S3 steep fabrics are observed through all the crustal levels, from upper crust at the eastern margin of the TBU through mid-crustal migmatites of Monotonous and Varied groups to the lower crustal Gföhl unit. Their spatial abundance (Figure 5) and vertical extent (Figure

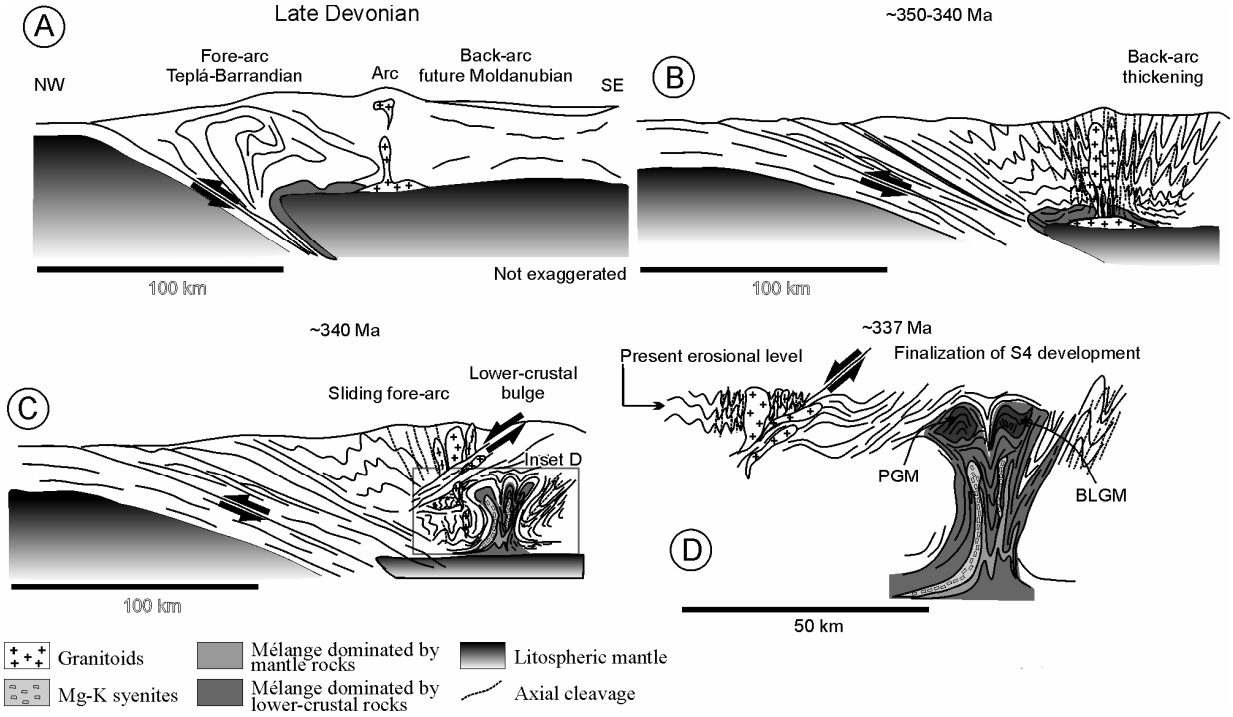

Figure 15. Geotectonic model of granulite lower-crustal exhumation with subsequent stacking and subhorizontal mid-crustal flow depicted along a 2D NW-SE lithospheric-scale profile. a) Late Devonian SE directed subduction leading to intermixing of distinct crustal levels according to numerical models of [*Gerya and Stockhert*, 2006]. b) Early Carboniferous subduction stage with intensive arc magmatism and shortening in the arc and back-arc domain. c) Prolonged shortening leads to extrusion of the lower crustal rocks from below the arc region, while the forearc block slides to the NW from the amplifying extrusion. d) Detail of the c) stage focused to our study area in the arc surroundings. D5 effect is not depicted.

11a) suggest homogeneous development of the steep foliation throughout all the arc and back-arc domains in a NW-SE transpressional regime. The S3 is developed only at the eastern edge of the TBU [e.g., *Žák, et al.*, 2005a] suggesting that the fore-arc upper crust behaved as a stiff block during the D3. The arc crust weakened by heating and intrusion of granitoid magmas presumably localized the strike-slip component of the horizontal transpression, while the back-arc region deformed by more or less coaxial shortening. The strain localization below the magmatic arc was responsible for the unusually massive amplification of F3 folds in the lower crust that resulted in localized exhumation of the deep-seated granulites to mid-crustal levels (Figure 15 b,c,d) in form of a ~20 - 30 km wide ductile isoclinal subvertical fan-like structure. Geometry and extent of this structure is inferred from detailed structural analysis of the generally NW dipping S3 fabrics preserved in the metasedimentary units and in the granulites (Figure 4, 5a), large extent of vertical low-reflectivity region depicting presumably steep fabrics across the whole crustal profile (Figure 11a) and significant depth extent of PGM estimated by gravity modeling (Figure 12b-d). Surrounding mid-crustal units would be in this case forced to develop neighboring marginal synclines to balance the voluminous vertical mass transfer through the ductile crust (Figure 15c,d), dragging the upper crustal Paleozoic varied sequences to the mid-crustal depths. The proposed rapid amplification of steep ascent channel due to horizontal compression offers an efficient exhumation mechanism for lower-crustal rocks as shown e.g. by [*Kisters, et al.*, 1996] on km scale steep folds in high-grade gneisses or by [*Štípská, et al.*, 2004a] on Variscan granulites in the NE part of the Bohemian Massif. Moreover the ascent was in our case enhanced by lubrication by Mg-K syenites that often intrude the granulite massif boundaries [*Janoušek and Holub*, 2007] and by

leucogranitic partial melts from surrounding metasediments [*Franěk, et al.*, 2006; *Kodym*, 1972].

The D4 vertical shortening follows immediately the D3 ascent, being localized at the margin of upper crustal TBU block (Figure 15c,d). Here it was lubricated by the late arc-related magmas and syenites and attained characteristics of a normal shear zone with dip-slip lineations [*Žák, et al.*, 2005a]. The TBU upper crust slid along this zone to the NW from the mid- and lower-crustal D3 bulge described above. It passively transported to the NW the S3 fabrics developed originally above the Moldanubian middle crust. The sliding was a subsurface expression of gravitational spreading of the roof of the crustal-scale bulge, being driven by the bulge amplification. The pervasive subhorizontal S4 distributed homogeneously in the western part of the studied area represents a mid-crustal expression of the same process. Here it resulted into significant spreading of the granulite bulge to the NW, while less intensive development of S4 fabric in the SE documents an asymmetric nature of this process.

Felsic granulites comparable to our rocks are exhumed around the 340 Ma event also at the eastern margin of Moldanubian domain and along the Saxothuringian suture zone. The D3-D4 mid-crustal evolution of the Moldanubian mélange in the studied southern Bohemia appears very similar to the structural scenario described by many authors from the eastern margin of Moldanubian where the high-grade rocks overthrust the Brunia continental margin [e.g., *Racek, et al.*, 2006; *Schulmann, et al.*, 2005; *Štípská, et al.*, 2004a; *Tajčmanová, et al.*, 2006]. The S3 can be correlated to the steep amphibolite-facies fabrics commonly present in relicts along the E margin of Moldanubian, which are interpreted to represent a fabric that achieved exhumation of the high-grade Gföhl rocks to mid-crustal levels. The S4 is comparable in extent, petrology and geometry to the shallowly dipping fabrics dominating the eastern Moldanubian [e.g., *Racek, et al.*, 2006]. The granulite exhumation in the Southern Bohemia is temporally related also to the granulite ascent along the Saxothuringian subduction zone in form of a narrow channel flow [*Konopásek and Schulmann*, 2005] which reveal the same age as the felsic granulites examined in this work (Figure 2). In both these cases exhumation is localized along a suture between two different continental microplates, which invokes ascent mechanisms different from our case. Nevertheless the proposed correlation allows to extend our interpretations to the whole southern part of Moldanubian and compare the fabric orientations to other terranes of the Bohemian Massif.

10.3 Strain switching during the single orogeny

The presented structural interpretations document two sudden changes in principal shortening direction, both being recorded in the weak partially molten crust of the Variscan root. The older switch from the NW-SE striking S_2 to the NE-SW trending S_3 shows 60-70° angular difference between strikes of these steep fabrics. The S_3 then strikes sub-parallel to the S_4, while another transition from NE-SW S_4 to NW-SE trending S_5 cleavage indicates the younger change of similar magnitude 70-80°. Based on radiometric data the first change is just poorly constrained by a minimum age of ~340 Ma, while the younger took place between ~337 and ~330 Ma.

Particularly the younger switch, recorded on a scale of the whole studied region, documents complexity of the Variscan collisional environment, and can be compared to sudden changes in shortening directions in other orogenic domains like the Alps [e.g., *Ceriani and Schmid*, 2004; *Peresson and Decker*, 1997]. Such changes in principal shortening point to common occurrence of switches in far-field driving forces which make modeling of the whole orogenies a true 3D problem that cannot be convincingly simulated in 2D using either analogue or numerical methods. We argue that application of 2D models [e.g., *Beaumont, et al.*, 2006; *Gerya and Stockhert*, 2006] should be confined to the individual stages of orogenic

processes, but the finite architecture of whole collisional zones can be simulated only by a 3D approach.

10.4 Comparison of the described evolution with other orogenic domains and numerical models of continental collisions

The results of our detailed study of Variscan middle and lower crust allow to estimate processes operating at these levels in present collisional domains. Many of collisional orogens show rather low thermal budget compared to the Variscan case, but we can still find well-studied "hot" domains which behaved presumably similar to the Variscan example. From these the Andean and Himalayan-Tibetan systems are the most famous, both of them representing a geotectonic setting common to Variscan orogen in Bohemian Massif, where the continental crust is thickened between subduction zone and rigid foreland.

The most pronounced feature of the Moldanubian, the thick domain of flat lying S_4 fabrics exhibiting syntectonic partial melting, can be correlated to subhorizontal mid-crustal layers detected in both the recent orogenic domains. Laterally extensive and thick mid-crustal layers of partially molten rocks have been imaged by seismic studies, being interpreted as attachment zones separating upper crustal semi-brittle deformations from ductile thickening in the lower crust. In the Andes this mid-crustal zone reaches thickness of 10-20 km [e.g., *Yuan, et al.*, 2000] occurring below the Altiplano and Puna plateaus and dipping shallowly against the subduction zone. The low velocity zone under Tibetan plateau is characterized by similar depth, thickness and lateral extent [e.g., *Kind, et al.*, 1996; *Nelson, et al.*, 1996].

Another fabrics analogous to S4 are reported e.g. from the upper Paleozoic Appalachian orogen in eastern USA [*Hatcher Jr and Merschat*, 2006] where they are in contrast ascribed to orogen-parallel tectonically forced channel flow in the mid-crustal partially molten rocks. Such process has been already for a decade numerically modeled by [*Beaumont, et al.*, 2001; *Beaumont, et al.*, 2004; *Beaumont, et al.*, 2006]. Their last models dealing with rheological heterogeneities in the thickened lower crust in a collisional setting resemble in a first approximation also our Moldanubian case.

PT conditions of S4 development of ~700-800 °C / 0.5-0.8 GPa resemble the conditions suggested for the recent mid-crustal attachment zones and shallow dip against subduction zone revealed by reflection seismics below Andes is comparable to the S4 attitude with respect to the Saxothuringian subduction. The flat S4 may represent structures developed in a sort of attachment zone separating ductile exhuming lower crust from the hypothetic upper crustal lid covering the Moldanubian domain during D3 and D4. The geometry and kinematical analysis of S4 then point to deformation mode operating at the boundary between brittle upper- and weak lower crust. The S4 exhibits too heterogeneous distribution to account for a channel flow processes during D4 in a sense of [*Beaumont, et al.*, 2006] mentioned above.

Regardless the nature of flat S_4 fabric, the relict S3 documents previous thickening, exhumation and imbrication of the partially molten middle and lower crust and S2 marks rapid exhumation of portions of orogenic root into shallower levels. Such multistage mixing of material from different crustal levels below brittle-ductile transition may well characterize processes operating in the lower crust below present-day plateau regions. The low viscosity of felsic granulites constituting significant portion of the base of Variscan thickened crust implies effective decoupling between crustal and mantle deformations.

11 Conclusions

- Structural evolution of the south Bohemian granulites reveals complexity not seen in eastern part of the Moldanubian domain. The granulites were exhumed along two distinct fabrics, the S_2 and S_3, instead of a single foliation known from the eastern Moldanubian.
- The steep and moderately dipping amphibolite-facies foliations S_3 and S_4 prevailing in the studied region are comparable in extent, petrology and geometry to the fabrics dominating the eastern margin of the Moldanubian domain, ca 130 km to the E.
- The gravimetry with structural geology indicates that the exposed south Bohemian granulites reach several km depth. Reflection seismics additionally depicts region of probable steep fabrics through the whole crust below granulites, which is interpreted as a possible continuation of the granulite-dominated mélange. The vertical region of low reflectivity represents then trace of the deformed granulite D3 crustal-scale ascent channel.
- Partially molten lower crust dominated by felsic granulites was incorporated into the middle levels in form of a D3 syn-compressional crustal-scale bulge. Once emplaced it deformed coherently with the surrounding middle crust. Such a new mechanism can explain presence of relatively small portions (X000 km^3) of HP HT rocks inside much shallower units in the internal parts of orogens.
- The subhorizontal S4 fabric immediately reworked S3, being induced by gravitational spreading of the amplified bulge. The S4 achieved sliding of the TBU upper crust to the NW from the bulge region and ductile thinning of the mid-crustal level in the Moldanubian domain.
- The restored older S2 as well as the youngest S_5 fabrics strike sub-perpendicularly to the NE-SW orogen trend marked by prevailing S3 and S4 foliations. The S2 marks a distinct older tectonic episode possibly related to Devonian subduction, when the felsic granulites were partially exhumed in frame of the lower crust. The development of S5 results from overlapping of two almost perpendicular deformational zones, Saxothuringian with Bavarian. The observed variations of principal shortening orientation ~ 70° exhibit magnitude similar to present orogenic areas, e.g. the Alps.
- Double switching of principal shortening direction during the Variscan collisional history points out complex architecture of natural orogens and restricts usage of numerical or analogue 2D models only to individual stages of an orogeny.

12 References

Aftalion, M., et al. (1989), Early Carboniferous U-Pb Zircon Age for Garnetiferous, Perpotassic Granulites, Blanský Les Massif, Czechoslovakia, *Neues Jahrb. Mineral.-Mon.hefte*, 145-152.

Aleksandrowski, P., et al. (1997), Kinematic data on major Variscan strike-slip faults and shear zones in the Polish Sudetes, northeast Bohemian Massif, *Geological Magazine*, *134*, 727-739.

Anczkiewicz, R., et al. (2007), Lu-Hf geochronology and trace element distribution in garnet: Implications for uplift and exhumation of ultra-high pressure granulites in the Sudetes, SW Poland, *Lithos*, *95*, 363-380.

Andersen, T. B., et al. (1993), Subduction and eduction of continental crust: Major mechanisms during continent-continent collision and orogenic extensional collapse, a model based on the south Norwegian Caledonides, *TERRA NOVA*, *3*, 303-310.

Babuška, V., and J. Plomerová (2001), Subcrustal lithosphere around the saxothuringian-Moldanubian Suture Zone - A model derived from anisotroy of seismic wave velocities, *Tectonophysics*, *332*, 185-199.
Beard, B. L., et al. (1992), Petrogenesis of Variscan high-temperature group A eclogites from the Moldanubian Zone of the Bohemian Massif, Czechoslovakia, *Contributions to Mineralogy and Petrology*, *111*, 468-483.
Beaumont, C., et al. (2001), Himalayan tectonics explained by extrusion of a low-viscosity crustal channel coupled to focused surface denudation, *Nature*, *414*, 738-742.
Beaumont, C., et al. (2004), Crustal channel flows: 1. Numerical models with applications to the tectonics of the Himalayan-Tibetan orogen, *Journal of Geophysical Research B: Solid Earth*, *109*.
Beaumont, C., et al. (2006), Crustal flow modes in large hot orogens, in *Geological Society Special Publication*, edited, pp. 91-145.
Behr, H. J. (1961), *Beitrage zur petrographischen und tektonischen Analyse des sachsischen Granulitgebirges*.
Behrmann, J. H., and D. C. Tanner (1997), Carboniferous tectonics of the Variscan basement collage in eastern Bavaria and western Bohemia, *Geologische Rundschau*, *86*, S15-S27.
Brueckner, H. K., et al. (1991), Nd and Sr age and isotope patterns from Variscan eclogites of the eastern Bohemian Massif, *Neues Jahrbuch für Mineralogie Abhandlungen*, *163*, 169-196.
Burg, J. P., and Y. Podladchikov (1999), Lithospheric scale folding: Numerical modelling and application to the Himalayan syntaxes, *Int. J. Earth Sci.*, *88*, 190-200.
Carswell, D. A., and P. J. O´Brien (1993), Thermobarometry and Geotectonic Significance of High-Pressure Granulites - Examples From the Moldanubian Zone of the Bohemian Massif in Lower Austria, *Journal of Petrology*, *34*, 427-459.
Ceriani, S., and S. M. Schmid (2004), From N-S collision to WNW-directed post-collisional thrusting and folding: Structural study of the Frontal Penninic Units in Savoie (Western Alps, France), *Eclogae Geologicae Helvetiae*, *97*, 347-369.
Cooke, R. A., et al. (2000), Garnet zoning and the identification of equilibrium mineral compositions in high-pressure-temperature granulites from the Moldanubian Zone, Austria, *Journal of Metamorphic Geology*, *18*, 551-569.
Čížek, P., and Č. Tomek (1991), Large-scale thin-skinned tectonics in the eastern boundary of the Bohemian Massif, *Tectonics*, *10*, 273-286.
de Sigoyer, J., et al. (2004), Exhumation of the ultrahigh-pressure Tso Morari unit in eastern Ladakh (NW Himalaya): A case study, *Tectonics*, *23*.
Dewey, J. F., et al. (1993), Orogenic uplift and collapse, crustal thickness, fabrics and metamorphic phase changes; the role of eclogites, in *Magmatic processes and plate tectonics.*, edited by H. M. Prichard, et al., pp. 325-343, Geological Society of London, London, United Kingdom.
Dorr, W., et al. (1998), U-Pb zircon ages and structural development of metagranitoids of the Tepla crystalline complex: evidence for pervasive Cambrian plutonism within the Bohemian massif (Czech Republic), *Geologische Rundschau*, *87*, 135-149.
Dudek, A. (1980), The crystalline basement block of the Outer Carpathians in Moravia, *Rozpravy Československé Akademie Věd*, *90*, 1-85.
Edel, J. B., et al. (2003), Anticlockwise and clockwise rotations of the Eastern Variscides accommodated by dextral lithospheric wrenching: palaeomagnetic and structural evidence, *J. Geol. Soc.*, *160*, 209-218.
Edel, J. B., and K. Weber (1995), Cadomian terranes, wrench faulting and thrusting in the central Europe Variscides: geophysical and geological evidence, *Geologische Rundschau*, *84*, 412-432.

England, P. C. (1987), Diffuse Continental Deformation - Length Scales, Rates and Metamorphic Evolution, *Philos. Trans. R. Soc. Lond. Ser. A-Math. Phys. Eng. Sci.*, *321*, 3-22.
Faryad, S. W., et al. (2006), P-T evolution and reaction textures in retrogressed eclogites from Světlík, the Moldanubian Zone (Czech Republic), *Mineral. Petrol.*, *88*, 297-319.
Fiala, J., et al. (1987), Moldanubian granulites: source material and petrogenetic considerations, *Neues Jahrbuch fur Mineralogie, Abhandlungen*, *157*, 133-165.
Finger, F., and H. P. Steyer (1995), A tectonic model for the eastern Variscides: indications from a chemical study of amphibolites in the south-eastern Bohemian Massif, Austria, *Geologica Carpathica*, *46*, 1-14.
Franěk, J., et al. (2006), Kinematic and rheological model of exhumation of high pressure granulites in the Variscan orogenic root: Example of the Blanský les granulite, Bohemian Massif, Czech Republic, *Mineral. Petrol.*, *86*, 253-276.
Franěk, J., et al. (in prep.), The precursor of Variscan felsic granulites, process of its granulitization, and inversed rheology of feldspars and quartz in the lower-crustal conditions.
Franke, W. (2000), The mid-European segment of the Variscides: Tectonostratigraphic units, terrane boundaries and plate tectonic evolution, *Geological Society Special Publication*, 35-56.
Friedl, G., et al. (2003), U-Pb shrimp dating and trace element investigations on multiple zoned zircons from a South-Bohemian granulite, *Journal of the Czech Geological Society*, *48*, 51.
Fuchs, G. (1976), Zur Entwicklung der Böhmischen Masse, *Jahrbuch des Geologischen Bundesanstalts*, *119*, 45-61.
Fuchs, G. (1986), Zur Diskussion um den Deckenbau der Böhmischen Masse, *Jb Geol B-A 129*, 41–49.
Gebauer, D., et al. (1989), The development of the Central European continental crust since the Early Archaean based on conventional and ion-microprobe dating of up to 3.84 b.y. old detrital zircons, *Tectonophysics*, *157*, 81-96.
Gerya, T., and B. Stockhert (2006), Two-dimensional numerical modeling of tectonic and metamorphic histories at active continental margins, *Int. J. Earth Sci.*, *95*, 250-274.
Hartley, A. J., and J. Otava (2001), Sediment provenance and dispersal in a deep marine foreland basin: The Lower Carboniferous Culm Basin, Czech Republic, *J. Geol. Soc.*, *158*, 137-150.
Hatcher Jr, R. D., and A. J. Merschat (2006), The Appalachian Inner Piedmont: An exhumed strike-parallel, tectonically forced orogenic channel, in *Geological Society Special Publication*, edited, pp. 517-541.
Hodges, K. V., et al. (2001), Southward extrusion of Tibetan crust and its effect on Himalayan tectonics, *Tectonics*, *20*, 799-809.
Hrouda, F. (1993), Variscan Magnetic Fabric Overprinting in Sedimentary and Crystalline Thrust Sheets in the NE Bohemian Massif, *Tectonics*, *12*, 507-518.
Hrubcová, P., et al. (2005), Crustal and uppermost mantle structure of the Bohemian Massif based on CELEBRATION 2000 data, *Journal of Geophysical Research B: Solid Earth*, *110*, 1-21.
Chemenda, A. I., et al. (1995), A mechanism for syn-collisional rock exhumation and associated normal faulting: Results from physical modelling., *Earth and Planetary Science Letters*, *132*, 225-232.
Chlupáč, I. (1994), Facies and biogeographic relationships in Devonian of the Bohemian Massif, *Courier Forschungsinstitut Senckenberg*, *169*, 299-317.

Jamieson, R. A., et al. (2002), Interaction of metamorphism, deformation and exhumation in large convergent orogens, *Journal of Metamorphic Geology*, *20*, 9-24.
Janoušek, V., et al. (2000), Modelling diverse processes in the petrogenesis of a composite batholith: the Central Bohemian Pluton, Central European Hercynides, *Journal of Petrology*, *41*, 511-543.
Janoušek, V., et al. (2004), Deciphering the petrogenesis of deeply buried granites: whole-rock geochemical constraints on the origin of largely undepleted felsic granulites from the Moldanubian Zone of the Bohemian Massif, *Trans. R. Soc. Edinb.-Earth Sci.*, *95*, 141-159.
Janoušek, V., et al. (2006), Low-pressure granulites of the Lišov Massif, Southern Bohemia: Visean metamorphism of Late Devonian plutonic arc rocks, *Journal of Petrology*, *47*, 705-744.
Janoušek, V., and F. V. Holub (2007), The causal link between HP-HT metamorphism and ultrapotassic magmatism in collisional orogens: case study from the Moldanubian Zone of the Bohemian Massif, *Proceedings of the Geologists Association*, *118*, 75-86.
Janoušek, V., et al. (1997), Izotopy stroncia a neodymu v amfibolitech pestré skupiny moldanubika v okolí Chýnova., 80-81 pp.
Ježek, J., et al. (2002), Strain partitioning in front of an obliquely convergent indenter, in *Continental collision and the tectonosedimentary evolution of forelands*, edited by G. Bertotti, et al., pp. 145–164, European Geophysical Society, Stephen Mueller Special Publication Series.
Kalt, A., et al. (1999), Metamorphic evolution of cordierite-bearing migmatites from the Bayerische Wald (Variscan Belt, Germany), *Journal of Petrology*, *40*, 601-627.
Kalt, A., et al. (1997), P-T-t Pfade variszicher Hochtemperatur-Metamorphite des Bayerischen Waldes, *European Journal of Mineralogy*, *9*, 19.
Kidan, T. W., and J. W. Cosgrove (1996), The deformation of multilayers by layer-normal compression; an experimental investigation, *Journal of Structural Geology*, *18*, 461-474.
Kind, R., et al. (1996), Evidence from earthquake data for a partially molten crustal layer in southern Tibet, *Science*, *274*, 1692-1694.
Kisters, A. F. M., et al. (1996), Steep structure formation in the Okiep copper district, South Africa: Bulk inhomogeneous shortening of a high-grade metamorphic granite-gneiss sequence, *J Struct Geol 18*, 735-751.
Klápová, H., et al. (1998), Eclogites from the Czech part of the Erzgebirge: multi-stage metamorphic and structural evolution, *J. Geol. Soc.*, *155*, 567-583.
Klemperer, S. L. (2006), Crustal flow in Tibet: Geophysical evidence for the physical state of Tibetan lithosphere, and inferred patterns of active flow, in *Geological Society Special Publication*, edited, pp. 39-70.
Kodym, O. (1972), Multiphase deformation in the Blanský les granulite massif (South Bohemia), *Krystalinikum 9*, 91-105.
Konopásek, J., and K. Schulmann (2005), Contrasting Early Carboniferous field geotherms: evidence for accretion of a thickened orogenic root and subducted Saxothuringian crust (Central European Variscides), *J. Geol. Soc.*, *162*, 463-470.
Konopásek, J., et al. (2002), Eclogite-facies metamorphism at the eastern margin of the Bohemian Massif - subduction prior to continental underthrusting?, *European Journal of Mineralogy*, *14*, 701-713.
Kossmat, F. (1927), Gliederung der varistischen Gebirgsbaues, *Abhandlungen des Sächsischen Geologischen Landesamts*, *1*, 1-39.
Košler, J., et al. (1999), Independent dating of cooling and decompression of high grade rocks in the southern Bohemian Massif with Ar-Ar, Sm-Nd and U-Pb techniques, *J C Abstr 4*, 39.

Kotková, J. (1993), Tectonometamorphic history of lower crust in Bohemian Massif: example of north Bohemian granulites, *Czech Geological Survey, Special papers*.
Kotkova, J., et al. (1996), Zircon dating of north Bohemian granulites, Czech Republic: Further evidence for the lower carboniferous high-pressure event in the Bohemian Massif, *Geologische Rundschau*, *85*, 154-161.
Koyi, H. A., et al. (1999), Numerical models of ductile rebound of crustal roots beneath mountain belts, *Geophysical Journal International*, *139*, 556-562.
Krabbendam, M., and J. F. Dewey (1998), Exhumation of UHP rocks by transtension in the Western Gneiss Region, Scandinavian Caledonides, *Geological Society Special Publication*, 159-181.
Kröner, A., et al. (2000), Zircon ages for high pressure granulites from South Bohemia, Czech Republic, and their connection to Carboniferous high temperature processes, *Contributions to Mineralogy and Petrology*, *138*, 127-142.
Kröner, A., et al. (1988), U-Pb zircon and Sm-Nd model ages of high grade Moldanubian metamsediments, Bohemian Massif, Czechoslovakia, *Contributions to Mineralogy and Petrology*, *99*, 257-266.
Kumpera, O., and P. Martinec (1995), The development of the Carboniferous accretionary wedge in the Moravian-Silesian Paleozoic Basin, *Journal - Czech Geological Society*, *40*, 47-64.
Lange, U., et al. (2005), Sm-Nd and U-Pb dating of high-pressure granulites from the Zlote and Rychleby Mts (Bohemian Massif, Poland and Czech Republic), *Journal of Metamorphic Geology*, *23*, 133-145.
Liew, T. C., et al. (1989), The Moldanubian granitoid plutons of Austria: Chemical and isotopic studies bearing on their environmental setting, *Chemical Geology*, *76*, 41-55.
Linner, M. (1996), Metamorphism and partial melting of paragneisses of the Monotonous Group, SE Moldanubicum (Austria), *Mineral. Petrol.*, *58*, 215-234.
Lister, G. S., and G. A. Davis (1989), The origin of metamorphic core complexes and detachment faults formed during Tertiary continental extension in the northern Colorado River region, USA, *Journal of Stuctural Geology*, *11*, 65-94.
Maluski, H., et al. (1995), Pre-Variscan, Variscan and early Alpine thermo - tectonic history of the northeastern Bohemian Massif: An 40Ar/39Ar study, *Geologische Rundschau*, *84*, 345-358.
Matte, P., et al. (1990), Terrane boundaries in the Bohemian Massif: result of the large–scale Variscan shearing, *Tectonophysics 177*, 151-170.
Mattern, F. (2001), Permo-Silesian movements between Baltica and western Europe: Tectonics and 'basin families', *Terra Nova*, *13*, 368-375.
Mazur, S., et al. (2006), The Variscan Orogen in Poland, *Geol. Q.*, *50*, 89-118.
Medaris, G., et al. (1995), Czech Eclogites - Terrane Settings and Implications for Variscan Tectonic Evolution of the Bohemian Massif, *European Journal of Mineralogy*, *7*, 7-28.
Milnes, A. G., and H. A. Koyi (2000), Ductile rebound of an orogenic root; case study and numerical model of gravity tectonics in the Western gneiss complex, Caledonides, southern Norway, *TERRA NOVA*, *12*, 1-7.
Nelson, K. D., et al. (1996), Partially molten middle crust beneath southern Tibet: Synthesis of project INDEPTH results, *Science*, *274*, 1684-1685.
O'Brien, P. J. (1993), Partially retrograded eclogites of the Münchberg Massiv, Germany: records of a multistage Variscan uplift history in the Bohemian Massif, *Journal of Metamorphic Geology*, *11*, 241-260.
O'Brien, P. J. (2006), Type-locality granulites: High-pressure rocks formed at eclogite-facies conditions, *Mineral. Petrol.*, *86*, 161-175.

O'Brien, P. J., and D. A. Carswell (1993), Tectonometamorphic Evolution of the Bohemian Massif - Evidence From High-Pressure Metamorphic Rocks, *Geologische Rundschau*, *82*, 531-555.
O'Brien, P. J., et al. (1997), Petrological and isotopic studies on palaeozoic high-pressure granulites, Gory Sowie Mts, Polish Sudetes, *Journal of Petrology*, *38*, 433-456.
O'Brien, P. J., and J. Rotzler (2003), High-pressure granulites: formation, recovery of peak conditions and implications for tectonics, *Journal of Metamorphic Geology*, *21*, 3-20.
O'Brien, P. J., and K. Seifert (1992), P–T–t paths as records of orogenic processes: examples and problems from the crystalline of the Bohemian Massif, *Terra Nostra 1992*, 58–59.
O'Brien, P. J., and S. Vrána (1995), Eclogites with a short-lived granulite facies overprint in the Moldanubian zone, Czech Republic: petrology, geochemistry and diffusion modelling of garnet zoning, *Geol Rundsch 84*, 473-488.
Peresson, H., and K. Decker (1997), Far-field effects of Late Miocene subduction in the Eastern Carpathians: E-W compression and inversion of structures in the Alpine-Carpathian-Pannonian region, *Tectonics*, *16*, 38-56.
Petrakakis, K. (1997), Evolution of Moldanubian rocks in Austria: review and synthesis, *Journal of Metamorphic Geology*, *15*, 203-222.
Pin, C., and D. Vielzeuf (1983), Granulites and Related Rocks in Variscan Median Europe - a Dualistic Interpretation, *Tectonophysics*, *93*, 47-74.
Pitra, P., et al. (1999), Late Variscan strike-slip tectonics between the Teplá- Barrandian and Moldanubian terranes (Czech Bohemian Massif): petrostructural evidence, *J. Geol. Soc.*, *156*, 1003-1020.
Platt, J. P. (1993), Exhumation of high-pressure rocks: a review of concepts and processes, *Terra Nova*, *5*, 119-133.
Plomerová, J., et al. (2003), BOHEMA 2001-2003. Passive seismic experiment to study lithosphere-asthenosphere system in the western parth of the Bohemian massif, *Stud. Geophys. Geod.*, *47*, 691-701.
Plomerová, J., et al. (2005), Passive seismic experiment Mosaic - A pilot study of mantle lithosphere anisotropy of the Bohemian Massif, *Stud. Geophys. Geod.*, *49*, 541-560.
Price, N. J., and J. W. Cosgrove (1990), *Analysis of Geological Structures*, 502 pp., Cambridge University Press, Cambridge.
Prince, C. I., et al. (2000), Comparison of laser ablation ICP-MS and isotope dilution REE analyses - implications for Sm-Nd garnet geochronology, *Chemical Geology*, *168*, 255-274.
Racek, M., et al. (2006), Metamorphic record of burial and exhumation of orogenic lower and middle crust: a new tectonothermal model for the Drosendorf window (Bohemian Massif, Austria), *Mineral. Petrol.*, *86*, 221-251.
Rajlich, P. (1988), Tektonika sz. okraje středočeského plutonu a variská transprese v bloku bohemika, *Sbor. geol Věd*, *4*, 9-81.
Rajlich, P., et al. (1986), Hercynian-Thrust Related Shear Zones and Deformation of the Varied Group on the Contact of Granulites Southern Moldanubian, Bohemian Massif, *Geologische Rundschau*, *75*, 665-683.
Rey, P., et al. (2001), Gravitational collapse of the continental crust: Definition, regimes and modes, *Tectonophysics*, *342*, 435-449.
Ring, U., and M. T. Brandon (1999), Ductile deformation and mass loss in the Franciscan Subduction Complex: implications for exhumation processes in accretionary wedges, *Geological Society Special Publication*, 55-86.
Schmadicke, E., et al. (1995), Variscan Sm-Nd and Ar-Ar ages of eclogite facies rocks from the Erzgebirge, Bohemian Massif, *Journal of Metamorphic Geology*, *13*, 537-552.

Schmidt, S., and H. J. Gotze (1999), Integration of data constraints and potential field modelling - an example from southern lower saxony, Germany, *Physics and Chemistry of the Earth, Part A: Solid Earth and Geodesy*, *24*, 191-196.
Schulmann, K., et al. (2005), Chronological constraints on the pre-orogenic history, burial and exhumation of deep-seated rocks along the eastern margin of the Variscan Orogen, Bohemian Massif, Czech Republic, *American Journal of Science*, *305*, 407-448.
Schulzschmalschlager, M. (1984), U-Pb Studies of zircons and monazites of the anterior Bavarian Forest, *Fortschritte der Mineralogie*, *62*, 223.
Siebel, W., et al. (2005), Geochronology and geochemistry of a dyke-host rock association and implications for the formation of the Bavarian Pfahl shear zone, Bohemian Massif, *Int. J. Earth Sci.*, *94*, 8-23.
Siebel, W., et al. (2003), Late-Variscan magmatism revisited: new implications from Pb-evaporation zircon ages on the emplacement of redwitzites and granites in NE Bavaria, *Int. J. Earth Sci.*, *92*, 36-53.
Siebel, W., et al. (2006), Zircon geochronology and compositional record of late- to post-kinematic granitoids associated with the Bavarian Pfahl zone (Bavarian Forest), *Mineral. Petrol.*, *86*, 45-62.
Sokoutis, D., et al. (2005), Lithospheric-scale structures from the perspective of analogue continental collision, *Tectonophysics*, *406*, 1-15.
Spotila, J. A., et al. (2001), Near-field transpressive deformation along the San Andreas fault zone in southern California, based on exhumation constrained by (U-Th)/He dating, *Journal of Geophysical Research B: Solid Earth*, *106*, 30909-30922.
Stockhert, B., and T. V. Gerya (2005), Pre-collisional high pressure metamorphism and nappe tectonics at active continental margins: A numerical simulation, *Terra Nova*, *17*, 102-110.
Suess, F. E. (1912), Die Moravischen Fenster und ihre Beziehung zum Grundgebirge des Hohen Gesenkes, *Akademie der Wissenschaften, Denkschrift Matematisch-Naturwissenschaftliche Klasse*, *88*, 541-631.
Suess, F. E. (1926), *Intrusionstektonik und Wandertektonik im variszichen Grundgebirge*, 268p pp., Verlag Bornttrager, Berlin.
Svojtka, M. (2001), Geochronologie a strukturní vývoj granulitů v jžní části moldanubika Českého masívu, PhD Thesis thesis, Charles University, Prague.
Synek, J., et al. (1990), Transpression and transtenssion in the Devonian and Culm of the Nízký Jeseník Mts., *Acta Univ. Carol. Geol.*, *2*, 209-234.
Šalanský, K. (1995), Magnetic map of the Czech Republic, Czech geological survey, Prague.
Štípská, P., et al. (2006), Separate or shared metamorphic histories of eclogites and surrounding rocks? An example from the Bohemian Massif, *Journal of Metamorphic Geology*, *24*, 219-240.
Štípská, P., and R. Powell (2005), Does ternary feldspar constrain the metamorphic conditions of high-grade meta-igneous rocks? Evidence from orthopyroxene granulites, Bohemian Massif, *Journal of Metamorphic Geology*, *23*, 627-647.
Štípská, P., et al. (2004a), Vertical extrusion and middle crustal spreading of omphacite granulite: a model of syn-convergent exhumation (Bohemian Massif, Czech Republic), *Journal of Metamorphic Geology*, *22*, 179-198.
Štípská, P., et al. (2004b), Vertical extrusion and middle crustal spreading of omphacite granulite: a model of syn-convergent exhumation (Bohemian Massif, Czech Republic), *J Metam Geol 22*, 179-198.
Tajčmanová, L., et al. (2007), Diffusion-controlled development of silica-undersaturated domains in felsic granulites of the Bohemian Massif (Variscan belt of Central Europe), *Contributions to Mineralogy and Petrology*, *153*, 237-250.

Tajčmanová, L., et al. (2006), Thermal evolution of the orogenic lower crust during exhumation within a thickened Moldanubian root of the Variscan belt of Central Europe, *Journal of Metamorphic Geology*, *24*, 119-134.
Talbot, C. J., and H. Koyi (1995), Palaeoproterozoic intraplating exposed by resultant gravity overturn near Kiruna, northern Sweden, *Precambrian Research*, *72*, 199-225.
Tollmann, A. (1982), Großräumiger variszischer Deckenbau im Moldanubikum und neue Gedanken zum Variszikum Europas, *Geotektonische Forschungen*, *64*, 1-91.
Tomek, Č., et al. (1997), Geological interpretation of the 9HR and 503M seismic profiles in Western Bohemia, in *Journal of Geological Sciences, Geological modelof Western Bohemia related to the KTB borehole in Germany*, edited by S. Vrána and V. Štědrá, pp. 43-50, Czech Geological Survey, Prague.
Turner, F. J., and L. E. Weiss (1963), *Structural analysis of metamorphic tectonites*, McGraw Hill, New York.
Van Breemen, O., et al. (1982), Geochronological studies of the Bohemian massif, Czechoslovakia, and their significance in the evolution of Central Europe, *Transactions of the Royal Society of Edinburgh: Earth Sciences*, *73*, 89-108.
Verner, K., et al. (2007), Magmatic fabrics and emplacement of the cone-sheet-bearing Knížecí Stolec durbachitic pluton (Moldanubian Unit, Bohemian Massif): implications for mid-crustal reworking of granulitic lower crust in the Central European Variscides, *Int. J. Earth Sci.*, in press.
von Raumer, J. F., et al. (2003), Gondwana-derived microcontinents - The constituents of the Variscan and Alpine collisional orogens, *Tectonophysics*, *365*, 7-22.
Vrána, S. (1989), Perpotassic Granulites from Southern Bohemia - a New Rock-Type Derived from Partial Melting of Crustal Rocks under Upper Mantle Conditions, *Contributions to Mineralogy and Petrology*, *103*, 510-522.
Vrána, S. (1997), Geology and petrology of the Moldanubian zone, *In*, Vrána S, Štědrá V (eds) Geological model of western Bohemia. Czech Geol Surv, Prague, pp 109-113.
Vrána, S., and J. Bártek (2005), Retrograde metamorphism in a regional shear zone and related chemical changes: The Kaplice Unit of muscovite-biotite gneisses in the Moldanubian Zone of southern Bohemia, Czech Republic, *Journal of the Czech Geological Society*, *50*, 43-57.
Vrána, S., et al. (1995), Moldanubian Zone: metamorphic evolution. In: Dallmeyer, D., Franke, W. and Weber, K. (eds), Pre-Permian Geology of the Central and Western Europe, 453-466.
Vrána, S., and M. Novák (2000), Petrology and geochemistry of granulite clasts in the Visean Luleč conglomerate, Kulm in central Moravia, Czech Republic, *B Czech Geol Surv*, *75*, 405-414.
Vrána, S., and J. Šrámek (1999), Geological interpretation of detailed gravity survey of the granulite complex in southern Bohemia and its structure, *B Czech Geol Surv 74*, 261- 277.
Wendt, J. I., et al. (1994), U-Pb zircon and Sm-Nd dating of Moldanubian HP/HT granulites from south Bohemia, Czech Republic, *Journal - Geological Society (London)*, *151*, 83-90.
Wendt, J. I., et al. (1993), Evidence from zircon dating for existence of approximately 2.1 Ga old crystalline basement in southern Bohemia, Czech Republic, *Geologische Rundschau*, *82*, 42-50.
Wernicke, B. (1981), Low-angle normal faults in the Basin and Range Province: nappe tectonics in an extending orogen, *Nature*, *291*, 645-648.
Winchester, J. A., et al. (2002), Palaeozoic amalgamation of Central Europe: New results from recent geological and geophysical investigations, *Tectonophysics*, *360*, 5-21.
Yardley, B. W. D. (1989), *An introduction to metamorphic petrology*, 248 pp., Longman Scientific & Technical, New York.

Yuan, X., et al. (2000), Subduction and collision processes in the Central Andes constrained by converted seismic phases, *Nature*, *408*, 958-961.
Zulauf, G. (2001), Structural style, deformation mechanisms and paleodifferential stress along an exposed crustal section: Constraints on the rheology of quartzofeldspathic rocks at supra- and infrastructural levels (Bohemian Massif), *Tectonophysics*, *332*, 211-237.
Zulauf, G., et al. (2002a), 10 km minimum throw along the West Bohemian shear zone: Evidence for dramatic crustal thickening and high topography in Bohemian Massif (European Variscides), *Int. J. Earth Sci.*, *91*, 850-864.
Zulauf, G., et al. (2002b), Evidence for high-temperature diffusional creep preserved by rapid cooling of lower crust (North Bohemian shear zone, Czech Republic), *Terra Nova*, *14*, 343-354.
Zulauf, G., et al. (1997), Late Cadomian crustal tilting and Cambrian transtension in the Tepla-Barrandian unit (Bohemian Massif, Central European Variscides), *Geologische Rundschau*, *86*, 571-584.
Žáček, V., and J. Cháb (1993), Metamorphism in the Teplá upland, Bohemian massif, Czech republic (preliminary report), *Věstník Českého geologického Ústavu*, *68*, 33-37.
Žák, J., et al. (2005a), Tectonic evolution of a continental magmatic arc from transpression in the upper crust to exhumation of mid-crustal orogenic root recorded by episodically emplaced plutons: The Central Bohemian Plutonic Complex (Bohemian Massif), *Int. J. Earth Sci.*, *94*, 385-400.
Žák, J., et al. (2005b), Multiple magmatic fabrics in the Sázava pluton (Bohemian Massif, Czech Republic): A result of superposition of wrench-dominated regional transpression on final emplacement, *Journal of Structural Geology*, *27*, 805-822.

13 Appendix 1.

Radiometric ages used for histogram calculations in Figure 2.

Central Bohemian plutonic complex, Ar
339±10 Ma, K-Ar on Bt, [*Dörr, et al.*, 1998]
342±8 Ma, K-Ar on Bt, [*Dörr, et al.*, 1998]
336±3,50 Ma, Ar-Ar on Bt, [*Janoušek, et al.*, 2000]
336±0 Ma, Ar-Ar on Bt, [*Matte, et al.*, 1990]
342±0 Ma, K-Ar on Bt, [*Wemmer and Ahrendt* , unpublished]

Central Bohemian plutonic complex, Pb
365±5 Ma, U-Pb on Zr, [*Košler, et al.*, 1993]
341±2 Ma, U-Pb on Zr, [*Dörr, et al.*, 1997]
342±8 Ma, Pb-Pb on Zr, [*Dörr, et al.*, 1998]
349±5 Ma, U-Pb on Zr, [*Dörr, et al.*, 1998]
349±12 Ma, Pb-Pb on Zr, [*Holub, et al.*, 1997]
351±11 Ma, Pb-Pb on Zr, [*Holub, et al.*, 1997]
346±10 Ma, Pb-Pb on Zr, [*Holub, et al.*, 1997]
343±6 Ma, Pb-Pb on Zr, [*Holub, et al.*, 1997]
341±7 Ma, Pb-Pb on Zr, [*Holub, et al.*, 1997]
354±3,50 Ma, U-Pb on Zr, [*Janoušek and Gerdes*, 2003]
337±1 Ma, U-Pb on Zr, [*Janoušek and Gerdes*, 2003]
369±4 Ma, Pb-Pb on Zr, [*Košler, et al.*, 1993]
375±5 Ma, Pb-Pb on Zr, [*Košler, et al.*, 1993]

373±5 Ma, U-Pb on Zr, [*Košler, et al.*, 1993]

Moldanubian batolith, Ar
331±0 Ma, Ar-Ar on Mu, [*Dallmeyer, et al.*, 1992]
325±0 Ma, Ar-Ar on Mu, [*Dallmeyer, et al.*, 1992]
326±1,50 Ma, Ar-Ar on Mu, [*Frank*, 1994]
327±4 Ma, Ar-Ar on Mu, [*Friedl, et al.*, 1996]
330±0 Ma, Ar-Ar on , [*Matte, et al.*, 1990]

Moldanubian batolith, Pb
323±4 Ma, U-Pb on Mo, [*Frasl and Finger*, 1991]
327±4 Ma, U-Pb on Mo, [*Frasl and Finger*, 1991]
319±6 Ma, U-Pb on Mo, [*Frasl and Finger*, 1991]
328±4 Ma, U-Pb on Zr, [*Friedl*, 1997]
302±2 Ma, U-Pb on Mo, [*Friedl, et al.*, 1992],
323±4 Ma, U-Pb on Mo, [*Friedl, et al.*, 1996]
327±5 Ma, U-Pb on Mo, [*Friedl, et al.*, 1996]
323±5 Ma, U-Pb on Mo, [*Friedl, et al.*, 1996]
328±5 Ma, U-Pb on Mo, [*Friedl, et al.*, 1996]
353±9 Ma, U-Pb on Zr, [*Klotzli and Parrish*, 1996]
338±2 Ma, U-Pb on Zr, [*Klotzli and Parrish*, 1996]
316±17 Ma, U-Pb on Zr, Xe, Mo, [*Quadt and Finger*, 1991]
327±5 Ma, U-Pb on Mo, [*Quadt and Finger*, 1991]
314±4 Ma, U-Pb on Xe, [*Quadt and Finger*, 1991]
318±4 Ma, U-Pb on Mo[*Quadt and Finger*, 1991]

Moldanubian granulites, Pb
338±1 Ma, U-Pb on Zr, [*Aftalion, et al.*, 1989]
346±5 Ma, U-Pb on Zr, [*Wendt, et al.*, 1994]
351±6 Ma, U-Pb on Zr, [*Wendt, et al.*, 1994]
346±12 Ma, U-Pb on Zr, [*Wendt, et al.*, 1994]
366±5 Ma, U-Pb on Zr, [*Wendt, et al.*, 1994]
373±12 Ma, U-Pb on Zr, [*Wendt, et al.*, 1994]
341±3,30 Ma, U-Pb on Zr, [*Kröner, et al.*, 2000]
338,20±3,20 Ma, U-Pb on Zr, [*Kröner, et al.*, 2000]
341,30±3,50 Ma, U-Pb on Zr, [*Kröner, et al.*, 2000]
339,30±2,90 Ma, U-Pb on Zr, [*Kröner, et al.*, 2000]
360±2 Ma, U-Pb on Zr, [*Kröner, et al.*, 2000]
399±6 Ma, U-Pb on Zr, [*Kröner, et al.*, 2000]
441±6 Ma, U-Pb on Zr, [*Kröner, et al.*, 2000]
357±2 Ma, U-Pb on Zr, [*Kröner, et al.*, 2000]
408±6 Ma, U-Pb on Zr, [*Kröner, et al.*, 2000]
340,40±2,90 Ma, U-Pb on Zr, [*Kröner, et al.*, 2000]
339,60±3,10 Ma, U-Pb on Zr, [*Kröner, et al.*, 2000]
367,80±3 Ma, U-Pb on Zr, [*Kröner, et al.*, 2000]
339,20±2,90 Ma, U-Pb on Zr, [*Kröner, et al.*, 2000]
469,30±3,80 Ma, U-Pb on Zr, [*Kröner, et al.*, 2000]
341,10±2,40 Ma, U-Pb on Zr, [*Kröner, et al.*, 1996]

Moldanubian domain in western Bavaria, Ar

320±6 Ma, K-Ar on Bt, [*Haare, et al.*, 1968]
320±8 Ma, K-Ar on Bt, [*Haare, et al.*, 1968]
316±6 Ma, K-Ar on Bt, [*Haare, et al.*, 1968]
325±6 Ma, K-Ar on Bt, [*Haare, et al.*, 1968]
323±8 Ma, K-Ar on Bt, [*Haare, et al.*, 1968]
314±6 Ma, K-Ar on Mu, [*Haare, et al.*, 1968]
314±12 Ma, K-Ar on Mu, [*Haare, et al.*, 1968]
314±0 Ma, K-Ar on Bt, [*Kreuzer, et al.*, 1989]
320±0 Ma, K-Ar on Bt, [*Kreuzer, et al.*, 1989]
309±0 Ma, Ar-Ar on Hbl, [*Kreuzer, et al.*, 1989]
328±0 Ma, Ar-Ar on Hbl, [*Kreuzer, et al.*, 1989]

Moldanubian domain in western Bavaria, Pb
359±0 Ma, U-Pb on Zr, [*Bues, et al.*, 2002]
332±0 Ma, U-Pb on Zr, [*Dörr, et al.*, 1998]
342±0 Ma, U-Pb on Zr, [*Dörr, et al.*, 1998]
322±0 Ma, U-Pb on Xe, [*Gebauer, et al.*, 1989]
384±0 Ma, U-Pb on Zr, [*Gebauer, et al.*, 1989]
324±0 Ma, U-Pb on Xe, [*Gebauer, et al.*, 1989]
316±0 Ma, U-Pb on Mo, [*Grauert, et al.*, 1974]
321±0 Ma, U-Pb on Mo, [*Grauert, et al.*, 1974]
322±0 Ma, U-Pb on Mo, [*Grauert, et al.*, 1974]
323±0 Ma, U-Pb on Mo, [*Grauert, et al.*, 1974]
310±0 Ma, U-Pb on Zr, [*Grauert, et al.*, 1974]
319±0 Ma, U-Pb on Zr, [*Grauert, et al.*, 1974]
320±3 Ma, U-Pb on Mo, [*Grauert, et al.*, 1974]
317±3 Ma, U-Pb on Mo, [*Grauert, et al.*, 1974]
322±0 Ma, U-Pb on Mo, [*Kalt, et al.*, 1997]
326±0 Ma, U-Pb on Mo, [*Kalt, et al.*, 1997]
331±7 Ma, Pb-Pb on Zr, [*Propach, et al.*, 2000]
320±3 Ma, U-Pb on Mo, [*Propach, et al.*, 2000]
318±2 Ma, U-Pb on Zr, [*Propach, et al.*, 2000]
319±4 Ma, U-Pb on Zr, [*Propach, et al.*, 2000]
356±7 Ma, U-Pb on Zr, [*Propach, et al.*, 2000]
321±3 Ma, U-Pb on Mo, [*Propach, et al.*, 2000]
315±4 Ma, U-Pb on Zr, [*Propach, et al.*, 2000]
317±3 Ma, U-Pb on Mo, [*Propach, et al.*, 2000]
318±3 Ma, U-Pb on Mo, [*Propach, et al.*, 2000]
320±2 Ma, U-Pb on Zr, [*Propach, et al.*, 2000]
318±3 Ma, U-Pb on Mo, [*Propach, et al.*, 2000]
316±24 Ma, Pb-Pb on Mo, [*Propach, et al.*, 2000]
323±2 Ma, U-Pb on Mo, [*Propach, et al.*, 2000]
322±0 Ma, U-Pb on Zr, [*Schulzschmalschlager*, 1984]
315±0 Ma, U-Pb on Mo, [*Schulzschmalschlager*, 1984]
309,90±2,90 Ma, Pb-Pb on Zr, [*Siebel, et al.*, 2003]
309,50±6,20 Ma, Pb-Pb on Zr, [*Siebel, et al.*, 2003]
315±1,20 Ma, Pb-Pb on Zr, [*Siebel, et al.*, 2003]
315,30±3,70 Ma, Pb-Pb on Zr, [*Siebel, et al.*, 2003]
324,20±4,20 Ma, Pb-Pb on Zr, [*Siebel, et al.*, 2003]
323±4,50 Ma, Pb-Pb on Zr, [*Siebel, et al.*, 2003]

321,60±4,70 Ma, Pb-Pb on Zr, [*Siebel, et al.*, 2003]
334,50±1,10 Ma, Pb-Pb on Zr, [*Siebel, et al.*, 2005]
334±3 Ma, Pb-Pb on Zr, [*Siebel, et al.*, 2005]
326±9 Ma, U-Pb on Zr, [*Siebel, et al.*, 2005]
331±9 Ma, U-Pb on Zr, [*Siebel, et al.*, 2005]
331±8 Ma, U-Pb on Zr, [*Siebel, et al.*, 2005]
321,80±4,80 Ma, U-Pb on Zr, [*Siebel, et al.*, 2005]
320±0 Ma, U-Pb on Mo, [*Teufel*, 1988]
324±0 Ma, U-Pb on Mo, [*Teufel*, 1988]

Saxothuringian – Teplá-Barrandian suture, Ar + Rb
371±4 Ma, K-Ar on Mu, [*Ahrendt, et al.*, 1997]
359±4 Ma, K-Ar on Bt, [*Ahrendt, et al.*, 1997]
377±3 Ma, K-Ar on Mu, [*Ahrendt, et al.*, 1997]
377±4 Ma, K-Ar on Bt, [*Ahrendt, et al.*, 1997]
377±3 Ma, Rb-Sr on Mu, [*Ahrendt, et al.*, 1997]
376±5 Ma, Rb-Sr on Mu, [*Ahrendt, et al.*, 1997]
378,70±3,50 Ma, Ar-Ar on pargasite, [*Bowes, et al.*, 2002]
379,50±4,30 Ma, Ar-Ar on pargasite, [*Bowes, et al.*, 2002]
371,50±2,30 Ma, Ar-Ar on Hbl, [*Dallmeyer and Urban*, 1994]
366,30±0,80 Ma, Ar-Ar on Mu, [*Dallmeyer and Urban*, 1994]
480±0 Ma, Rb-Sr on Mu, [*Glodny*, 1995]
475±0 Ma, Rb-Sr on Mu, [*Glodny*, 1995]
380±0 Ma, K-Ar on Hbl, [*Kreuzer, et al.*, 1989]
370±0 Ma, K-Ar on mineral, [*Kreuzer, et al.*, 1989]
376±0 Ma, Rb-Sr on mica, [*Krohe and Wawrzenitz*, 2000]
373±0 Ma, Rb-Sr on mica, [*Krohe and Wawrzenitz*, 2000]
370±8 Ma, Rb-Sr on mineral-WR, [*Sollner*, 1981]

Saxothuringian – Teplá-Barrandian suture, Pb
377±7 Ma, Sm-Nd on Grt-Omph, [*Beard, et al.*, 1995]
367±4 Ma, Sm-Nd on Grt-Omph, [*Beard, et al.*, 1995]
496±1 Ma, U-Pb on Zr, [*Bowes and Aftalion*, 1991]
362±12 Ma, U-Pb on Zr, [*Bowes and Aftalion*, 1991]
380±18 Ma, U-Pb on Zr, [*Gebauer and Grunenfelder*, 1979]
525±36 Ma, U-Pb on Zr, [*Gebauer and Grunenfelder*, 1979]
380±0 Ma, U-Pb on Mo, [*Krohe and Wawrzenitz*, 2000]
375±0 Ma, U-Pb on Mo, [*Krohe and Wawrzenitz*, 2000]
484±2 Ma, U-Pb on Mo, [*Krohe and Wawrzenitz*, 2000]
384±2 Ma, Sm-Nd on Grt-Omph, [*Stosch and Lugmair*, 1990]
385±2 Ma, Sm-Nd on MultiMineral-WR, [*Stosch and Lugmair*, 1990]
385±15 Ma, Sm-Nd on Grt, [*Quadt*, 1994]
398±20 Ma, Sm-Nd on Grt, [*Quadt*, 1994]
475±0 Ma, U-Pb on Zr, [*Quadt*, 1994]
493±0 Ma, U-Pb on Zr, [*Quadt*, 1994]

Erzgebirge crystalline complex at the Saxothuringian – Teplá-Barrandian suture, Ar
341±4 Ma, Ar-Ar on Mu, [*Zulauf, et al.*, 2002b]
344±3 Ma, Ar-Ar on Bt, [*Zulauf, et al.*, 2002b]
344±4 Ma, Ar-Ar on Mu, [*Zulauf, et al.*, 2002b]

347±3 Ma, Ar-Ar on Bt, [*Zulauf, et al.*, 2002b]

Erzgebirge crystalline complex at the Saxothuringian – Teplá-Barrandian suture, Pb
348±10 Ma, U-Pb on Zr, [*Kotková*, 1993]
339±1,50 Ma, Pb-Pb on Zr, [*Kotková*, 1993]
339±1,40 Ma, Pb-Pb on Zr, [*Kotková*, 1993]
346±14 Ma, U-Pb on Rt, [*Kotková*, 1993]
345±11 Ma, U-Pb on Zr, [*Kotková, et al.*, 1996]
342±1 Ma, U-Pb on Mo, [*Zulauf, et al.*, 2002b]

Teplá-Barrandian unit, Ar
378,70±3,50 Ma, Ar-Ar on pargasite, [*Bowes, et al.*, 2002]
379,50±4,30 Ma, Ar-Ar on pargasite, [*Bowes, et al.*, 2002]
495±6 Ma, K-Ar on Bt, [*Bues, et al.*, 2002]
547±7 Ma, K-Ar on Hbl, [*Bues, et al.*, 2002]
549±7 Ma, K-Ar on Hbl, [*Bues, et al.*, 2002]
371,50±2,30 Ma, Ar-Ar on Hbl, [*Dallmeyer and Urban*, 1994]
366,30±0,80 Ma, Ar-Ar on Mu, [*Dallmeyer and Urban*, 1994]
375±0 Ma, Ar-Ar on Mu, [*Dallmeyer and Urban*, 1994]
516±0 Ma, Ar-Ar on Hbl, [*Dallmeyer and Urban*, 1998]
383±0 Ma, Ar-Ar on Hbl, [*Dallmeyer and Urban*, 1998]
371±0 Ma, K-Ar on Hbl, [*Dallmeyer and Urban*, 1998]
366±0 Ma, K-Ar on Hbl, [*Dallmeyer and Urban*, 1998]
362±0 Ma, Ar-Ar on white mica, [*Dallmeyer and Urban*, 1998]
385±0 Ma, Ar-Ar on Hbl, [*Fischer, et al.*, 1968]
444±0 Ma, K-Ar on Hbl, *Henjes and Kunst* (unpublished)
518±8 Ma, Ar-Ar on Bt, [*Kreuzer, et al.*, 1990]
321±0 Ma, K-Ar on Bt, [*Kreuzer, et al.*, 1992]
328±0 Ma, K-Ar on Bt, [*Kreuzer, et al.*, 1992]
320±0 Ma, K-Ar on Bt, [*Kreuzer, et al.*, 1992]
375±0 Ma, K-Ar on Bt, [*Kreuzer, et al.*, 1992]
329±0 Ma, Ar-Ar on Hbl, [*Kreuzer, et al.*, 1992]
334±0 Ma, Ar-Ar on Hbl, [*Kreuzer, et al.*, 1992]
351±0 Ma, Ar-Ar on Hbl, [*Kreuzer, et al.*, 1992]
363±0 Ma, Ar-Ar on Hbl, [*Kreuzer, et al.*, 1992]
326±0 Ma, K-Ar on Hbl, [*Kreuzer, et al.*, 1992]
491±0 Ma, K-Ar on Hbl, [*Kreuzer, et al.*, 1992]
407±0 Ma, K-Ar on Hbl, [*Kreuzer, et al.*, 1992]
340±0 Ma, Ar-Ar on Mu, [*Vejnar*, 1962]
475±0 Ma, K-Ar on white mica, [*Vejnar*, 1962]
371±8 Ma, K-Ar on Sericite, [*Wemmer and Ahrendt*, 1997]
483±10 Ma, K-Ar on white mica, [*Wemmer and Ahrendt*, 1997]
498±11 Ma, K-Ar on white mica, [*Wemmer and Ahrendt*, 1997]
362±0 Ma, K-Ar on white mica, [*Wemmer and Ahrendt*, 1997]
306±0 Ma, K-Ar on Bt, [*Zulauf, et al.*, 2002a]
296±0 Ma, K-Ar on Bt, [*Zulauf, et al.*, 2002a]
271±0 Ma, K-Ar on Bt, [*Zulauf, et al.*, 2002a]
385±0 Ma, K-Ar on Bt, [*Zulauf, et al.*, 2002a]
350±0 Ma, K-Ar on white mica, [*Zulauf, et al.*, 2002a]
361±0 Ma, K-Ar on white mica, [*Zulauf, et al.*, 2002a]

362±0 Ma, K-Ar on white mica, [*Zulauf, et al.*, 2002a]
362±0 Ma, K-Ar on white mica, [*Zulauf, et al.*, 2002a]
371±0 Ma, K-Ar on white mica, [*Zulauf, et al.*, 2002a]
295±0 Ma, K-Ar on white mica, [*Zulauf, et al.*, 2002a]

Teplá-Barrandian unit, Pb
496±1 Ma, U-Pb on Zr, [*Bowes and Aftalion*, 1991]
362±12 Ma, U-Pb on Zr, [*Bowes and Aftalion*, 1991]
320±0 Ma, U-Pb on Zr, [*Dörr, et al.*, 1998]
337±0 Ma, U-Pb on Zr, [*Dörr, et al.*, 1998]
315±0 Ma, U-Pb on Zr, [*Dörr, et al.*, 1998]
524±0 Ma, U-Pb on Zr, [*Dörr, et al.*, 1996]
342±0 Ma, U-Pb on Zr, [*Dörr, et al.*, 1997]
523±0 Ma, U-Pb on Zr, [*Dörr, et al.*, 2002]
522±0 Ma, U-Pb on Zr, [*Dörr, et al.*, 2002]
511±0 Ma, U-Pb on Zr, [*Gebauer and Bauberger*, 1993]
522±0 Ma, U-Pb on Zr, [*Zulauf, et al.*, 1997]
523±0 Ma, U-Pb on Zr, [*Zulauf, et al.*, 1997]

Aftalion, M., et al. (1989), Early Carboniferous U-Pb Zircon Age for Garnetiferous, Perpotassic Granulites, Blansky Les Massif, Czechoslovakia, *Neues Jahrb. Mineral.-Mon.hefte*, 145-152.

Ahrendt, H., et al. (1997), Rb-Sr and K-Ar mineral data of the KTB and the surrounding area and their bearing on the tectonothermal evolution of the metamorphic basement rocks, *Geologische Rundschau*, *86*, S251-S257.

Beard, B. L., et al. (1995), Geochronology and geochemistry of eclogites from the Mariánské Lázně Complex, Czech Republic: Implications for Variscan orogenesis, *Geologische Rundschau*, *84*, 552-567.

Bowes, D. R., and M. Aftalion (1991), U-Pb isotopic evidence for early Ordovician and late Proterozoic units in the Maránské Lázně Complex, Central European Hercynides, *Neues Jahrbuch für Mineralogie Abhandlungen*, *1991*, 315-326.

Bowes, D. R., et al. (2002), Ar-40/Ar-39 isotopic evidence for mid-devonian post-metamorphic pegmatite emplacement in the Marianske Lazne Complex, Bohemian Massif, Central European Hercynides, *Neues Jahrbuch Fur Mineralogie-Monatshefte*, 445-457.

Bues, C., et al. (2002), Emplacement depths and radiometric ages of Paleozoic plutons of the Neukirchen-Kdyne? massif: Differential uplift and exhumation of Cadomian basement due to Carboniferous orogenic collapse (Bohemian Massif), *Tectonophysics*, *352*, 225-243.

Dallmeyer, R. D., et al. (1992), Chronology of late Paleozoic tectonothermal activity in the southeastern Bohemian Massif, Austria (Moldanubian and Moravo- Silesian zones): 40Ar/39Ar mineral age controls, *Tectonophysics*, *210*, 135-153.

Dallmeyer, R. D., and M. Urban (1994), Variscan vs. Cadomian tectonotermal evolution within the Tepla-Barrandian zone, Bohemian Massif, Czech Republic: evidence from 40Ar/39Ar mineral and whole rock slate/phyllite ages, *Journal of the Czech Geological Society*, *39*, 21-22.

Dallmeyer, R. D., and M. Urban (1998), Variscan vs Cadomian tectonothermal activity in northwestern sectors of the Tepla-Barrandian zone, Czech Republic: constraints from Ar-40/Ar-39 ages, *Geologische Rundschau*, *87*, 94-106.

Dörr, W., et al. (1998), U-Pb zircon ages, geochemistry and structural development of metagranitiods of the Teplá Crystalline Complex - Evidence for pervasive Cambrian plutonism within the Bohemian Massif (Czech Republic), *Geologische Rundschau*, *87*, 135-149.
Dörr, W., et al. (2002), Neoproterozoic to Early Cambrian history of an active plate margin in the Tepla-Barrandian unit - a correlation of U-Pb isotopic-dilution-TIMS ages (Bohemia, Czech Republic), *Tectonophysics*, *352*, 65-85.
Dörr, W., et al. (1997), Dating of collapse related plutons along the West- and Central Bohemian shear zone, European Variscides, *Terra Nostra*, *5*, 31-34.
Dörr, W., et al. (1996), The Tepla-Barrandian/Moldanubian s.str. boundary: preliminary geochronological results from fault related plutons, *Terra Nostra*, *2*, 34-38.
Fischer, G., et al. (1968), Hornblendealter aus dem ostbayerischen Grundgebirge, *Neues Jahrb. Mineral.*, 352– 385.
Frank, W. (1994), Geochronology and evolution of the South Bohemian Massif: a review, *Mitt Osterreichischen Mineralogischen Gesellschaft*, *139*, 41-43.
Frasl, G., and F. Finger (1991), Geologisch-petrographische Exkursion in den Osterreichischen Teil des Sudbohmischen Batholiths, *Eur J Mineral*, *3*, 23-40.
Friedl, G. (1997), U/Pb-Datierungen an Zirkonen und Monaziten aus Gesteinen vom Osterreichischen Anteil der Bohmischen Masse, University of Salzburg.
Friedl, G., et al. (1992), Neue U/Pb Altersdaten aus der sudlichen Bohmischen Masse, *Frankfurter Geowiss Arb*, *All*, 217.
Friedl, G., et al. (1996), Timing der Intrusionstatigkeit Im Sudbohmischen Batholith, paper presented at 6 Symposium Tektonik-Strukturgeologie-Kristallingeologie, Erweiterte Kurzfassungen, Facultas-Universitatsverlag, Wien.
Gebauer, D., and W. Bauberger (1993), Geochronologische Ubersicht. In: Geologische Karte von Bayern 1:25000, Erlauterungen zum Blatt Nr. 6439 Tannesberg. Bayern, Geol. L.-Amt, Munchen.
Gebauer, D., and M. Grunenfelder (1979), U-Pb and Rb-Sr mineral dating of eclogites and their country rocks Example: Munchberg Gneiss massif, northeast Bavaria, *Earth Planet Sci Lett*, *42*, 35-44.
Gebauer, D., et al. (1989), The development of the Central European continental crust since the Early Archaean based on conventional and ion-microprobe dating of up to 3.84 b.y. old detrital zircons, *Tectonophysics*, *157*, 81-96.
Glodny, J. (1995), KTB, Munchen.
Grauert, B., et al. (1974), Geochronology of a polymetamorphic and anatectic gneiss region: The Moldanubicum and the area Lam-Deggendorf, eastern Bavaria, Germany., *Contributions to Mineralogy and Petrology*, *45*, 37-63.
Haare, W., et al. (1968), Unverofentlicher Zwischenbericht Nr. 5/67 der Bundesanstalt fur Bodenvorschung, Hannover.
Holub, F. V., et al. (1997), Radiometric dating of granitic rocks from the Central Bohemian Plutonic Complex (Czech Republic): constraints on the chronology of thermal and tectonic events along the Moldanubian-Barrandian boundary, *Comptes Rendus De L Academie Des Sciences Serie Ii Fascicule a-Sciences De La Terre Et Des Planetes*, *325*, 19-26.
Janoušek, V., et al. (2000), Modelling diverse processes in the petrogenesis of a composite batholith: the Central Bohemian Pluton, Central European Hercynides, *Journal of Petrology*, *41*, 511-543.
Janoušek, V., and A. Gerdes (2003), Timing the magmatic activity within the Central Bohemian Pluton, Czech Republic: conventional U-Pb ages for the Sazava and Tabor intrusions and their geotectonic significance, *J Czech Geol Soc*, *48*, 70-71.

Kalt, A., et al. (1997), P-T-t Pfade variszicher Hochtemperatur-Metamorphite des Bayerischen Waldes, *European Journal of Mineralogy*, *9*, 19.
Klotzli, U. S., and R. R. Parrish (1996), Zircon U/Pb and Pb/Pb geochronology of the Rastenberg granodiorite, South Bohemian Massif, Austria, *Mineralogy and Petrology*, *58*, 197-214.
Košler, J., et al. (1993), Mid-late Devonian plutonic activity in the Bohemian Massif: U-Pb zircon isotopic evidence from the Stare Sedlo and Mirotice gneiss complexes, Czech Republic, *Neues Jahrbuch fur Mineralogie, Monatshefte*, 417-431.
Kotková, J. (1993), Tectonometamorphic history of lower crust in Bohemian Massif: example of north Bohemian granulites, *Czech Geological Survey, Special papers*.
Kotková, J., et al. (1996), Zircon dating of North Bohemian granulites, Czech Republic: Further evidence for the Lower Carboniferous high-pressure event in the Bohemian Massif, *Geologische Rundschau*, *85*, 154-161.
Kreuzer, H., et al. (1990), Ar-Ar conformation for Cambrian, early Devonian and mid-Carboniferous tectonic units at the western margin of the Bohemian Massif, paper presented at 6. Rundgesprach Geodynamik des europ. Variszikums, Clausthal-Zellerfeld.
Kreuzer, H., et al. (1989), K-Ar geochronology of different tectonic units at the northwestern margin of the Bohemian Massif, *Tectonophysics*, *157*, 149-178.
Kreuzer, H., et al. (1992), K-Ar dating on the Teplá-Domažlice Zone at the western margin of the Bohemian Massif, *Proceedings of the First International Conference on the Bohemian Massif, 26.9-1.10. 1988*, 168-175.
Krohe, A., and N. Wawrzenitz (2000), Domainal variations of U-Pb monazite ages and Rb-Sr whole-rock dates in polymetamorphic paragneisses (KTB Drill Core, Germany): influence of strain and deformation mechanisms on isotope systems, *Journal of Metamorphic Geology*, *18*, 271-291.
Kröner, A., et al. (2000), Zircon ages for high pressure granulites from South Bohemia, Czech Republic, and their connection to Carboniferous high temperature processes, *Contributions to Mineralogy and Petrology*, *138*, 127-142.
Kröner, A., et al. (1996), SHRIMP zircon ages for HP-HT granulites from the Moldanubian zone of southern Bohemia, paper presented at EOS 77.
Matte, P., et al. (1990), Terrane boundaries in the Bohemian Massif: result of large-scale Variscan shearing, *Tectonophysics*, *177*, 151-170.
Propach, G., et al. (2000), Zircon and monazite U-Pb ages of Variscan granitoid rocks and gneisses in the Moldanubian zone of eastern Bavaria, Germany, *Neues Jahrbuch Fur Geologie Und Palaontologie-Monatshefte*, 345-377.
Quadt, A. v. (1994), U-Pb zircon data and Pb-Sr-Nd isotope geochemistry from meta-gabbros from the KTB bore hole, *J Czech Geol Soc*, *39*, 87-88.
Quadt, A. v., and F. Finger (1991), Geochronologische untersuchungen im osterreischen teil des Sudbohmisches batoliths: U-Pb datierungen an zirkonen, monaziten und xenotimen des Weinsberges granits, *European Journal of Mineralogy*, *3*, 281.
Schulzschmalschlager, M. (1984), U-Pb Studies of zircons and monazites of the anterior Bavarian Forest, *Fortschritte der Mineralogie*, *62*, 223.
Siebel, W., et al. (2005), Geochronology and geochemistry of a dyke-host rock association and implications for the formation of the Bavarian Pfahl shear zone, Bohemian Massif, *International Journal of Earth Sciences*, *94*, 8-23.
Siebel, W., et al. (2003), Late-Variscan magmatism revisited: new implications from Pb-evaporation zircon ages on the emplacement of redwitzites and granites in NE Bavaria, *International Journal of Earth Sciences*, *92*, 36-53.

Sollner, F. (1981), Rb-Sr Dating of rocks from the Munchberg gneiss-massif, NE-Bavaria (Germany) 2nd mineral datings, *Neues Jahrbuch fur Mineralogie-Abhandlungen*, 142-178.

Stosch, H. G., and G. W. Lugmair (1990), Geochemistry and evolution of MORB - type eclogites from the Münchberg Massif, southern Germany, *Earth and Planetary Science Letters*, *99*, 230-249.

Teufel, S. (1988), Vergleichende U-Pb- und Rb-Sr-Altersbestimmungen an Gesteinen des Ubergangsbereiches Saxothuringikum/Moldanubikum, NE-Bayern, *Gottinger Arb. Geol. Palaont.*, *35*, 87.

Vejnar, Z. (1962), Zum problem des absoluten Alters der kristallinen Schiefer und der Intrusiva des Westbohmischen Kristallins, *Krystalinikum*, *1*, 149-159.

Wemmer, K., and H. Ahrendt (1997), Comparative K-Ar and Rb-Sr age determinations of retrograde processes on rocks from the KTB deep drilling project, *Geologische Rundschau*, *86*, S272-S285.

Wendt, J. I., et al. (1994), U-Pb zircon and Sm-Nd dating of Moldanubian HP/HT granulites from south Bohemia, Czech Republic, *Journal - Geological Society (London)*, *151*, 83-90.

Zulauf, G., et al. (2002a), 10 km minimum throw along the West Bohemian shear zone: Evidence for dramatic crustal thickening and high topography in Bohemian Massif (European Variscides), *International Journal of Earth Sciences*, *91*, 850-864.

Zulauf, G., et al. (2002b), Evidence for high-temperature diffusional creep preserved by rapid cooling of lower crust (North Bohemian shear zone, Czech Republic), *Terra Nova*, *14*, 343-354.

Zulauf, G., et al. (1997), Late Cadomian crustal tilting and Cambrian transtension in the Tepla-Barrandian unit (Bohemian Massif, Central European Variscides), *Geologische Rundschau*, *86*, 571-584.

The precursor of Variscan felsic granulites, process of its granulitization, and inversed rheology of feldspars and quartz in the lower-crustal conditions

Jan Franěk[1,2], Karel Schulmann[1], Ondrej Lexa[1,2], Stanislav Ulrich[2,3], Jakub Haloda[4], Patricie Týcová[4]

1 Université Louis Pasteur, EOST, UMR 7517, 1 Rue Blessig, Strasbourg 67084, France
2 Institute of Petrology and Structural Geology, Albertov 6, 128 43 Prague 2, Czech Republic
3 Geophysical institute of the Czech academy of sciences, Boční II/1401, 14131 Prague 4, Czech Republic
4 Czech Geological Survey, Geologická 6, 152 00 Prague 5, Czech Republic

1 Abstract

Microstructural and microchemical study of Variscan felsic granulites from the Blanský les massif in the Moldanubian domain of the Bohemian Massif shows that precursor of these rocks was a high-pressure alkali feldspar – quartz – garnet – biotite – kyanite bearing coarse-grained hypersolvus banded orthogneiss. It underwent an unusual process of almost static isochemical recrystalization into a plagioclase - K-feldspar fine-grained matrix containing subordinate large quartz ribbons. The newly formed matrix feldspar grains maintained roughly the lattice orientation of parental perthite crystals. Such fine-grained matrix underwent mylonitization and decompression with small amount of partial melt via very efficient combination of GBS with dislocation creep and presumably grain-boundary diffusion. After exhumation to mid-crustal levels the cooling granulites deformed by much less effective dislocation creep similarly to common orthogneisses. The early evolution recognized for the Blanský les felsic granulites may be extrapolated also to other Variscan felsic granulites including the Saxonian granulite massif. The low viscosity of the granulitic mylonite fabric suggests that part of the Variscan lower crust was weakened by several orders of magnitude at the onset of granulite exhumation. The study also sheds new light on common rheology of felsic minerals at lower crustal conditions. While Qtz keeps the same deformational mechanism throughout the complex history of the described felsic rocks, feldspars accommodate deformations by various mechanisms depending on actual conditions, which invokes rapid switches in rheology of the feldspar-dominated rocks.

Keywords: Felsic granulites, Quantitative microstructural analysis, Quartz and feldspar rheology, Moldanubian domain, Variscan belt.

2 Introduction

Deformational mechanisms governing rheology of lower crustal rocks are often hard to determine due to annealing of the HP microstructures during exhumation, eventually recrystalization in later deformations or retrogressive chemical reactions. Under granulite-facies conditions the ductile strain is usually accommodated by dislocation creep, or diffusion creep sometimes complemented by grain boundary sliding mechanism (GBS) (Martelat et al., 1999). All of these mechanisms may cooperate in HT environment, each having variable importance. Grain boundary diffusion or presence of fluids, eventually partial melt, may favor

the GBS on the expense of other mechanisms and allow for a granular flow with superplastic characteristics, particularly in case of fine-grained rocks. Experimental works on crystal-melt mixtures (Rosenberg & Handy, 2005) define a rheological boundary at several percent of melt content (MCT) when stiffness of the mixture suddenly drops, presumably due to such a change of dominant deformational mechanism.

Feldspars (Fsp) belong to the essential constituents of the Earth crust, but their deformational behavior isn't yet fully understood due to complexity of partial mixing of end-members and changes in crystallographic structure. We present microstructural analysis from exceptionally preserved samples of lower-crustal felsic granulites from an 8x2 km (Franěk et al., 2006) domain of almost intact granulite-facies fabrics. It forms part of Blanský Les granulite massif (BLG) in southern Bohemian Moldanubian domain, which belongs to Paleozoic Variscan collisional chain in central Europe. The microstructural study combined with published petrological PT estimates indicate switching of Fsp rheology during the granulite formation and exhumation, that is ascribed to chemically and deformationally driven recrystalization, variable grain size, changing temperature and amount with distribution of partial melts.

The feldspar recrystalization driven mainly by chemical disequilibrium of the Or-Ab-An solid solution has been studied on natural examples (Putnis, 2002) or experimentally (Stunitz & Tullis, 2001), but these studies focused mainly on LT water-assisted processes below ~500°C. There the original chemically unstable Fsp undergoes dissolution and reprecipitates as two separate feldspars of different composition. Such studies cannot be easily extrapolated to our water under-saturated HT situation at minimally 850°C (Štípská & Powell, 2005), where the available fluid is represented by partial melt rather than water.

Felsic granulites represent the far most abundant deep crustal rocks exposed in Variscan chain. Unraveling their complex deformational behavior then allows for broader considerations on the rheology of Variscan lower with middle crust at certain stages of the orogeny.

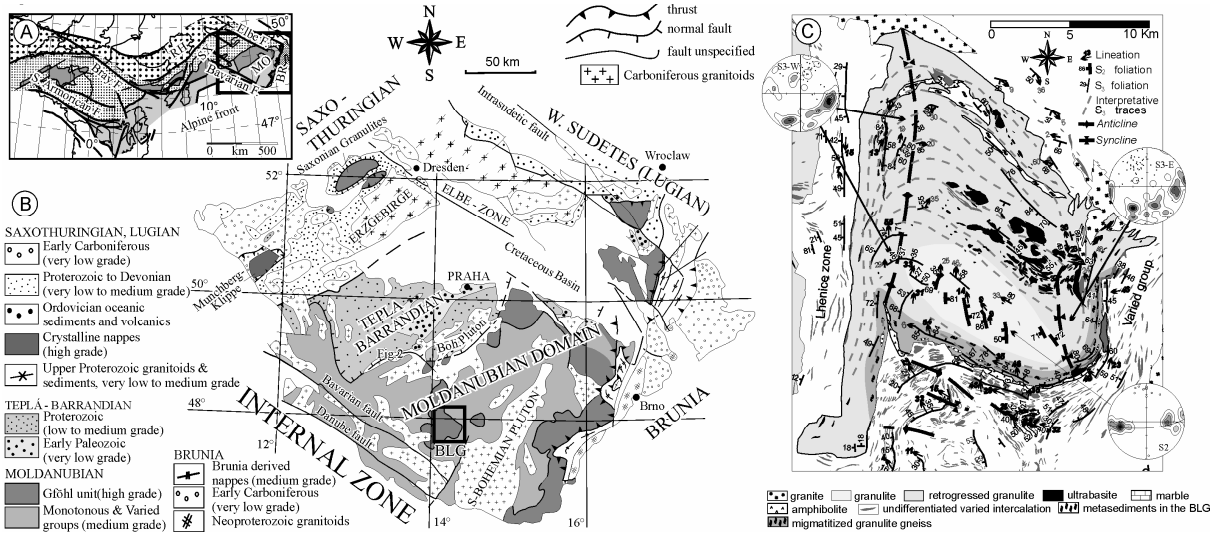

Fig. 1. (A) Position of the Bohemian Massif in frame of Variscan chain in Europe. (B) Simplified geological units constituting the Bohemian Massif. Rectangle marks the study area depicted in detail C. Modified after (Franke, 2000). (C) Structural map of the Blanský les granulite massif modified after (Franěk et al., 2006). Stereographic projections depict contoured densities of foliation poles and dots mark corresponding lineations: S_2 - 11 foliations and 15 lineations, S_3 - W 51 foliations and 35 lineations, S3 - E 51 foliations and 54 lineations. Note that in all cases the foliation poles are distributed along great circle(s) while the lineations plunge parallel to π-axes corresponding to these great circles.

2.1 Geological setting

The Bohemian Massif (Fig. 1A, B) represents the easternmost exposure of Variscan orogen in Europe. During the 380-300 Ma complex subduction - collision a ~300 km wide orogenic chain has developed, showing tectonic zonation comparable to other European Variscan fragments. From the NW to the SE following tectonic sequence is developed: undeformed Paleozoic Saxothuringian sediments to high-grade Saxothuringian crystalline, suture zone and lower-grade Teplá-Barrandian unit. Further to the SE the arc-related granitoid plutons separate the Teplá-Barrandian folded Paleozoic sediments from high-grade Moldanubian unit, which shows widespread anatexis and contains slices of lower-crustal and mantle rocks. This pervasively deformed root domain is further to the E bounded by the Brunia microplate (e.g. Schulmann et al., 2005), which is almost unaffected by Variscan tectonometamorphic processes.

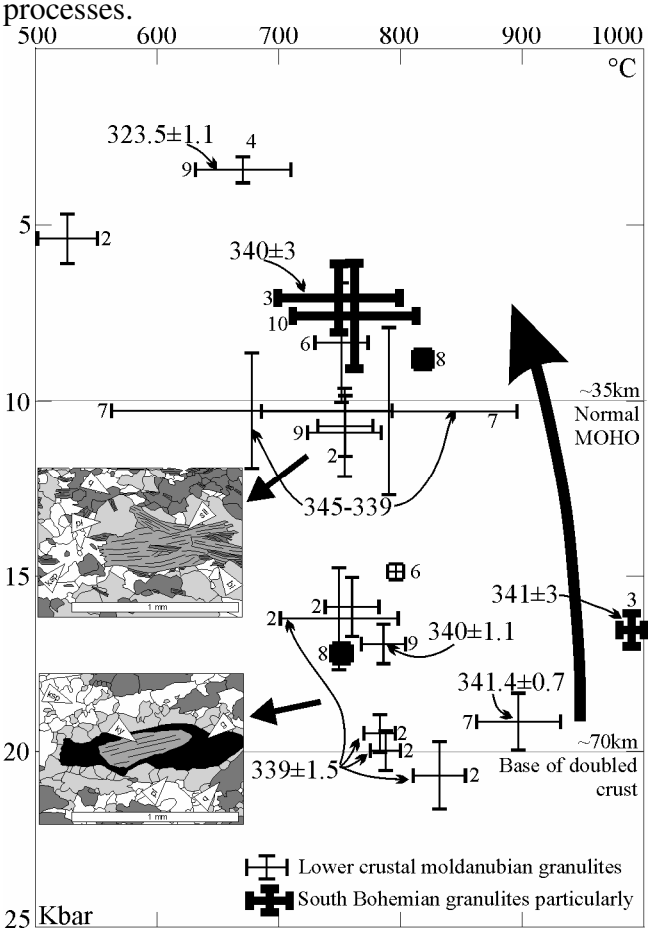

Fig. 2. PT estimates from Moldanubian granulites accompanied by relevant radiometric ages suggest almost isothermal rapid exhumation from peak metamorphic conditions to mid-crustal levels. Results from south Bohemian bodies emphasized by thick lines.

The Moldanubian zone exhibits complex mixing of middle- with lower-crustal segments, offering an excellent opportunity to examine the exhumation processes operating in the collisional setting. The exhumed lower crust designated as Gföhl unit (Matte et al., 1990) represents felsic granulites with anatectic gneisses that enclose small bodies of mafic granulites, mantle rocks and eclogites. Mid-crustal level dominated by paragneisses and called Drosendorf unit (Tollmann, 1982) was according to lithology divided by (Fuchs, 1976; Matte et al., 1990) into Monotonous group, with only limited content of intercalations like amphibolites or quartzites, and Varied group bearing significant portion of amphibolites, quartzites and marbles. The studied large Blanský les granulite massif in Southern Bohemia, which belongs to the Gföhl unit, is located in a complex stack of Monotonous and Varied rocks being accompanied by several neighboring granulite bodies.

2.2 Deformational history of the Blanský les granulite

(Franěk et al., 2006) revealed succession of three ductile fabrics inside the BLG (Fig. 1C) documenting two-stage exhumation history of the lower-crustal rocks. S_1 compositional banding of ~1 cm thick Qtz and Fsp dominated bands was almost entirely reworked by D_2 episode. The S_2 penetrative cleavage, parallel to axial planes of passive F_2 folds, is marked by remnants of thinned and rotated compositional banding inherited from S_1 and by stretching lineation defined by strong elongation of Qtz ribbons and Bt aggregates. Both S_1 and S_2 exhibit syntectonic mineral assemblages Grt-Ky-Bt-Kfs-Pl-Qtz (mineral

abbreviations are after (Kretz, 1983)) indicating granulite-facies conditions and they are preserved mainly in large elliptical domain inside the BLG. Decompressional Pl rims around Ky (Tajčmanová et al., 2007), syntectonic with D_2 phase, indicate significant uplift during this stage. On the edges of the mentioned relict domain the S_2 is transposed into S_3 amphibolite-facies fabrics via outcrop scale folds with developing axial cleavage. The S_3 dominates in majority of the BLG, showing syntectonic retrogressive breakdown of previous Grt to Bt and Ky to Sil. It was interpreted by (Franěk et al., 2006) as a result of mid-crustal horizontal shortening accompanied by imbrications.

2.3 Geochronology and petrology of the South Bohemian granulites

PT estimates (Fig. 2) of peak metamorphic conditions were calculated by various authors using either conventional thermobarometry to obtain ~ 1000 ºC / 1.6 GPa (e.g. Carswell & O´Brien, 1993; Cooke, 2000; O'Brien & Seifert, 1992; Vrána, 1989) or thermodynamic modeling in Thermocalc software which yields 750-850 °C / 1.6-1.8 GPa (Štípská & Powell, 2005) or TWEEQU that gives 970-1000 °C/1.6-1.7 GPa (Kröner et al., 2000). The thermodynamic models give for the amphibolite-facies overprint 700 – 800 °C / 0.5-0.7 GPa (Štípská & Powell, 2005), 700-800 °C / 0.6-0.8 GPa (Kröner et al., 2000) or 710-810 °C / 0.75-0.77 GPa (Verner et al., 2007).

Radiometric ages (Fig. 3) ascribed to crystallization of protolith of the South Bohemian felsic granulites span between 469±4 and 357±2 Ma (U-Pb method on Zrn, Kröner et al., 2000; Wendt et al., 1994). Subsequent peak HP metamorphism took place between 351±6 Ma (Wendt et al., 1994) and 341±3Ma (Kröner et al., 2000). Retrogression under amphibolite-facies conditions proceeded immediately after exhumation, marked by ages from 340±3 to 338±3 Ma (both U-Pb on Zrn, Kröner et al., 2000). Cooling below ~500°C constrains the 331±1 Ma Ar-Ar age on Hbl from an amphibolite adjacent to the BLG (Košler et al., 1999). The petrological results combined with radiometric ages suggest very rapid almost isothermal exhumation of the felsic granulites from the lower- to mid-crustal levels.

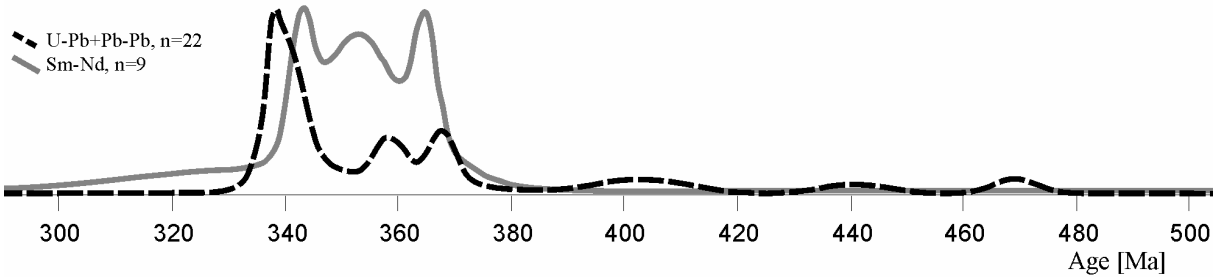

Fig. 3. Radiometric Sm-Nd, U-Pb and Pb-Pb ages from the south Bohemian granulites presented as a sum of probability curves for individual published values. For individual ages and citations see Appendix 1.

2.4 Granulite precursor

The question of felsic granulite precursor hasn't been unambiguously resolved yet. Based on geochemical arguments the protolith of the felsic granulites is considered to be a granitic igneous rock (e.g. Fiala et al., 1987; Finger et al., 2003; Jakes, 1997; Janoušek et al., 2004; Janoušek et al., 2006; Kotkova & Harley, 1999). (Janoušek et al., 2004) suggest an Ordovician granitic protolith with model age around 450 Ma, supported also by radiometric U-Pb zircon ages of (Kröner et al., 2000) or (Friedl et al., 2003). On the contrary (Schulmann et al., 2005) proposed a Devonian age of the granulite protolith (around 370 - 400 Ma), which would originate by melting of continental crust in the back arc region of the Saxothuringian subduction. The protolith major element composition corresponds to end-members of granitic

fractionation trend and excludes any sedimentary precursor, the LIL elements are enriched and Eu exhibits negative anomaly (Janoušek et al., 2004). The only chemical difference against common granites represents depletion of granulites in U and Th. Solitary experimental work related to the studied granulites performed (Tropper et al., 2005), who heated a granitic protolith to the peak 1000 °C / 1.6 GPa, simulating subsequent almost isothermal decompression to 900 °C / 1.2 GPa and mid-crustal cooling to 800 °C / 1.2 GPa. Apart from ca 30 mol% melting by simulated lower-crustal heating, the samples revealed large degree of decompressional melting during subsequent pressure decrease, which increased the melt content from 33 to 41%. The melt rapidly crystallized during mid-crustal cooling so that almost none finally remained at 800 °C / 1.2 GPa. Despite they didn't simulate probable contemporaneous outflux of melt as well as hydration documented during exhumation (e.g. Franěk et al., 2006), their results still pose important constraints on the timing and extent of partial melting in the natural granulites. Additionally they produced only single alkali feldspar above 850 °C on the expense of previous K- and Na- rich complementary ones.

3 Microstructural and petrographical characteristics of fabrics in felsic granulites

3.1 S_1 compositional banding

S_1 fabric is characterized by ~1cm alternation of Qtz and Fsp dominated bands, which were observed as limited remnants throughout the relict domain of granulitic fabrics inside the BLG (Fig. 4). On the microscopic scale the bands are often internally recrystalized into S_2 microstructure, but on several localities a mosaic of large microperthites has been preserved inside the thick Fsp-dominated bands. The individual perthite (Pth) grains are separated from each other by the fine-grained granulitic S_2 matrix. Mutual textural relations of the matrix and Pth porphyroblasts, particularly finger-like matrix domains pervading into porphyroblasts, imply that the perthites represent precursor of the matrix and that the Fsp-dominated bands originally constituted of such large perthites (Fig. 5A).

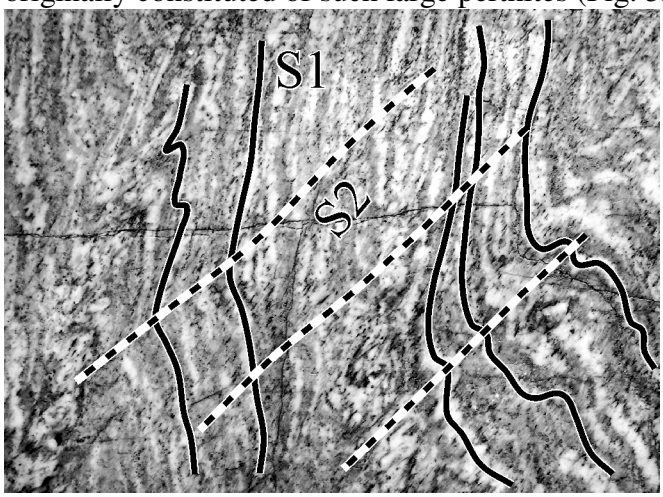

Fig. 4. Field photograph of passive F_2 folds depicting penetrative development of S_2 axial cleavage across the folded S_1 compositional banding.

50 thin-sections containing the large Pth porphyroblasts were prepared from samples of S_1 banding. The sections are oriented with respect to penetrative S_2 mylonitic foliation, representing mainly XY sections or less commonly XZ or YZ planes (X direction is parallel to lineation, Z perpendicular to foliation). They expose ~250 grains of large unzoned perthites which represent decomposed original alkali feldspars of 68.2% Or 27.3% Ab 4.5% An average composition that was acquired by areal analyses of regions containing ~100 Pl microscopic exsolutions. The relict Pth porphyroblasts reveal two generations of perthitic exsolutions (Fig. 6B). The coarser ones, presumably older, exhibit elongated rhomboidal shapes and constant An_{20-25} composition, with grain boundaries preferentially oriented in two directions. The second generation of exsolutions represent micro- to crypto-perthitic films whose composition cannot be determined directly because of small thickness, but we can infer almost pure albite

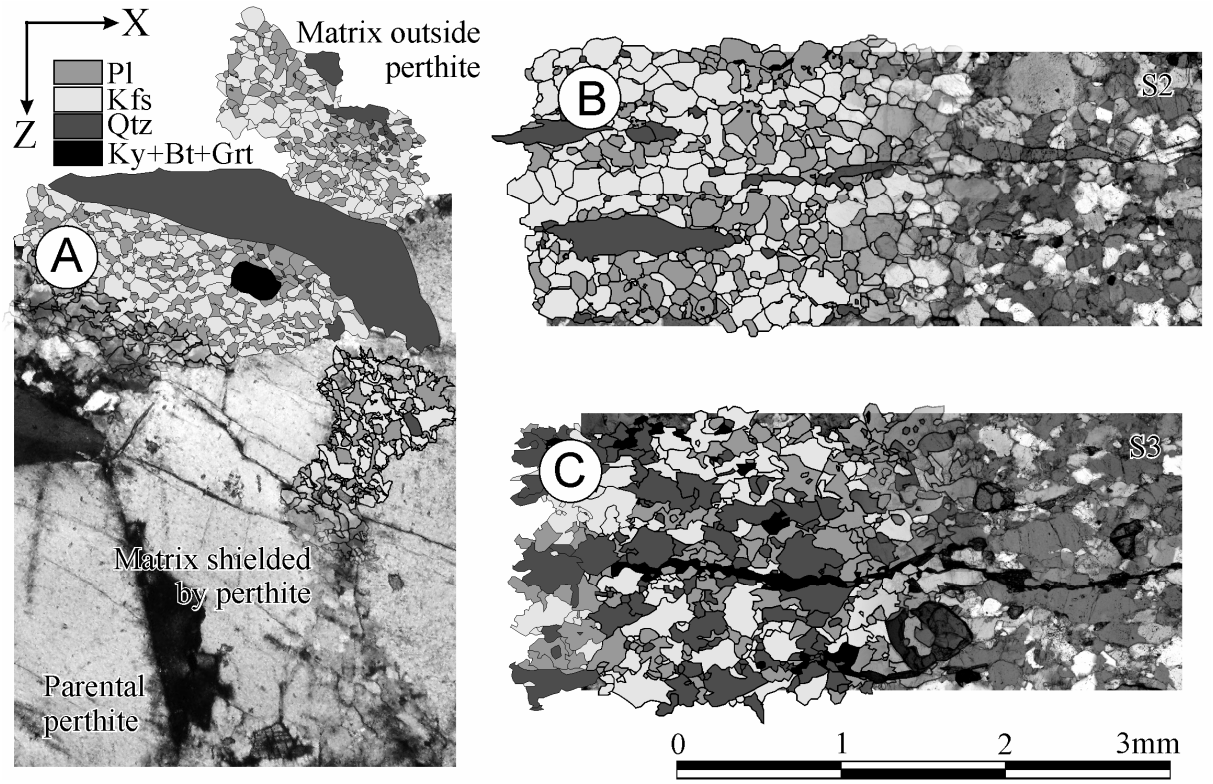

Fig. 5. Microphotographs of representative X-Z thin sections (X is parallel to lineation, Z normal to foliation plane) with corresponding digitalizations, that were subsequently used for quantitative microstructural analysis. (A) Granulitization inside perthite and faintly deformed granulitic matrix outside the perthite grain. (B) Progressively developed granulite-facies S_2. (C) Amphibolite-facies S_3 fabric.

composition from Ca compositional maps. In average the Kfs domains of the perthite contain 87.1% Or, 12.3% Ab and 0.6% An, while the microscopic Pl exsolutions bear 0.8% Or, 76.7% Ab and 22.5% An. All of the ~250 observed Fsp porphyroblasts represent perthites, suggesting that during their crystallization all the feldspar components were incorporated into a single alkali feldspar dominated by Or end-member. This may be correlated with the experimental work of (Tropper et al., 2005) focused on South-Bohemian felsic granulites, where only single alkali feldspar existed above 850ºC.

The perthites bear often inclusions of Qtz, Grt and Ky or more rarely Bt, Zrn, Ap rimmed by Mnz, Ilm, Rt and Fe-sulphide (Fig. 6D,E,F,G,H). Qtz inclusions are almost always built of a single crystal with oval or euhedral shapes up to 1 mm large, being occasionally split into mosaic of smaller sub-grains. Grt crystals enclosed in perthites, max 1.2 mm in diameter, exhibit euhedral shapes with sharp edges and flat compositional profile of 54,4% Alm 24,0% Prp 18,8% Grs 2,8% Sps which changes only at crystal rims to 60.4% Alm 28.1% Prp 10.6% Grs 0.9% Sps. Ky inclusions show elongated subhedral shapes probably due to consummation in a decompressional reaction with surrounding alkali Fsp (Tajčmanová et al., 2007), Bt inclusions exhibit short prismatic habitus and bear in average 4.17 wt % TiO_2. Except Ky and late chloritization of Bt none of the observed inclusions show signs of chemical breakdown.

The microstructural and petrographical character of S_1 cannot be examined completely, because the Qtz bands are initially to entirely disintegrated into syn-D_2 ribbons and Qtz inclusions enclosed in Pth may not represent D_1, but pre-D_1 feature. Several large Qtz grains protected in perthite pressure shadows exhibit amoeboid shapes reaching size of 4 mm, but these shapes may also not represent typical examples of S_1 Qtz microstructure. The perthite grains reach size up to 1.7 cm with circular to slightly elliptical geometry, preserving rarely Pth-Pth or Qtz-Pth grain boundaries. Whereas the Qtz-Pth boundaries are always straight, the

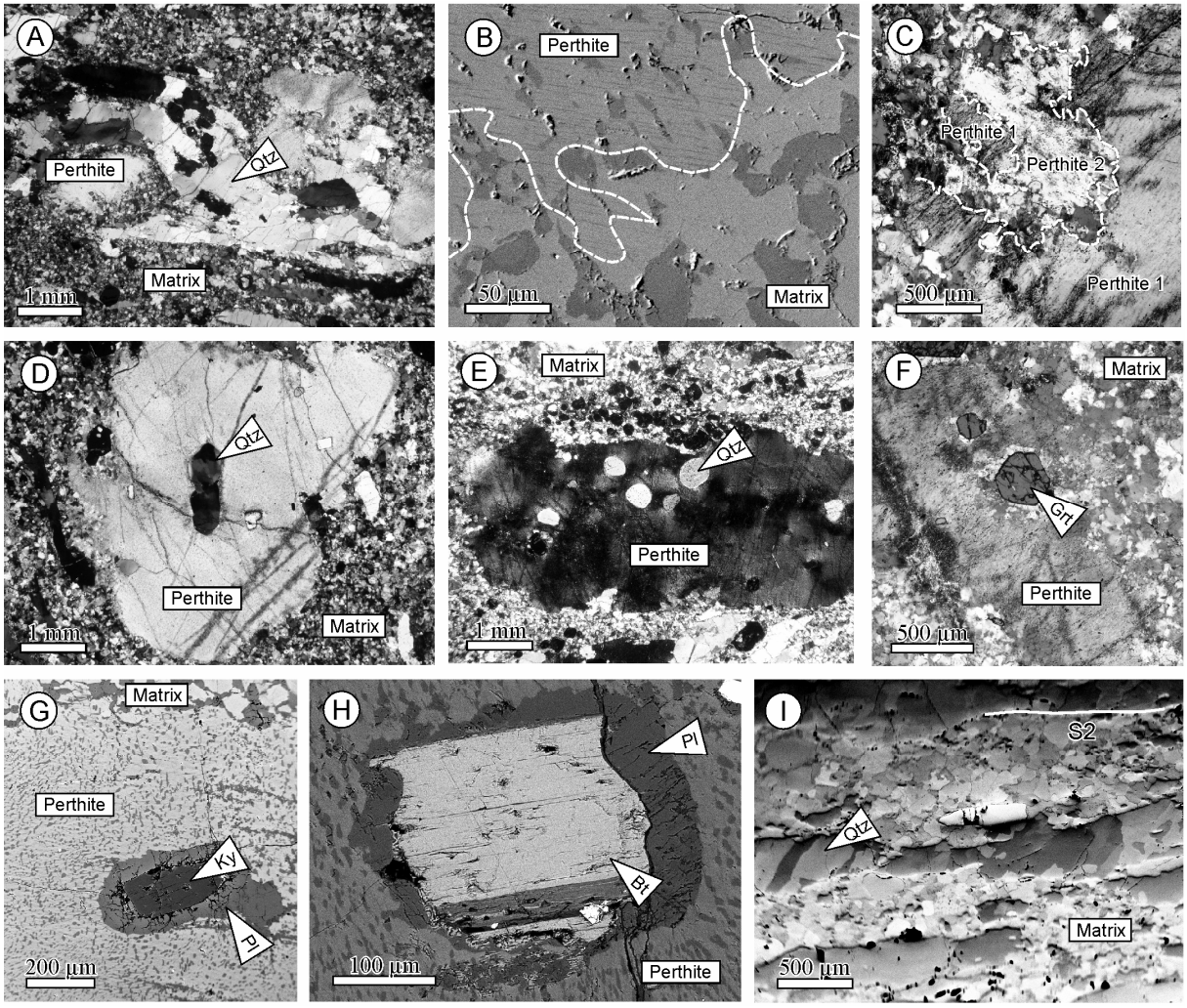

Fig. 6. (A) Qtz ribbons encapsulating perthite porphyroblast that is partially recrystalized to granulitic matrix. The mutual relations suggest that the Qtz encircled the porphyroblast already before granulitization. Crossed polarizers. (B) Detailed BSE image of the sharp transition between parental perthite and shielded granulitic matrix marked by disappearance of cryptoperthitic films in the matrix. (C) Relict curved boundary between two perthites depicting their interface during D_1 deformation. Crossed polarizers. (D) Euhedral Qtz inclusion in perthite exhibiting mosaic of small subgrains. Crossed polarizers. (E) Strain free drop-like Qtz inclusions inside perthite. Crossed polarizers. (F) Euhedral Grt inclusions in perthite showing onset of granulitization at their edges. Crossed polarizers. (G) Ky inclusion inside perthite, rimmed by thick Pl envelope developed during decompression. BSE image. (H) BSE picture of inclusion of short prismatic Bt crystal rimmed by Pl inside perthite. The lower dark part represents late breakdown of the Ti-rich Bt into Chl + Ilm. (I) FSD image of large Qtz ribbons parallelized with S_2 fabric, showing crystallographically determined subgrain boundaries developed during D_2 mylonitization.

Pth-Pth interfaces show significant curvature resembling sutures produced by grain-boundary migration processes or step-like twin intergrowths (Fig. 6C). Lattice preferred orientation (LPO) of perthite porphyroblasts wasn't studied because their large grain-size doesn't allow collecting sufficient amount of measurements per thin section.

Quantitative bulk rock chemical analysis of S_1 relict samples of felsic granulite with widely preserved large perthites (Oxide wt %: SiO_2 71.98, TiO_2 0.42, Al_2O_3 13.53, Fe_2O_3 1.18, FeO 2.10, MnO 0.03, MgO 0.73, CaO 1.93, Na_2O 2.76, K_2O 4.01, P_2O_5 0.15, H_2O- 0.22, H_2O+ 0.56, CO_2 0.03, Sum 99.63) reveals major element composition very similar to the average of felsic granulites from the whole Bohemian Massif summarized e.g. by (Janoušek et al., 2004).

Particularly the SiO_2, Al_2O_3, Na_2O and K_2O contents are in accord with the average values, while the MgO is slightly higher and CaO with FeO are strongly enriched in our sample compared to the reported average. The overall compositional similarity proves that the examined relict samples do not represent an exceptional domain but rather typical felsic granulite, and that their interpretations may be extrapolated to the other felsic granulites in the Bohemian Massif. The compositional banding resembling the S_1 fabric in the BLG was reported as the oldest fabric also from the large Saxonian granulite massif in the Saxothuringian domain (Behr, 1961). For example Figs. 9A, B in his publication depict samples of S_1 compositional banding texturally equal to the BLG S_1 fabric. Additionally the relict perthites from the Saxonian felsic granulites enclose undeformed crystals of kyanite and drop-like quartz (bild 31c in Behr, 1961) similarly to the BLG samples.

3.2 Decompressional S_2 granulitic mylonite

The penetratively developed S_2 mylonitic foliation predominating in the relict granulite-facies domain of the BLG exhibits abundant syntectonic decompressional features suggesting that the S_2 achieved significant exhumation of the felsic granulites (Franěk et al., 2006). The most striking S_2 feature represents separation of the main constituents Qtz, Kfs and Pl into two distinct media – the predominating fine-grained granulitic Kfs-Pl-Qtz matrix and the subordinate large elongated Qtz ribbons defining penetrative lineation (Fig. 5B). Disintegration of the coarse-grained S_1 into this mixture proceeded via spectacular process which must be examined first.

3.2.1 Initiation of S_2 microstructure

The process of perthite recrystalization into the fine-grained matrix (granulitization) can be observed in numerous finger-like domains of granulitic matrix pervading into the perthite porphyroblasts (Fig. 7A). Such domains of newly formed matrix were shielded by the surrounding stiff perthites from significant deformation at any later time. The granulitization

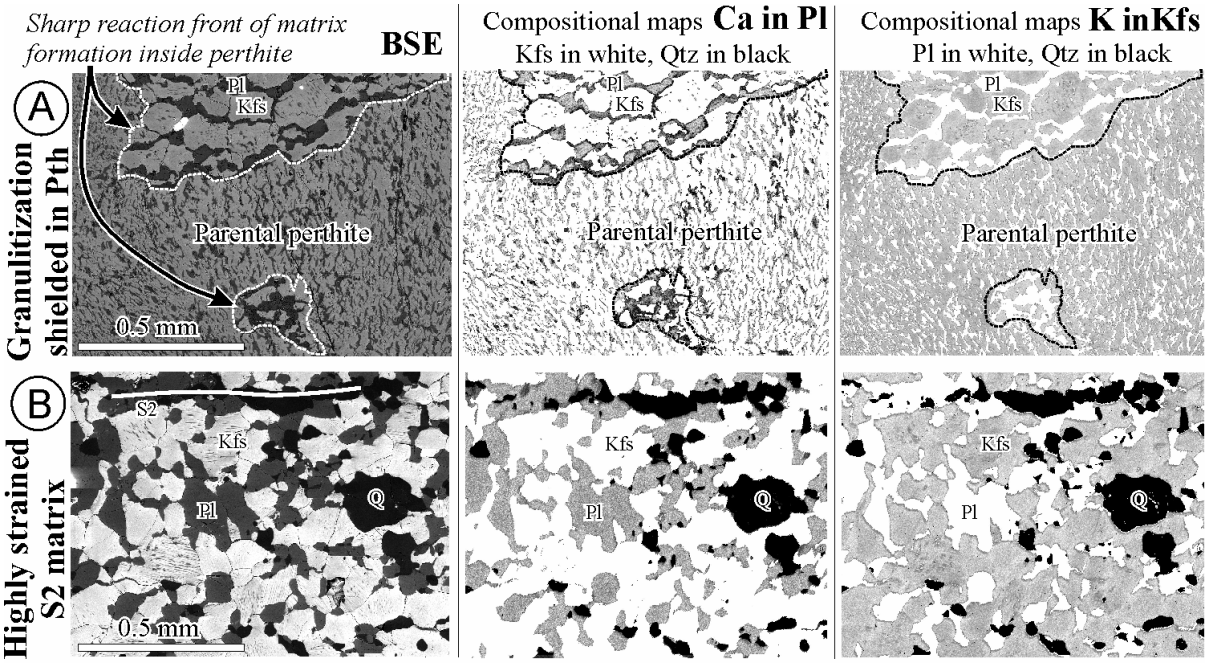

Fig. 7. Compositional maps of Ca and K from matrix shielded inside parental perthites (A) and progressively deformed matrix in S_2 fabric (B). In case of Ca the Kfs and Qtz grains are masked by white and black color to stress out the Ca zonality in Pl. Similarly the Pl and Qtz grains are masked in the K distribution map to point out the K zonality in Kfs. The BSE images are offered for better orientation in phase distribution.

heterogeneously consumed the Pth porphyroblasts in random directions, as all of the XZ, YZ and XY sections show random orientations of the recrystalized domains inside Pth. Small remnants of parental Pth grains occasionally escaped granulitization, being distinguished from the S_2 matrix by the presence of microperthitic exsolutions (Fig. 7B).

The granulitization initiates inside intact perthite grains or along Pth-Pth and Grt-Pth grain boundaries, while at Qtz-Pth or Ky-Pth boundaries it occurs only rarely. Distortion of the perthite crystal lattice is often observed in continuity of the recrystalized domains, being marked by undulose extinction, but it is not possible to decide whether the distortion was a cause or a consequence of the recrystalization.

The Pth porphyroblasts are often tightly encircled by Qtz ribbons documenting that the Pth was stronger than the Qtz. In some instances the Qtz ribbons encapsulate lens shaped domain partially made of Pth grain and partially of the matrix (Fig. 6A), while the matrix analysis given later suggest that the matrix was weaker than the Qtz ribbons. This relation suggests that these ribbons developed and encircled the Pth grain already before its partial granulitization, otherwise they would squeeze the matrix outwards. On the other hand the Qtz grains released during granulitization from relict perthites (Fig. 5A) are being immediately squeezed into ribbon forms parallel to S_2 foliation suggesting contemporaneity of granulitization with Qtz ribbon formation. The Qtz ribbons define L_2 stretching lineation, i.e. developed during D_2 phase. Development of the Qtz ribbons before and during granulitization process implies that the granulitization proceeded also during the D_2 episode.

The Kfs grains in the shielded matrix show mainly oval shapes of mild ellipticity in contrast to variable geometry of Pl that spans from circular grains at Kfs triple junctions to highly elongated grains coating boundaries between Kfs crystals or between new Kfs and relict Pth (Fig. 7A). At the granulitization front the mutual grain boundaries of Kfs and Pl are curved and irregular, while farther to the matrix the feldspar boundaries straighten presumably to minimize their surface energy (Fig. 7A and 12B).

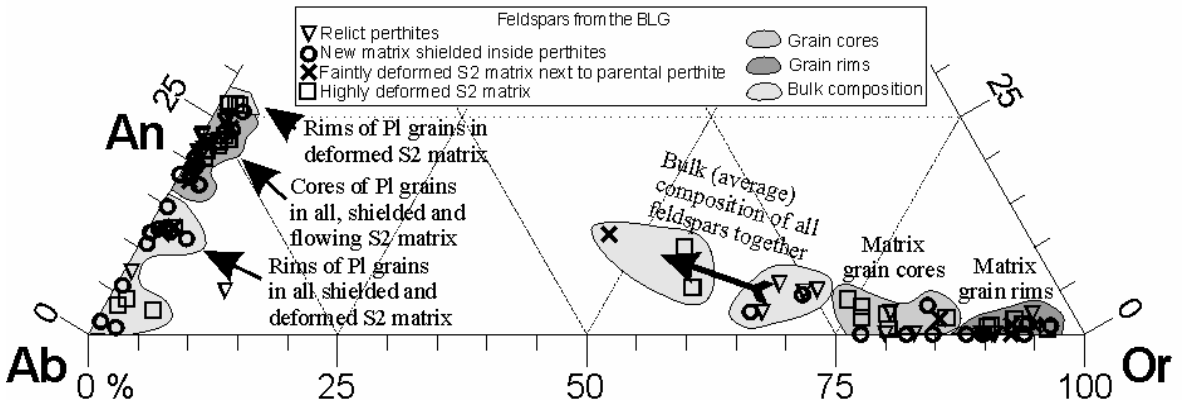

Fig. 8. Ternary plot of feldspar compositions acquired from microchemical analyses. Similar bulk compositions of parental perthites and shielded matrix are contrasted against areal analyses of deformed matrix. Zonality of Pl and to lesser extent also Kfs is pointed out as description of data clusters.

To unravel chemical processes operating during granulitization, compositional maps of the recrystalized domains were examined, being complemented by spot or areal analyses of representative places (Fig. 7). The analyses, plotted in Fig. 8, were conducted on scanning electron microscopes equipped with an EDX analyzer, particularly on a scanning electron microscope Tescan VEGA\\ XMU at 15kV and 0.4nA at the CGS, Université Louis Pasteur in Strasbourg, and at a scanning electron microscope CamScan CS 3200 at 15kV and 3nA at the LAREM laboratory of the Czech geological survey in Prague. Feldspar compositions were

recalculated to end-member proportions using Norm software. Areal analyses of matrix shielded inside Pth (region of ca 100 grains) yield average composition of 67.3% Or, 29.1% Ab and 3.6% An similarly to the neighboring parental perthites. In average the Kfs grains contain 87.6% Or, 11.8% Ab and 0.6% An, Pl centers consist of 1.5% Or, 78.1% Ab and 20.4% An.

Compositional maps reveal sharp reaction front separating parental Pth from the newly formed matrix (Fig. 7A). The boundary is easily distinguishable due to presence of characteristic small sheet-like microperthitic exsolutions in the Pth, while the new matrix bears Kfs free of them. Kfs grains reveal mild gradual zonality from Or_{82} in the wide cores to Or_{93} at the grain boundaries. The matrix Pl grains, also free of exsolutions, exhibit An_{18-23} cores which are roughly 2x larger than the string microperthitic exsolutions and located often in triple junctions of Kfs grains. They are surrounded by wide Pl rims of An_{11-12} composition that usually connect several of these cores. In places irregular patches of pure albite occur at the edges of Pl grains. Abrupt boundaries between these three Pl compositional zones exclude their continuous development during a single event.

3.2.2 Faintly deformed granulitic matrix

The Kfs-Pl-Qtz matrix located directly at the edge of parental Pth and suffering already initial deformation (Fig. 5A) has been briefly examined to provide a bridge between evolution of shielded regions almost lacking deformation and pervasively flowing S_2 matrix.

Microstructures of feldspars in the initially flowing matrix exhibit similar grain sizes, shapes, and distribution of phases as the shielded domains. On the other hand it differs by occurrence of Qtz grains, which suggests addition of new chemical components in comparison to Qtz-free shielded matrix. Microchemical view prove significant differences, as the areal analyses of initially deformed matrix yield average feldspar composition of 46.5% Or, 42.0% Ab and 11.5% An, values significantly different from both the parental perthites and shielded matrix. The Kfs grains bear 90.9% Or, 8.1% Ab and 1.0% An, Pl exhibits in average 1.6% Or, 76.5% Ab and 21.9% An.

The compositional map acquired at the edge of a decomposing perthite reveals mild gradual zonality of Kfs, where the rims are depleted in Ab component similarly to the shielded matrix during granulitization. Distinct pattern exhibits

Pl zoning, where only isolated remnants of An_{11-13} domains survive among An_{24} homogenous areas with ill-defined enrichment in An content at grain boundaries, a feature not observed in the shielded matrix.

3.2.3 Texture characteristics of penetrative S_2

Microstructure of progressively developed S_2 doesn't differ significantly from the shielded granulitic matrix and throughout the 8 km wide relict granulite-facies domain the S_2 macroscopic as well microscopic textures exhibit striking uniformity. The homogeneity of S_2 on scale of thin sections, outcrop and the whole S_2 – dominated region suggests, that our microstructural interpretations can be convincingly extrapolated to all the S_2 fabrics in the BLG. The above used methods in combination with extensive LPO measurements allow to define D_2 deformational mechanisms and to constrain rheology of the ascending granulites in the lower crust.

The S_2 is defined by weak mm - scale mylonitic compositional banding of stripes of granulitic matrix and stripes rich in large Qtz ribbons. The attenuation of S1 well-defined cm - thick bands into the S_2 foliation documents significant strain during the D_2 evolution (Fig. 4). Numerous tiny Qtz grains nucleate in triple junctions of Fsp grains and the quartz ribbons are being dynamically disintegrated into the homogeneous matrix of uniform grain size suggesting that they are rheologically stronger than the surrounding matrix. Grt grains

dispersed in the matrix behave as rigid objects that undergo fracturation and rounding of crystal edges, Ky crystals deform by folding and kinking. Isolated Bt flakes lie parallel to the S_2 foliation and together with Qtz ribbons define a strong penetrative lineation.

Areal analysis of a granulitic matrix region covering ~ 100 grains yield for all the involved feldspars average composition of 56.4% Or, 35.9% Ab and 7.7% An (Fig. 8). Average composition of Kfs is characterized by 84.7% Or, 13.5% Ab and 1.8% An, while Pl constitutes of 1.8% Or, 74.6% Ab and 23.6% An.

Two compositional maps acquired from the Fsp-dominated matrix (Fig. 7B) reveal typical mild zonality of Kfs reflecting loss of Na around grain boundaries, while Pl exhibits uniform An-rich composition of majority of grains. One of the two samples exhibit thin (5-10 μm) Na-rich rims around all the Pl grains, while the other is lacking such feature. These films often continue from Pl rims into interfaces between Kfs grains to separate them from each other. They are much thinner than the An_{11-12} rims in the shielded granulitic matrix and differ also in more sodic An_3 composition. These films can be interpreted either as a result of release of Na from Kfs rims via volume diffusion or as a result of melt crystallization along the grain boundaries. As the Qtz would be needed to crystallize together with the Kfs and Pl films from the hypothetic partial melt, but it is absent in the near surroundings of many of these films, we suggest that the Pl films formed by solid-state volume diffusion of Na out of Kfs to precipitate as Ab-rich films or rims of the Pl grains. Again an ill-defined increase in Ca is visible at the Pl rims, supported by chemical analyses yielding 2-3% higher An content at rims than in the homogenous large centers of Pl grains. Such observation is consistent with decompression, which is suggested to occur during the S_2 develompent.

The above mentioned Saxonian granulites document also penetrative reworking of the S_1 banding by younger S_2 cleavage characterized by fine-grained granulitic matrix containing large Qtz ribbons (Tafel 3, Figs 9a,b in Behr, 1961), which exhibit comparable relationship as the S_1-S_2 transition and S_2 characteristics observed in the BLG.

3.2.4 S_3 amphibolite-facies overprint

The S_3 fabrics prevailing in the felsic granulites of the BLG reveal highly variable degree of retrogression of the previous mineral assemblage. Hydration of granulites increases towards massif's boundaries where it is accompanied by partial anatexis (Franěk et al., 2006; Kodym, 1972). The resulting S_3 microstructure resembles rather a common Bt + Sil ± Grt containing orthogneiss than the preceding granulite and we present characteristics of this fabric to demonstrate an important and abrupt switch in deformational behavior and rheology of the felsic rocks of granitic composition at the lower-middle crust interface. For the analyses we have chosen samples less affected by hydration, where Bt doesn't coalesce into continuous bands and dominant portion of strain is unambiguously achieved by deformation of Qtz, Kfs and Pl mixture. This let's us compare deformational behavior of these minerals to the S_2 fabric.

Grain size of the Qtz, Kfs and Pl doesn't change significantly compared to S_2 but all these phases tend to form irregular grain boundaries and merge into monomineralic aggregates. The microstructure is on the scale of a thin-section homogenous, entirely disappears the differentiation to Qtz ribbons and fine-grained Fsp-dominated matrix characteristic for S_2 foliation. The abundant Bt flakes lie parallel to the foliation planes, whereas Sil in some instances defines lineation. The recrystalization processes of Qtz, Kfs and Pl operating during D_3 are sufficiently clarified using the LPO and microstructural analysis, so that chemical composition of S_3 phases was not examined in detail.

3.3 Quantitative microstructural analysis

The previous section has defined five stages of microstructural evolution: 0 - coarse grained precursor of the felsic granulites, 1 - granulitic matrix shielded inside perthites, 2 - faintly deformed granulitic matrix adjacent to parental perthites, 3 - pervasively deformed granulitic matrix mixed with large Qtz ribbons in S_2 fabric, 4 - microstructure in S3 fabric developed under amphibolite-facies conditions. The 0. stage is not enough constrained for any comprehensive characterization. To compare the four following stages we have quantified several parameters characterizing the corresponding microstructures using the PolyLX toolbox (Lexa et al., 2005) for Matlab® software package and CSD corrections program (e.g. Higgins, 1998). Four thin sections oriented parallel to lineation and perpendicular to foliation (X-Z sections) from representative samples of S_2 (956 and 1252 grains) and S_3 fabrics (848 and 886 grains) were digitalized and imported into the PolyLX and CSD corrections software. The individual shielded domains exhibiting granulitization do not contain enough grains for a textural analysis, so that four of these digitalized domains were merged together to yield 801 grains. Before merging the individual domains were rotated so that the traces of S_2 foliation outside perthites acquired the uniform horizontal orientation. Next to one of these domains the faintly deformed matrix outside perthite was digitalized covering 868 grains.

From the available quantitative characteristics we present bulk grain boundary preferred orientation (GBPO) plotted against contact frequencies (Fig. 9A), slope of linear regression from crystal size distribution (CSD) analysis vs. regression intercept (Fig. 9B) and bulk shape

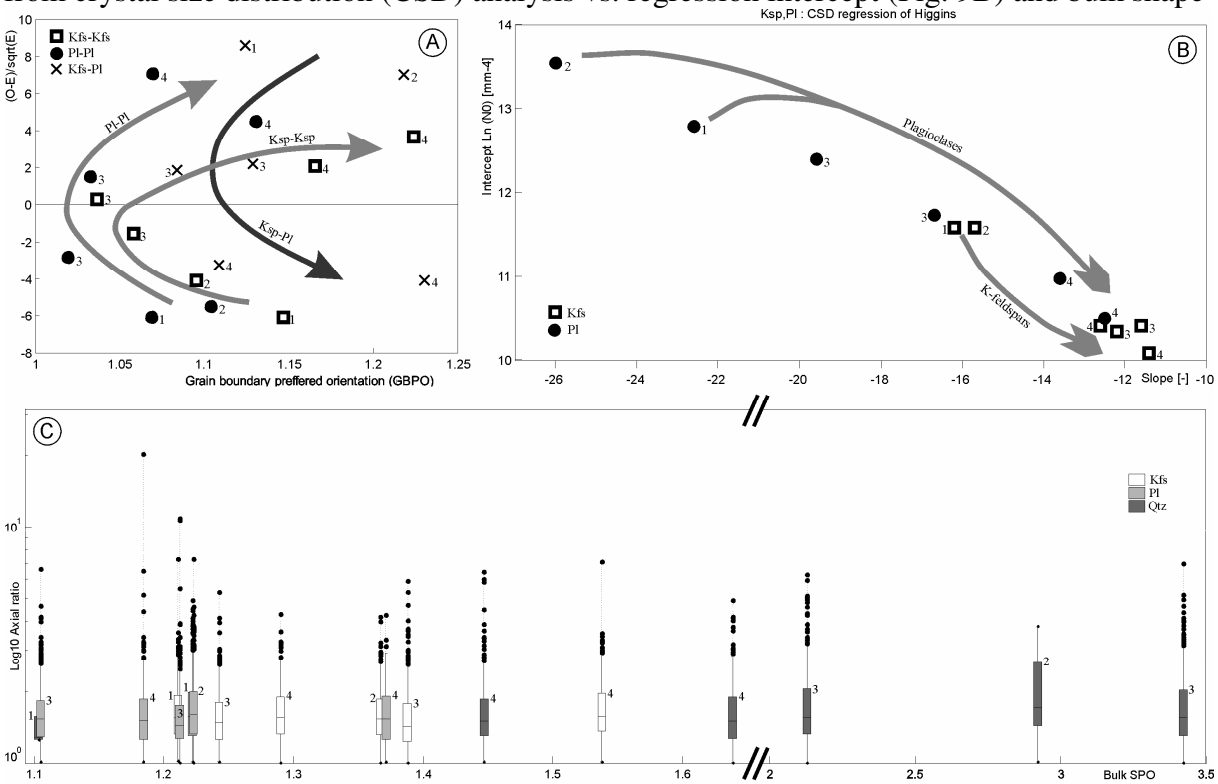

Fig. 9. Microstructural analyses performed using the PolyLX software. (A) Degree of grain boundary preferred orientation vs. contact frequencies for like and unlike boundaries of feldspars. (B) Values of slope and upper intercept of linear regression to crystal size distribution (CSD) curves for both feldspars. (C) Box plots of axial ratio of Qtz, Kfs and Pl grains plotted against bulk shape preferred orientation (SPO) of these phases. Indexes at individual data points refer to evolution stages – 1. Granulitic matrix shielded inside perthites 2. Faintly deformed granulitic matrix outside perthites 3. Pervasively deformed granulitic matrix in S_2 fabric 4. Microstructure of S_3 fabric developed under amphibolite-facies conditions.

EAD [mm]	1-Shielded matrix		2-Matrix out of Pth		3-Pervasive S2		4-Pervasive S3	
	Kfs	Pl	Kfs	Pl	Kfs	Pl	Kfs	Pl
N	334	463	332	467	472	464	253	303
Mean	0.0627	0.0470	0.0710	0.0459	0.0958	0.0732	0.0880	0.0819
St. dev.	0.0382	0.0296	0.0347	0.0225	0.0532	0.0401	0.0637	0.0564
Geomean	0.0515	0.0402	0.0620	0.0406	0.0817	0.0638	0.0702	0.0652
Geo st.dev.	1.9963	1.7481	1.8449	1.7766	1.8729	1.6961	1.9442	2.0760
Min	0.0006	0.0097	0.0001	0.0000	0.0002	0.0093	0.0169	0.0005
Quartile1	0.0337	0.0268	0.0448	0.0292	0.0565	0.0463	0.0427	0.0409
Median	0.0563	0.0423	0.0671	0.0403	0.0839	0.0647	0.0674	0.0672
Quartile3	0.0844	0.0594	0.0908	0.0590	0.1267	0.0906	0.1092	0.1115
Max	0.2500	0.3226	0.1923	0.1416	0.4812	0.3350	0.3209	0.3691
Trimean	0.0577	0.0427	0.0675	0.0422	0.0877	0.0666	0.0717	0.0717

Tab. 1. EAD (Equal Area Diameter) statistical characteristics depicting Kfs and Pl grain size evolution from the granulitization process to amphibolite-facies syntectonic retrogression.

preferred orientation (SPO) against axial ratios (Fig. 9C). The grain size of both feldspars is given in Tab. 1 as statistic of equal area diameter (EAD) values.

The contact frequency method (CFM) compares the observed (O) count of contacts between two phases with the value expected (E) for a perfectly random distribution. The boundaries are designated as "like" for contacts between grains of one phase or "unlike" in case of boundary between two different phases. The resulting values (O-E)/sqrt(E) from one sample are positive for like contacts and negative for unlike contacts if the corresponding microstructure tends to form monomineralic aggregates. On the other hand the unlikes exhibit positive values while the likes are negative when the phases tend to intermix with each other. The CSD linear regression analyzes a recalculated grain size histogram of individual phases to obtain slope of regression line and its intercept with y axis. The intercept values are proportional to the nucleation rate of the examined phase, while the slope is proportional to growth rate of existing grains. Individual absolute values are in deformed rocks meaningless, but allow to compare ratio between nucleation and grain growth among more samples. The shape, SPO and GBPO of recrystallized grains strongly depend on types of active deformation mechanisms. The aspect ratio, SPO and GBPO are relatively high for grains deformed by dislocation creep while low values characterize diffusion creep or grain boundary sliding, which are accommodated by diffusional transfer of atoms and molecules or slip and rotation of individual grains (Behrmann & Mainprice, 1987; Boullier & Gueguen, 1975). A statistical characteristic of grain size is presented because of its sensitivity to stress and temperature (Schmid et al., 1999). Due to lognormal distribution of grain sizes the median was considered to represent the most reliable statistical value (Lexa et al., 2005).

3.3.1 Granulitization

Grain size (EAD) statistic exhibits for Kfs the median value 0.06 mm, while Pl is characterized by the size of 0.05 mm. The low shape preferred orientation (SPO) of both phases (1.21 for Kfs and 1.22 for Pl) complements low grain boundary preferred orientation ~1.1 and low axial ratio 1.26-2 for both phases. The contact frequency method (CFM) yields like contacts far below random distribution (around -6), whereas the unlike count lies high above it (at 8.5). Such disproportion suggests very regular distribution of Kfs and Pl grains without any tendency to form monomineralic aggregates. Boundary straightness is higher for the unlike contacts than for the like ones. The CSD analysis reveals differing values for Kfs and Pl grains. During the granulitization the intercept reaches 11.6 for Kfs and 12.8 for Pl, but the slope yields -16.2 for Kfs and -22.6 for Pl. The values suggest that there was much higher nucleation rate compared to grain growth for Pl than for Kfs.

3.3.2 Faintly deformed S_2 matrix

Microstructural analysis reveals for feldspars characteristics similar to the shielded matrix, differing only in significant content of small grains of interstitial Qtz. Grain size distribution

of Kfs reaches median at 0.07 mm, while distribution of Pl shows the size of 0.05 mm and Qtz yields 0.06 mm. SPO of feldspars remains low (Pl 1.2 and Kfs 1.4), but Qtz exhibit value 2.9, despite all the three phases show low axial ratios around 1.6. The GBPO of Qtz-Kfs and Qtz-Pl interfaces reach high values of 2.1-2.3, while the other boundaries maintain low degree of preferred orientation 1.1-1.2. Also boundary straightness rises in case of Qtz-Kfs and Qtz-Pl pairs to a value of ~8, while the other boundaries yield ~2. The CFM yields low values of -4 for Kfs-Kfs and -5.5 for Pl-Pl boundaries, while the Qtz-Qtz contacts lie at a value of 3 above random distribution. The Kfs-Pl boundaries show high value of 7 and Qtz-Kfs with Qtz-Pl give 3 and 1.5 particularly. Such set of data suggests that the Kfs grains remain separated by Pl and vice versa, while Qtz tend to coalesce into aggregates that are sharply bounded against surrounding Fsp matrix. The CSD calculations yield intercept at 11.6 and slope -15.7 for Kfs, but the Pl exhibits intercept at 13.5 while slope reaches -26.0, a disproportion implying that Pl nucleation was much more important than growth of existing grains compared to Kfs.

3.3.3 Microstructures of highly deformed S_2

Grain size distribution exhibits median of 0.1 mm for Kfs, ill-defined maximum around 0.07 mm for Pl and 0.04 mm median for Qtz. SPO remains very low for Kfs (1.2-1.4) and Pl (1.1-1.2), while Qtz exhibits distinct values 2.1-3.4. GBPO for Kfs-Kfs and Pl-Pl boundaries reaches almost to 1.0 and Kfs-Pl boundaries show also very low preferred orientation of ~1.1. Qtz-Qtz values don't change substantially, giving 1.25-1.45 and Qtz-Kfs with Qtz-Pl interfaces yield 1.54-1.61 and 1.45-1.57 respectively. Boundary straightness is generally lower for like contacts (~1.6-10) than for unlikes (6.3-10). CFM values of feldspars oscillate around 0 value for both like and unlike contacts documenting change to a random mutual distribution of the two phases. The Kfs-Qtz and Pl-Qtz boundaries yield negative values while Qtz-Qtz are very positive which reflects abundance of monomineralic Qtz ribbons in matrix of intermixed two feldspars. Generally the CFM analysis combined with optical observations implies that the feldspar dominated bands behave in a very different way than Qtz. The CSD computation reveals decrease of nucleation vs. growth rate ratio for Pl, which is nevertheless still higher than for Kfs.

3.3.4 Retrogressive S_3

EAD grain size median reaches 0.09 mm for Kfs and 0.08 mm for Pl, while Qtz shows histogram with ill-defined region of most common values around 0.09 mm. The SPO mildly increases to 1.3-1.5 for Kfs, and to 1.2-1.35 for Pl, while Qtz exhibits strong decrease to 1.4-1.6. Kfs-Qtz and Pl-Qtz boundaries yield GBPO between 1.3-1.5, values systematically higher than rest of boundaries which range between 1.1 and 1.2. Boundary straightness spans between 1.3 – 16 for all the mentioned phase contacts. CFM results in moderate positive values for like boundaries while the unlikes reach moderately negative values. These can result only from formation of monomineralic aggregates that contrast with previous D_2 mixing of phases. According to CSD analysis the ratio of nucleation and growth rate is almost the same for both feldspars. The Bt grains were excluded from the presented S3 analyses because the Bt behaves differently than Qtz, Kfs or Pl and also due to its insufficient content in analyzed samples.

3.4 Lattice preferred orientation study

The recrystalization mechanism of the perthites described above appears so unusual that the LPO study of individual feldspar grains was additionally employed to complement microstructural data and chemical analyses. The LPOs are also used to clarify possible deformational mechanisms affecting the Qtz, Kfs and Pl grains during D_2 and D_3 episodes.

The strong LPO usually originates during plastic deformation via dislocation creep, while the diffusional creep or GBS do not increase LPO of deforming grains. The slip systems accommodating dislocation creep are well known for Qtz and abundantly but not entirely described for Pl with Kfs. To interpret the active slip systems we used inverse polar figures (IPFs) projecting lineation and poles to foliation into Qtz, Kfs and Pl crystals. In these stereographic projections the foliation poles point to crystallographic slip planes while the lineations indicate slip directions, assuming that plastic deformation proceeds via dislocation creep. To ascertain high quality of measurements the crystal lattice orientations were picked manually via Electron Back-Scattered Diffraction method (EBSD) on scanning electron microscope in the LAREM laboratory of the Czech geological survey in Prague.

3.4.1 Shielded and faintly deformed S_2 matrix

EBSD study of crystal lattice orientation of perthites and Kfs with Pl in the newly formed matrix was conducted in five domains where the matrix was protected from younger deformations by the surrounding perthite. Kfs and Pl grains always reveal roughly the same lattice orientation as Kfs with Pl domains in parental perthites (Fig. 10). The matrix Pl grains form generally tighter cluster around the parental Pth orientation, while the matrix Kfs shows more scattering. In case of two from the five measured samples has been documented continuous scattering of the uniform orientation when passing from the shielded domain to unprotected matrix outside the perthite porphyroblast. The matrix grains outside perthites quickly loose the orientation inherited from their parental grain and their random scatter together with elongation of neighboring Qtz inclusions prove progressive flow of the surrounding matrix during granulitization.

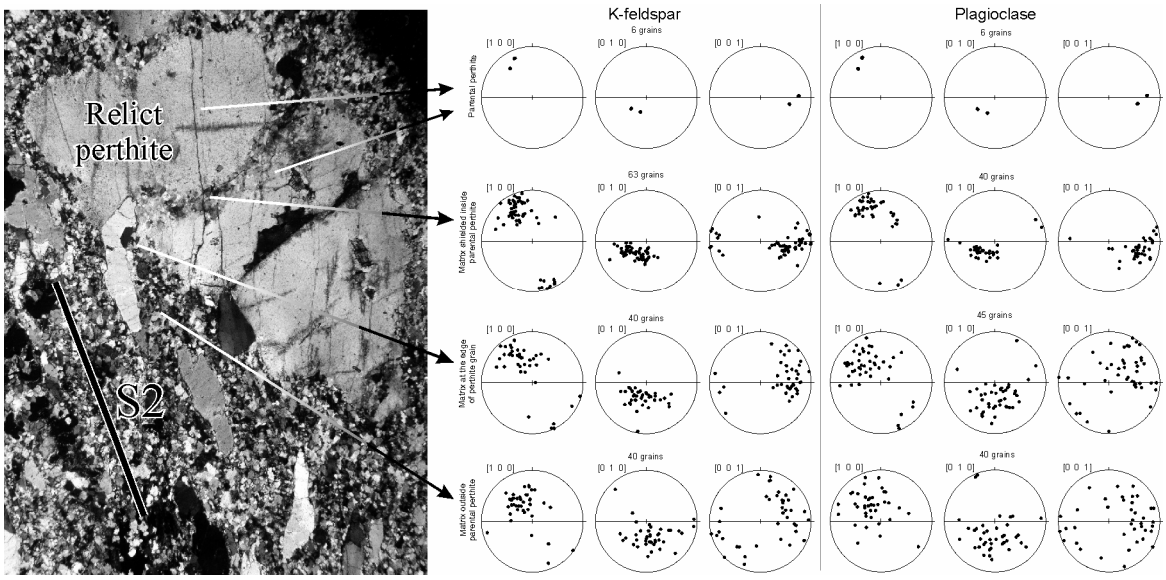

Fig. 10. EBSD measurements of a domain undergoing granulitization process and initial D_2 deformation. The LPOs of both Kfs background and Pl exsolutions in parental perthite are compared to LPOs of both feldspars in granulitic matrix located inside the perthite, at the edge of the perthite and in the deformed matrix adjacent to the perthite grain. The elongation of Qtz grains points out D_2 strain intensity and depicts orientation of S_2 fabric. Lower hemisphere non-polar equal-area projections.

3.4.2 Highly deformed S_2

The LPOs of Qtz, Kfs and Pl were measured in four thin sections of intensive S_2 fabric cut parallel to XZ plane of the D_2 strain ellipsoid. The IPFs revealed similar positions of strongest clusters in each sample, nevertheless for feldspars the maxima were too weakly defined due to

insufficient number of measurements per thin section. To allow for convincing interpretation of the resulting patterns we have merged all data from the four samples together to obtain 581 grains of Qtz, 608 of Kfs and 549 of Pl from the granulitic matrix (Fig. 11A).

The IPFs of matrix Qtz show strong maximum of foliation poles at position of rhombic with weaker maximum at prismatic planes, while lineations project to the <a> direction or to a girdle between <a> and <c> directions. This characteristics point to dominance of rhombic slip in <a> + <c> directions, with subordinate activity of prismatic <a> slip (Schmid & Casey, 1986). Rather different behavior exhibit the large Qtz ribbons examined in one of the samples, suggesting dominant activity of prismatic <a> slip with only minor influence of rhombic slip planes (Franěk et al., 2006). Compared to the matrix Qtz it implies sensitivity of the Qtz slip systems to size of the deformed grains. Fore-scatter detector (FSD) orientation maps reveal very irregular size and distribution of subgrains inside the single ribbons with prevalence of ~50° inclination of subgrain boundaries to the lineation direction. Assuming the prevailing prismatic slip system, these boundaries represent rhombic planes of the individual crystals, i.e. the subgrain shape is strongly dictated by crystallographic planes and their boundaries are not oriented randomly.

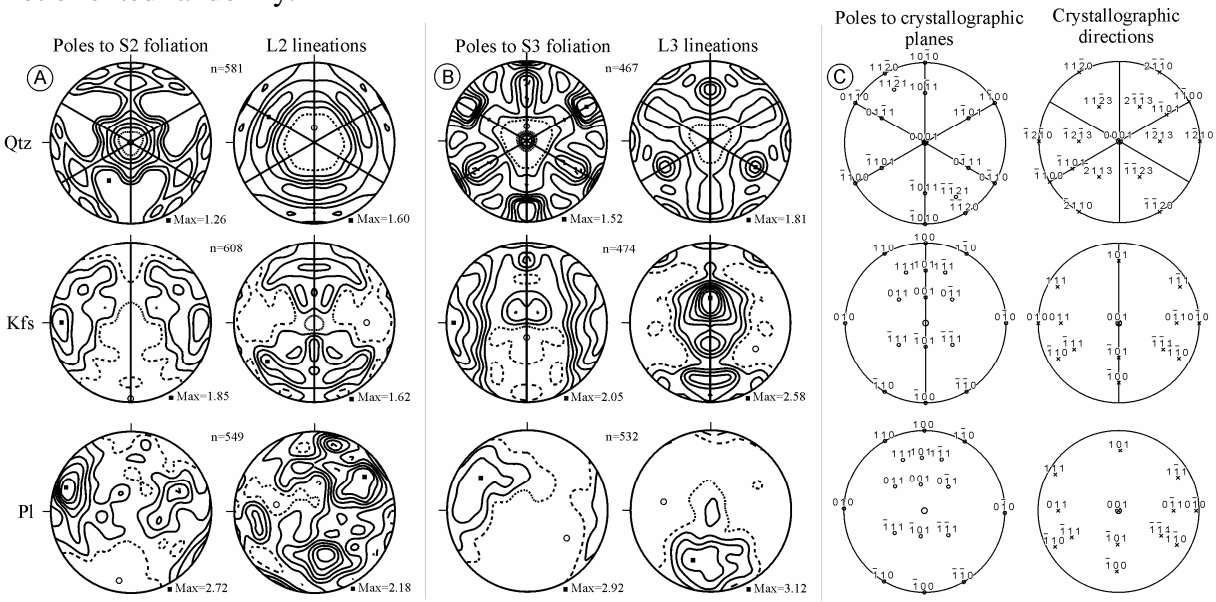

Fig. 11. Inverse polar diagrams of LPO measurements of Qtz, Kfs and Pl from felsic granulites exhibiting penetrative S_2 (A) and S_3 fabrics (B). The S_2 data are compiled from 4, the S_3 are merged from 3 studied thin sections. Poles to foliation and lineations are plotted in order to reveal possible active slip planes and slip directions. Positions of simple crystallographic planes and directions in the Qtz, Kfs and Pl crystals are indicated in (C). Upper hemisphere non-polar equal-area projections.

The IPFs of Kfs and Pl yield pronounced maxima around (010) plane which achieves most often slips in feldspars (Kruse et al., 2001). Particularly the Kfs exhibits strong maximum at the (010) with subordinate ones near (021) and (111) planes, while the maxima for slip directions lie at [101],[$\bar{1}$01],[100] and [$\bar{1}$10] positions. These can be partially ascribed to (010) [100] and (010) [101] slip systems (both Tullis, 1983). Majority of LPOs cannot be explained by slip systems described for Kfs, nevertheless the strong maximum at (010) typical slip plane suggests that the Kfs deforms by dislocation glide along this plane in slip directions not described so far. In the Pl projections the strongest maximum of foliation poles spans between (010) and (021) plane poles with subordinate peak at (0$\bar{2}$1). Highest lineation concentrations are reached near [1$\bar{1}$1] direction, while the [100] and [101] are less important. The maxima suggest activity of (010) [100] (Montardi & Mainprice, 1987) and (021) [100] (Jensen & Starkey, 1985) slip systems, while the significant amount of measured Pl grains

seem to glide along (010) or (021) planes in different unpublished directions. The maxima in IPFs for both feldspars are stronger than for Qtz and suggest development of the LPO via dislocation creep, despite the potential active slip directions haven't been described yet. We won't further speculate about possible new slip system(s) in the feldspars at HT HP conditions because such an attempt necessitates additional TEM studies and goes beyond the scope of the present article.

3.4.3 S_3

Three XZ thin sections were analyzed in a similar way as the S_2 samples. Also for similar reasons the measurements were merged together to obtain 467 measurements of Qtz, 474 of Kfs and 532 of Pl, which were plotted as IPFs (Fig. 11B). The resulting pattern reveals simpler distribution than the S_2 projections. The Qtz exhibits well defined maxima of foliation poles at position of prismatic planes and concentration of lineations at <a> with <-1101> directions. According to described Qtz slip systems (Schmid & Casey, 1986) such a pattern may be best explained by slip along prismatic planes in <a> direction or in combination of <a> and <c> directions.

In case of Kfs the poles to foliations concentrate near (010) plane while the lineations project mainly between [001] and [102] directions, showing subordinate maxima near [100] and $[10\bar{2}]$. These presumably indicate dominance of (010) [100] and (010) [001] slip systems (Montardi & Mainprice, 1987; Tullis, 1983). Foliation poles in the Pl IPFs exhibit strongest maximum among (010), (021) and (121) planes with subordinate peak at (012). The lineations reveal strong maximum at [100] and weak cluster at [001] direction. These indicate dislocation glide along the above mentioned (010) [100], (010) [001] (Montardi & Mainprice, 1987; Tullis, 1983) and (021) [100] (Jensen & Starkey, 1985) slip systems.

4 Discussion

4.1 Precursor of felsic granulites at D_1 episode

The observed structural succession, regular field distribution of S_1 relicts and microstructural relations imply that the perthite porphyroblasts preserved locally in the S_1 compositional banding represent remnants of the precursor of BLG felsic granulites. The characteristic strict separation of Qtz from Fsp cannot arise from any chemically driven differentiation, but it may be interpreted only as a result of deformational segregation of two materials with different plasticity. The length and thickness of the bands indicate significant strain during the D_1 segregation. The perthitic exsolutions in alkali feldspars exhibit regular undistorted pattern suggesting that they weren't present during D_1 plastic deformation. We rather argue that the exsolution proceeded between D_1 and D_2 phases and in turn that the S_1 necessarily developed under hypersolvus HT conditions. Abundant inclusions of Ky or high-grosular Grt suggest that the large alkali feldspars crystallized at HP conditions. Consequently the original syn-D_1 rock was HP hypersolvus coarse-grained orthogneiss plastically deformed under lower-crustal conditions in Ky stability field. The overall low Ca content of the large Fsp porphyroblasts doesn't allow to apply the two feldspar thermometry with sufficient accuracy to determine the absolute temperature during the D_1 event.

Petrological or geochemical arguments cannot help to distinguish if the observed relict Pth developed by magmatic or solid-state crystallization, but the inclusions preserved in the large perthite porphyroblasts offer a hint to answer this question. The abundant rectangular, hexagonal or drop-like shaped quartz single crystal inclusions without any SPO point to lack of plastic deformation between the growth of the quartz crystals and feldspar porphyroblasts. Such inclusions are referred to represent idiomorphic quartz crystals trapped by growing feldspar in a magmatic or subvolcanic evolution of granites, or to melt-assisted

recrystalization of quartz and feldspar in banded migmatites at leucosome-melanosome boundaries (p. 111, 192 in Mehnert, 1968). The inclusions of HP minerals exclude possible subvolcanic crystallization of the alkali feldspars, thus the more likely seem a melt-assisted metamorphic growth of the porphyroblasts. Lack of significant strain during their growth is suggested by euhedral shapes of quartz grains, sharp edges of euhedral Grt or prismatic habitus of Bt inclusions. None of the two possibilities can be fully excluded, but the melt-assisted recrystalization in a predominantly solid rock seems as a more plausible explanation to the observed Pth features.

The absolute timing of alkali feldspar crystallization and D_1 deformation isn't convincingly established as yet. (Kröner et al., 2000) has drilled out zircons enclosed in perthites of South Bohemian felsic granulites to obtain ages around 340 Ma, comparable within error with the ages reported for HP metamorphism (e.g. Kröner et al., 2000; Wendt et al., 1994) and exhumation (e.g. Kröner et al., 2000) of these rocks. These zircon inclusions should determine maximum age of crystallization of the alkali feldspars, but due to HT granulite-facies environment the age may possibly result from partial resetting of the U-Pb isotopic system in the zircon crystals.

Based on similarity of perthite inclusions, S_1 banding and S_2 mylonites in the BLG with oldest structures described from the Saxonian Granulitgebirge (Behr, 1961), the interpretations of the granulite precursor can be extrapolated to the latter massif. It cannot be excluded that also other Variscan felsic granulites evolved from such hypersolvus coarse-grained orthogneisses.

4.2 Granulitization process

The exsolution of string perthitic Pl postdates the D_1 phase as suggested above, and predates D_2 granulitization because the newly formed Kfs in granulitic matrix is already free of such exsolutions. As the perthite exsolution is triggered by cooling, this succession implies decrease in temperature between D_1 and D_2 stages. The temperature drop particularly between exsolution and granulitization is documented also by the T-dependent Ca content in Pl, which attains slightly higher Ca concentrations in the perthitic exsolutions in the large alkali feldspars than in the An-rich cores of the fine-grained shielded matrix. The spatial relations and compositional similarity suggest that the An-rich cores of matrix Pl nucleated on the preexisting perthitic Pl exsolutions. Low SPO and high count of unlike grain boundaries are in accord with almost static development of the granulitic matrix driven by tendency to active intermixing of the two different phases and minimization of surface energy by grain shape simplification..

Recrystalization processes are always strongly enhanced by action of differential stress and strain, in case of heterogeneous recrystalization leading to preferred orientation of the recrystalized domains. The largely random orientations of disintegrated domains inside Pth in all the XZ, YZ and XY sections then suggest that the matrix formed in almost static conditions. BSE images show that the new grains developed at a sharp recrystalization front pervading gradually into intact Pth grains (Fig. 6B,7A). The equivalent bulk chemical composition of Pth and shielded granulitic matrix (Fig. 8) indicates that the recrystalization proceeded in a chemically closed system by redistribution of Or, Ab and An components on a micro scale. Such characteristics resemble exsolution of Pl in perthites, but in case of granulitization an interconnected net of grain boundaries developed with almost equidimensional Kfs grain shapes surrounded by Pl that lack crystallographically determined SPO. The question arises why the unstable alkali feldspar disintegrated into fine-grained mosaic of Kfs and Pl grains, when the decomposition usually leads only to coarsening of Pl perthitic exsolutions inside intact crystal lattice of the original Kfs-dominated feldspar grain. The coherent perthitic microstructure bears enormously high surface energy but there's

usually no mechanism to overcome the coherency and recrystalize to more stable and non-coherent geometries. The different behavior observed in our samples cannot be explained by chemical inhomogeneities as the Pth and shielded matrix exhibit same chemical composition. The isolated An_{20} cores of new matrix Pl are connected via the An_{12} rims – a generation of Pl that is missing in parental perthites and that must have evolved during the granulitization. These irregularly oriented Pl rims coat boundaries between Kfs grains suggesting that these grain boundaries existed already before the Pl crystallization. In turn the granulitization was initiated by breakage of the parental Pth into small grains, being followed by gradual Pl redistribution along these boundaries (e.g. lower part of Fig. 7A). The Pl perthitic exsolutions served as crystallization centers along which the An_{12} Pl have precipitated, being released partially from surrounding Kfs by volume diffusion.

Several driving mechanisms could induce the observed breakage. The feldspar solid solutions do not exhibit only partial mixing among end members, but the complexity of behavior is raised by crystal structure changes from monoclinic HT forms to triclinic ones at lower temperatures. Transition of Kfs-dominated alkali feldspars or pure Kfs from monoclinic high sanidine to monoclinic low sanidine occurs between ~900 - 700°C, followed by change to triclinic microcline via transitional orthoclase at ~500°C (e.g. Brown & Parsons, 1989), but the presented temperatures relate to alkali feldspar system without considering eventual subtle Ca content. In case of Pl the HT monoclinic monalbite reorganizes to triclinic high albite between 980 to ~1160°C (Ribbe, 1983) depending on An content, and subsequently transforms to triclinic low albite between 725 and 620°C (e.g. Brown & Parsons, 1989). According to thermobarometry of felsic granulites the original alkali feldspar kept monoclinic symmetry until granulitization, the Kfs in granulitic matrix was during whole D_2 monoclinic sanidine, while the Pl born the triclinic high albite structure.

In general, formation of new grains from parental alkali feldspars govern the configurational, surface and strain energies (Kuhl & Schmid, 2007). Chemical with surface arguments lead to coalescence of existing grains, while the only mechanism to develop new grain boundaries represent deformation causing increase in strain energy. Based on these assumptions we suspect that the Pth breakage at the beginning of granulitization process was triggered by subtle straining of the decomposing Pth grains. Crystal lattice of both the Kfs and Pl domains of parental Pth reveal uniform orientation, suggesting that Pl exsolution proceeded along coherent solvus, possibly by spinodal decomposition mechanism (Brown & Parsons, 1989).

Mild scatter of shielded matrix LPOs in comparison to parental Pth grains (Fig. 10) may be explained by non-coherent nucleation of the grains or by subsequent plastic deformation of the matrix. Based on systematic scatter of the LPOs we suggest that the matrix nucleation was originally non-coherent, resembling decomposition of alkali feldspar along a strain free solvus (SFS). The SFS in feldspars lies at higher temperatures than the coherent solvus (e.g.Yund & Tullis, 1983) suggesting that the matrix should than form before microperthite exsolution. Our samples show opposite succession, but the natural examples of hypersolvus rocks exhibit also coherent exsolution of perthites before eventual decomposition along SFS. For the feldspars it is probably too hard to overcome coherency and the strain-free noncoherent recrystalization occurs in praxis only after some water or external stress is imposed on the alkali feldspar grains (Brown & Parsons, 1989 and references therein). As a lack of hydrous phases and presumably lack of water characterizes all the granulite-facies evolution of our rocks, the activity of external stresses seems to be a possible cause of noncoherent recrystalization of the Pth porphyroblasts. Such hypothesis is supported by the fact that granulitization often initiates at inclusion boundaries which are likely to concentrate stresses or that undulose extinction is observed in parental grains around decomposed regions indicating elastic distortion of crystal lattice, i.e. local increase of strain energy at the recrystalized domains.

Both the microstructural and LPO considerations point to an activity of subtle strain during granulitization process, but at the same time the LPO of matrix implies very limited intensity of the deformation and indicates that the chemical or surface energy disequilibrium was necessary to drive the recrystalization. Consequently the breakage and recrystalization of parental Pth appear to result from an interplay of subtle strain and high disequilibrium of the Pth at given PT conditions.

4.3 Lower crustal ascent and strength of felsic granulites

The relict granulite facies S_2 fabrics allow for reconstruction of the early exhumation mechanism in form of a subvertical ascent channel proposed by (Franěk et al., 2006), because the subsequent cooling history froze these fabrics enabling us to observe them continuously on a km-scale. The destruction of S_1 banding and elongation of isolated Qtz ribbons prove high plastic strain imposed on the S_2 fabric, while textural analysis of the prevailing fine-grained feldspar dominated matrix reveals only weak signs of plastic deformation. Several possible deformational mechanisms accommodating the high strain at given PT conditions comprise dislocation creep, grain boundary sliding (GBS) and diffusional creep via volume diffusion or diffusion along grain boundaries.

The contact frequency analysis of S_2 (Fig. 9A) reveals intermixing of all the three major phases to almost ideally random distribution. If the Qtz, Kfs and Pl would deform dominantly by dislocation creep, they would rather tend to coalescence into monomineralic bands due to different intra-crystalline plasticity of the individual phases. The observed mixing of all three minerals at high strains implies that the grains didn't deform predominantly by intra-crystalline slip, thus their different plasticity didn't lead to phase segregation. The SPO and GBPO of both feldspars in S_2 reach lowest values from all the samples analyzed and the axial ratio of matrix grains shows low values as well (Fig. 9A,C). CSD calculations show decrease in nucleation compared to grain growth rate of both Kfs and Pl, when compared to the initial stages of matrix development. This is in accord with increased grain size of both the feldspars.

The IPFs of the three principal phases reveal strong maxima for all of them. The Qtz LPO is fully explainable by the slip systems described in literature, while the Pl and to lesser extent also Kfs partly exhibit maxima of potential slip directions that are incompatible with slip systems described in feldspars. Because the other maxima fit to the reported slip systems and the complex crystal structure of feldspars offers numerous slip systems for a dislocation glide (e.g. Kruse et al., 2001; Stunitz et al., 2003; Tullis, 1983) we suggest that feldspars in the examined granulitic matrix deformed via dislocation glide along slip systems which are in part not reported yet.

Despite strong LPOs, the quantitative textural characteristic of the fine-grained matrix is incompatible with dominance of dislocation creep deformation mechanism, and rather points to diffusion creep or GBS processes. Volume diffusion is generally a slow process that cannot accomodate high strains attained in the short time span of granulite exhumation, but the more efficient grain boundary diffusion is highly likely to operate in such a fine grained matrix under granulite-facies temperatures. The latter mode of diffusion usually enables GBS which would represent a very efficient mechanism to accommodate high strain rates in the fine-grained S_2 matrix. The GBS would be additionally enhanced by presence of syntectonic partial melt suggested by microscopic and microchemical observations. The content of partial melt wasn't sufficient enough to lubricate all matrix grain boundaries so that in domains devoid of the melt a dislocation creep operated as an additional important deformational mechanism. (Tajčmanová et al., 2007; Tajčmanová et al., 2006) report in petrological study of comparable Moldanubian felsic granulites relatively low partial melt content <5% but very efficient solid-state diffusion at the peak 850 °C / 1.8 GPa conditions and during Pl corona

formation around Ky marking decompression stage equivalent to our D_2 phase. Microstructural evidence for dominance of grain-size sensitive creep in mylonites is usually not available, however for the S_2 matrix grain sizes at temperatures over 800 °C the published deformational maps clearly predict dominance of diffusion-controlled creep (Rybacki & Dresen, 2004). It is not possible to unambiguously evaluate relative importance of dislocation creep, GBS and grain boundary diffusion, but the observations suggest that the S_2 matrix arose from competition between dislocation creep inducing strong LPO and GBS assisted by diffusion along grain boundaries. The grain-size sensitive mechanisms may not necessarily lead to loss of LPO acquired in previous or contemporaneous dislocation creep, as suggested e.g. by (Jiang et al., 2000). This precedent explains how the observed strong LPO could have been maintained during cooperation of the mentioned deformational mechanisms.

As mentioned, the interstitial small Qtz crystals with Ab-rich discontinuous films at Pl boundaries imply presence of syn-deformational intergranular partial melt in the granulitic matrix, a feature suggested already by (Franěk et al., 2006). Syn-deformational partial melting during the rapid D_2 decompressional phase is in agreement with the thermodynamical modeling of (Tajčmanová et al., 2007) or with the experimental works of (Tropper et al., 2005) who produced significant amount of partial melt during simulated isothermal decompression of the felsic rock from granulite facies conditions. Experimental studies (e.g. Dell'Angelo, 1987; Rosenberg & Handy, 2005) also demonstrated that the presence of several percent of silicate melts may decrease bulk strength of the rock by several orders of magnitude. Diffusion along grain boundaries with the fluid phase partially coating the grains in this case probably enhances the GBS mechanism, which for our felsic matrix implies highly ductile behavior attaining characteristics of a superplastic flow (Behrmann & Mainprice, 1987; Boullier & Gueguen, 1975). The partially molten matrix prevailing over Qtz ribbons would then form a framework of interconnected weak layers (IWL) evoking low bulk viscosity of the rock. Extreme weakness of granulites during D_2 was independently documented by (Franěk et al., 2006) by the geometrical analysis of F_2 folds which revealed passive amplification mechanism and flow character of this early folding.

4.4 D_3 switch in rheology of feldspars vs. quartz

Microstructural characteristics of the S_3 microfabric differ in majority of attributes from the S_2 quantitative description. The high number of like boundaries (Fig. 9A) point to significant coalescence of individual phases into monomineralic aggregates, the SPO, GBPO and axial ratio of both feldspars increase too. Qtz grains exhibit decrease in SPO as well as in axial ratios. The proportion between nucleation and growth rate of Kfs remains comparable with S_2, while the Pl exhibits lower nucleation compared to growth rate. IPFs of all the three examined phases reveal slip systems reported in the literature, with predominance of those usual in naturally deformed rocks.

The tendency to monomineralic aggregate distribution, high preferred orientation and general prevalence of grain growth over nucleation compared to S_2 are in accord with the strong LPO, suggesting that the Qtz, Kfs and Pl deformed during D_3 predominantly by dislocation creep mechanism. Slip systems of all the three phases significantly differ from those active in granulite-facies samples and no signs of diffusion creep or previously active GBS mechanisms have been detected. The irregular grain boundaries in S_3 microstructure are also typical of dislocation creep rather than the GBS mechanism. Dislocation creep was in places enhanced by creep along stripes of coalesced Bt flakes and flow along melt segregation bands. The dominance of less effective dislocation creep documented in S_3 microstructure indicates hardening of the felsic granulites, where the less plastic feldspars built a load-bearing framework (LBF, Handy, 1990) that determined high bulk strength of the retrograde felsic rock in mid-crustal levels.

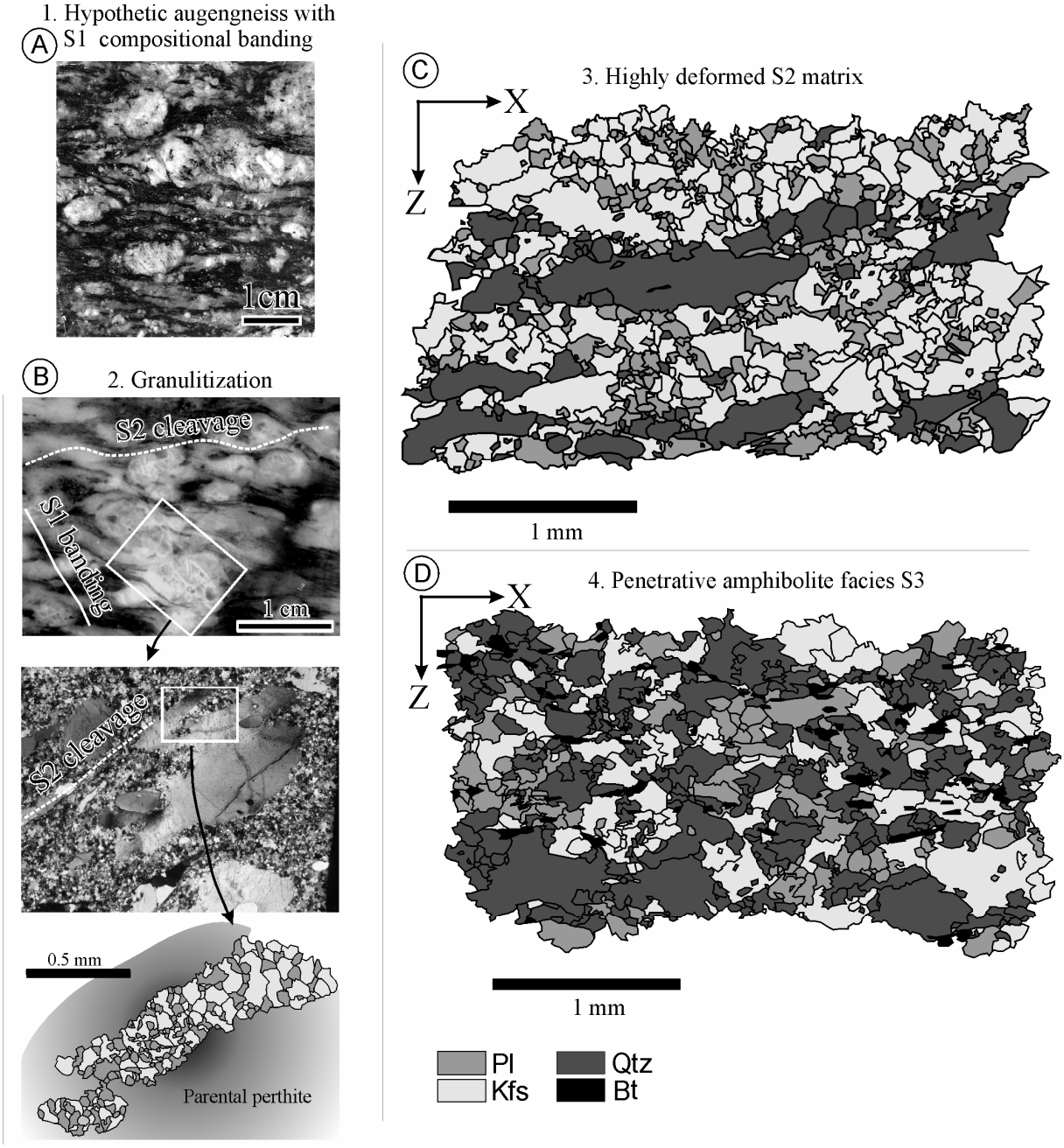

Fig. 12. Interpretative sketch of succession of the 4 described microstructural evolution stages. (A) D_1 Augen gneiss (B) Granulitization process (C) D_2 granulitic mylonite with interstitial Qtz suggesting presence of intergranular melt, 4) S_3 MP MT fabric.

5 Conclusions

Precursor of BLG felsic granulites was a high-pressure alkali feldspar – quartz – garnet – biotite – kyanite bearing coarse-grained hypersolvus banded orthogneiss which developed via deformational segregation of Qtz from Fsp.

Granulitization process is almost static disintegration of ~1 cm large parental microperthites into a plagioclase - K-feldspar fine-grained matrix. It takes place via recrystalization of metastable perthites driven by perthite instability accompanied with subtle strain. Newly formed matrix grains maintain roughly the LPO of parental perthite crystal.

The fine-grained S_2 granulitic matrix with tiny content of partial melt deformed via combination of GBS with dislocation creep and presumably grain-boundary diffusion to form an IWL structure. In other words the granulitization of coarse-grained Fsp aggregate produced matrix that was directly capable of grain size-sensitive flow. This caused break of the strength of the polyphase matrix and weakened the whole volume of such felsic lower-crustal rocks. Subsequently these were rapidly extruded upwards through the orogenic root.

After cooling and crystallization of the syn-D_2 partial melt along grain boundaries, the granulites deformed during D_3 episode by much less effective dislocation creep similarly to common orthogneisses (Fig. 12). Local hydration produced partial melt that segregated from solid matrix into isolated bands instead of coating grain boundaries.

When compared to data published from other Variscan felsic granulites in the Bohemian Massif, it appears that all described granulite-facies fabrics reveal similar petrological and microstructural features as the S_2 in the BLG (Behr, 1961; Racek et al., 2006; Schulmann et al., 2005; Štípská et al., 2004; Tajčmanová et al., 2006). Results concerning early granulite history from the BLG can be then extrapolated to the Saxonian granulite massif which shows comparable early evolution, and possibly may be applied also to other Variscan felsic granulites. Combined with abundance of felsic granulites in Moldanubian zone and rheological characteristics it states that significant part of the Variscan lower crust was weakened by several orders of magnitude at the onset of granulite exhumation.

While Qtz keeps the same deformational mechanism throughout the complex history of the described felsic rocks, feldspars accommodate deformations by various mechanisms depending on actual conditions.

Our observations document a rapid weakening of Fsp-rich rocks under lower-crustal conditions. Similar processes may lower the viscosity of any other rock containing perthitic feldspars when subjected to deformation at suitable PT conditions, while subsequent switch in deformation mechanism may invoke hardening. It directly implies that geotectonic rheological considerations based purely on the Byerlee and Weertmann laws are too simplistic and should be modified.

6 Acknowledgments

The work was supported by a grant of the Czech Science Foundation (GACR 205/05/2187). We are grateful to Jean-Emmanuel Martelat for constructive suggestions.

7 References

Behr, H. J., 1961. *Beitrage zur petrographischen und tektonischen Analyse des sachsischen Granulitgebirges*.

Behrmann, J. H. & Mainprice, D., 1987. Deformation mechanisms in a high-temperature quartz-feldspar mylonite: evidence for super-plastic flow in the lower crust. *Tectonophysics 140*, 297-305.

Boullier, A. M. & Gueguen, Y., 1975. SP-mylonites; origin of some mylonites by superplastic flow. *Contrib Mineral Petrol 50*, 93-104.

Brown, W. L. & Parsons, I., 1989. Alkali feldspars: ordering rates, phase transformations and behaviour diagrams for igneous rocks. *Mineralogical Magazine*, **53**, 25-42.

Carswell, D. A. & O´Brien, P. J., 1993. Thermobarometry and Geotectonic Significance of High-Pressure Granulites - Examples From the Moldanubian Zone of the Bohemian Massif in Lower Austria. *Journal of Petrology*, **34**(3), 427-459.

Cooke, R. A., 2000. High-pressure/temperature metamorphism in the St. Leonhard Granulite Massif, Austria: Evidence from intermediate pyroxene-bearing granulites. *International Journal of Earth Sciences*, **89**(3), 647-651.

Dell'Angelo, L. N., Tullis, J. , and Yund, R.A., 1987. Transition from dislocation creep to melt-enhanced diffusion creep in fine-grained granitic aggregates. **139**, 325-332.

Fiala, J., Matejovska, O. & Vankova, V., 1987. Moldanubian granulites: source material and petrogenetic considerations. *Neues Jahrbuch fur Mineralogie, Abhandlungen*, **157**(2), 133-165.

Finger, F., Cooke, R., Janous?ek, V., Konzett, J., Pin, C., Roberts, M. P. & Tropper, P., 2003. Petrogenesis of the south Bohemian granulites: The importance of crystal-melt relationships. *Journal of the Czech Geological Society*, **48**(1-2), 44-45.

Franěk, J., Schulman, K. & Lexa, O., 2006. Kinematic and rheological model of exhumation of high pressure granulites in the Variscan orogenic root: Example of the Blanský les granulite, Bohemian Massif, Czech Republic. *Mineralogy and Petrology*, **86**(3-4), 253-276.

Franke, W., 2000. The mid-European segment of the Variscides: Tectonostratigraphic units, terrane boundaries and plate tectonic evolution. *Geological Society Special Publication*(179), 35-56.

Friedl, G., Cooke, R., Finger, F., McNaughton, N. J. & Fletcher, I., 2003. U-Pb shrimp dating and trace element investigations on multiple zoned zircons from a South-Bohemian granulite. *Journal of the Czech Geological Society*, **48**(1-2), 51.

Fuchs, G., 1976. Zur Entwicklung der Böhmischen Masse. *Jahrbuch des Geologischen Bundesanstalts*, **119**, 45-61.

Handy, M., 1990. The solid state flow of polymineralic rocks. *Journal of Geophysical Research*, **95**, 8647-8661.

Higgins, M. D., 1998. Origin of anorthosite by textural coarsening: quantitative measurements of a natural sequence of textural development. *Journal of Petrology*, **39**(7), 1307-1323.

Jakes, P., 1997. Melting in high-P region - Case of Bohemian granulites. *Acta Universitatis Carolinae, Geologica*, **41**(3-4), 113-125.

Janoušek, V., Finger, F., Roberts, M., Fryda, J., Pin, C. & Dolejs, D., 2004. Deciphering the petrogenesis of deeply buried granites: whole-rock geochemical constraints on the origin of largely undepleted felsic granulites from the Moldanubian Zone of the Bohemian Massif. *Transactions of the Royal Society of Edinburgh-Earth Sciences*, **95**, 141-159.

Janoušek, V., Gerdes, A., Vrana, S., Finger, F., Erban, V., Friedl, G. & Braithwaite, C. J. R., 2006. Low-pressure granulites of the Lišov Massif, Southern Bohemia: Visean metamorphism of Late Devonian plutonic arc rocks. *Journal of Petrology*, **47**(4), 705-744.

Jensen, L. N. & Starkey, J., 1985. Plagioclase microfabrics in a ductile shear zone from the Jotun Nappe, Norway. *J Struct Geol 7*, 527-539.

Jiang, Z., Prior, D. J. & Wheeler, J., 2000. Albite crystallographic preferred orientation and grain misorientation distribution in a low-grade mylonite: Implications for granular flow. *Journal of Structural Geology*, **22**(11-12), 1663-1674.

Kodym, O., 1972. Multiphase deformation in the Blanský les granulite massif (South Bohemia). *Krystalinikum 9*, 91-105.

Košler, J., Kelley, S. P., Vance, D. & Svojtka, M., 1999. Independent dating of cooling and decompression of high grade rocks in the southern Bohemian Massif with Ar-Ar, Sm-Nd and U-Pb techniques. *J C Abstr 4*, 39.

Kotkova, J. & Harley, S. L., 1999. Formation and evolution of high-pressure leucogranulites: Experimental constraints and unresolved issues. *Physics and Chemistry of the Earth Part a-Solid Earth and Geodesy*, **24**(3), 299-304.

Kretz, R., 1983. Symbols for rock forming minerals. *American Mineralogist*, **68**, 277-279.

Kröner, A., O'Brien, P. J., Nemchin, A. A. & Pidgeon, R. T., 2000. Zircon ages for high pressure granulites from South Bohemia, Czech Republic, and their connection to Carboniferous high temperature processes. *Contributions to Mineralogy and Petrology*, **138**(2), 127-142.

Kruse, R., Stu?nitz, H. & Kunze, K., 2001. Dynamic recrystallization processes in plagioclase porphyroclasts. *Journal of Structural Geology*, **23**(11), 1781-1802.

Kuhl, E. & Schmid, D. W., 2007. Computational modeling of mineral unmixing and growth. *Computational mechanics*, **39**(4), 439-451.

Lexa, O., Stipska, P., Schulmann, K., Baratoux, L. & Kroner, A., 2005. Contrasting textural record of two distinct metamorphic events of similar P-T conditions and different durations. *Journal of Metamorphic Geology*, **23**(8), 649-666.

Martelat, J. E., Schulmann, K., Lardeaux, J. M., Nicollet, C. & Cardon, H., 1999. Granulite microfabrics and deformation mechanisms in southern Madagascar. *Journal of Structural Geology*, **21**(6), 671-687.

Matte, P., Maluski, H., Rajlich, P. & Franke, W., 1990. Terrane boundaries in the Bohemian Massif: result of the large–scale Variscan shearing. *Tectonophysics 177*, 151-170.

Mehnert, K. R., 1968. *Migmatites and the origin of granitic rocks*. Elsevier, Amsterdam London New York.

Montardi, Y. & Mainprice, D., 1987. A transmission electron microscopy study of the natural plastic deformation of calcic plagioclases (An 68-70). *B Mineral 110*, 1-14.

O'Brien, P. J. & Seifert, K., 1992. P–T–t paths as records of orogenic processes: examples and problems from the crystalline of the Bohemian Massif. *Terra Nostra 1992*, 58–59.

Putnis, A., 2002. Mineral replacement reactions: From macroscopic observations to microscopic mechanisms. *Mineralogical Magazine*, **66**(5), 689-708.

Racek, M., Stipska, P., Pitra, P., Schulmann, K. & Lexa, O., 2006. Metamorphic record of burial and exhumation of orogenic lower and middle crust: a new tectonothermal model for the Drosendorf window (Bohemian Massif, Austria). *Mineralogy and Petrology*, **86**(3-4), 221-251.

Ribbe, P. H., 1983. Feldspar mineralogy, Mineralogical society of America, Washington.

Rosenberg, C. L. & Handy, M. R., 2005. Experimental deformation of partially melted granite revisited: Implications for the continental crust. *Journal of Metamorphic Geology*, **23**(1), 19-28.

Rybacki, E. & Dresen, G., 2004. Deformation mechanism maps for feldspar rocks. *Tectonophysics*, **382**(3-4), 173-187.

Schmid, S. M. & Casey, M., 1986. Complete fabric analysis of some commonly observed quartz c-axis patterns. In: *Mineral and Rock Deformation: Laboratory Studies* (eds Hobbs, B. E. & Heard, H. C.) *Geophys. Monograph*, pp. 263-286.

Schmid, S. M., Heilbronner, R. & Stunitz, H., 1999. Deformation mechanisms in nature and experiment. *Tectonophysics 303*, VII-IX.

Schulmann, K., Kroner, A., Hegner, E., Wendt, I., Konopasek, J., Lexa, O. & Stipska, P., 2005. Chronological constraints on the pre-orogenic history, burial and exhumation of deep-seated rocks along the eastern margin of the Variscan Orogen, Bohemian Massif, Czech Republic. *American Journal of Science*, **305**(5), 407-448.

Stunitz, H., Fitz Gerald, J. D. & Tullis, J., 2003. Dislocation generation, slip systems, and dynamic recrystallization in experimentally deformed plagioclase single crystals. *Tectonophysics*, **372**(3-4), 215-233.
Stunitz, H. & Tullis, J., 2001. Weakening and strain localization produced by syn-deformational reaction of plagioclase. *International Journal of Earth Sciences*, **90**(1), 136-148.
Štípská, P. & Powell, R., 2005. Does ternary feldspar constrain the metamorphic conditions of high-grade meta-igneous rocks? Evidence from orthopyroxene granulites, Bohemian Massif. *Journal of Metamorphic Geology*, **23**(8), 627-647.
Štípská, P., Schulmann, K. & Kroner, A., 2004. Vertical extrusion and middle crustal spreading of omphacite granulite: a model of syn-convergent exhumation (Bohemian Massif, Czech Republic). *Journal of Metamorphic Geology*, **22**(3), 179-198.
Tajčmanová, L., Konopásek, J. & Connolly, J. A. D., 2007. Diffusion-controlled development of silica-undersaturated domains in felsic granulites of the Bohemian Massif (Variscan belt of Central Europe). *Contributions to Mineralogy and Petrology*, **153**(2), 237-250.
Tajčmanová, L., Konopásek, J. & Schulmann, K., 2006. Thermal evolution of the orogenic lower crust during exhumation within a thickened Moldanubian root of the Variscan belt of Central Europe. *Journal of Metamorphic Geology*, **24**(2), 119-134.
Tollmann, A., 1982. Großräumiger variszischer Deckenbau im Moldanubikum und neue Gedanken zum Variszikum Europas. *Geotektonische Forschungen*, **64**, 1-91.
Tropper, P., Konzett, J. & Finger, F., 2005. Experimental constraints on the formation of high-P/high-T granulites in the Southern Bohemian Massif. *European Journal of Mineralogy*, **17**(2), 343-356.
Tullis, J., 1983. Deformation of feldspars. In: *Feldspar mineralogy* (ed Ribbe, P. H.), pp. 297-323, Mineralogical society of America, Washington.
Verner, K., Žák, J., Nahodilová, R. & Holub, F. V., 2007. Magmatic fabrics and emplacement of the cone-sheet-bearing Knížecí Stolec durbachitic pluton (Moldanubian Unit, Bohemian Massif): implications for mid-crustal reworking of granulitic lower crust in the Central European Variscides. *International Journal of Earth Sciences*, in press.
Vrána, S., 1989. Perpotassic Granulites from Southern Bohemia - a New Rock-Type Derived from Partial Melting of Crustal Rocks under Upper Mantle Conditions. *Contributions to Mineralogy and Petrology*, **103**(4), 510-522.
Wendt, J. I., Kroner, A., Fiala, J. & Todt, W., 1994. U-Pb zircon and Sm-Nd dating of Moldanubian HP/HT granulites from south Bohemia, Czech Republic. *Journal - Geological Society (London)*, **151**(1), 83-90.
Yund, R. A. & Tullis, J., 1983. Subsolidus phase relations in the alkali feldspars with emphasis on coherent phases. In: *Feldspar mineralogy* (ed Ribbe, P. H.), pp. 141-176, Mineralogical society of America, Washington.

8 Apendix 1

Radiometric ages used for plots in Figure 3 with corresponding references.

South Bohemian granulites, Pb-Pb and U-Pb ages
338±1 Ma, U-Pb on Zrn, (Aftalion et al., 1989)
346±5 Ma, U-Pb on Zrn, (Wendt et al., 1994)
351±6 Ma, U-Pb on Zrn, (Wendt et al., 1994)
346±12 Ma, U-Pb on Zrn, (Wendt et al., 1994)
366±5 Ma, U-Pb on Zrn, (Wendt et al., 1994)

373±12 Ma, U-Pb on Zrn, (Wendt et al., 1994)
368±2 Ma, U-Pb on Zrn, (Janoušek & Holub, 2007)
341±3.30 Ma, U-Pb on Zrn, (Kröner et al., 2000)
338.20±3.20 Ma, U-Pb on Zrn, (Kröner et al., 2000)
341.30±3.50 Ma, U-Pb on Zrn, (Kröner et al., 2000)
339.30±2.90 Ma, U-Pb on Zrn, (Kröner et al., 2000)
360±2 Ma, U-Pb on Zrn, (Kröner et al., 2000)
399±6 Ma, U-Pb on Zrn, (Kröner et al., 2000)
441±6 Ma, U-Pb on Zrn, (Kröner et al., 2000)
357±2 Ma, U-Pb on Zrn, (Kröner et al., 2000)
408±6 Ma, U-Pb on Zrn, (Kröner et al., 2000)
340.40±2.90 Ma, U-Pb on Zrn, (Kröner et al., 2000)
339.60±3.10 Ma, U-Pb on Zrn, (Kröner et al., 2000)
367.80±3 Ma, U-Pb on Zrn, (Kröner et al., 2000)
339.20±2.90 Ma, U-Pb on Zrn, (Kröner et al., 2000)
469.30±3.80 Ma, U-Pb on Zrn, (Kröner et al., 2000)
341.10±2.40 Ma, U-Pb on Zrn, (Kröner et al., 1996)

South Bohemian granulites, Sm-Nd ages
351 ± 6 on WR-Grt core (Košler et al., 1999)
343 ± 2 on Grt (Janoušek & Holub, 2007)
365 ± 2 on Grt (Janoušek & Holub, 2007)
360 ± 10 on WR-Grt (Prince et al., 2000)
354 ± 5 on WR-Grt core (Prince et al., 2000)
349 ± 6 on WR-Grt (Prince et al., 2000)
362 ± 7 on WR-Grt (Prince et al., 2000)
343 ± 21 on mineral-WR (Kröner et al., 1996)
327 ± 19 on mineral-WR (Van Breemen et al., 1982)

Aftalion, M., Bowes, D. R. & Vrana, S., 1989. Early Carboniferous U-Pb Zircon Age for Garnetiferous, Perpotassic Granulites, Blanský Les Massif, Czechoslovakia. *Neues Jahrbuch Fur Mineralogie-Monatshefte*(4), 145-152.

Janoušek, V. & Holub, F. V., 2007. The causal link between HP-HT metamorphism and ultrapotassic magmatism in collisional orogens: case study from the Moldanubian Zone of the Bohemian Massif. *Proceedings of the Geologists Association*, **118**, 75-86.

Košler, J., Kelley, S. P., Vance, D. & Svojtka, M., 1999. Independent dating of cooling and decompression of high grade rocks in the southern Bohemian Massif with Ar-Ar, Sm-Nd and U-Pb techniques. *J C Abstr 4*, 39.

Kröner, A., O'Brien, P. J., Nemchin, A. A. & Pidgeon, R. T., 2000. Zircon ages for high pressure granulites from South Bohemia, Czech Republic, and their connection to Carboniferous high temperature processes. *Contributions to Mineralogy and Petrology*, **138**(2), 127-142.

Kröner, A., O'Brien, P. J. & Pidgeon, R. T., 1996. SHRIMP zircon ages for HP-HT granulites from the Moldanubian zone of southern Bohemia. In: *EOS 77*.

Prince, C. I., Kosler, J., Vance, D. & Gunther, D., 2000. Comparison of laser ablation ICP-MS and isotope dilution REE analyses - implications for Sm-Nd garnet geochronology. *Chemical Geology*, **168**(3-4), 255-274.

Van Breemen, O., Aftalion, M., Bowes, D. R., Dudek, A., Misar, Z., Povondra, P. & Vrana, S., 1982. Geochronological studies of the Bohemian massif, Czechoslovakia, and their

significance in the evolution of Central Europe. *Transactions of the Royal Society of Edinburgh: Earth Sciences*, **73**(2), 89-108.
Wendt, J. I., Kroner, A., Fiala, J. & Todt, W., 1994. U-Pb zircon and Sm-Nd dating of Moldanubian HP/HT granulites from south Bohemia, Czech Republic. *Journal - Geological Society (London)*, **151**(1), 83-90.

General conclusions

Apart from results in the individual articles above, the presented study of the high-grade rocks leads to several general suggestions which overcome its regional scope:

- Despite the structural analysis and distinguishing of deformational episodes is not in the fashion in present structural geology, this study dealing with multiple deformational phases demonstrates that it remains a powerful tool in unraveling tectonic history when field structural measurements are combined with other methods like petrography or microstructural analysis.
- Lower-crustal rocks can be exhumed in relatively small portions in the centre of an orogenic domain, e.g. in form of a steep amplifying extrusion interpreted in Southern Bohemian Moldanubian domain. They can create themselves a new ascent path instead of following some preexisting structure.
- Extensive regions of flat anastomosing crustal fabrics may develop in kinematic continuity with overall horizontal shortening and steep fabric development in deeper or shallower crustal levels, resembling attachment zones between supra- and infra-structure.
- The large changes in direction of far-field forces acting on a single orogen are shown to operate on a scale of ~10Ma, being caused probably by rearrangement of colliding microplates. Such an observation indicates that the Variscan chain as well as other orogens may exhibit complex 3D architecture which cannot be completely explained by 2D models.

- While quartz keeps the same deformational mechanism throughout the complex ductile deformations of the studied felsic rocks, feldspars accommodate strain by various mechanisms depending on actual conditions.
- Our microstructural observations document abrupt weakening of feldspar-rich rocks under lower-crustal high temperature conditions. The studied lower-crustal rocks first underwent significant weakening caused by disintegration to a fine-grained matrix (granulitization) with subsequent activity of grain boundary sliding mechanism, second they hardened due to cooling and dominant activity of dislocation creep. Similar processes could lower the viscosity of any other rock containing perthitic feldspars when subjected to deformation at

suitable PT conditions, producing matrix that is directly capable of grain size-sensitive flow. Later change of deformation mechanisms may invoke rapid hardening of such weakened rock. In both cases the rheology changes due to switch in dominant deformational mechanism, both changes taking place in frame of the single orogeny.

- The felsic granulites probably represented an important constituent of the Variscan lower crust and the described weakening probably affected majority of these lower-crustal felsic rocks during this orogeny. If so, the weakened granulites would then achieve effective decoupling of crustal and mantle deformations during part of the collision. Generally the documented transient rheology of crustal rocks differing in space and time indicates, that degree of coupling between mantle and lower crust or lower with upper crust isn't constant property of a particular lithosphere, but that it changes together with evolving rheology of the involved rocks.

French resumé

Des microstructures à la déformation crustale dans un orogéne collisionnel: approches pluri -disciplinaires

Le propos de cette thèse est l'étude de la réponse des roches de croûte profonde lors de la collision continentale. L'exemple utilisé est la racine de la chaîne Varisque, qui affleure dans le Massif de Bohème (République Tchèque). Nous étudions les processus orogéniques depuis l'échelle microscopique du grain constituant les roches jusqu'à celle de l'affleurement sur une superficie d'envrion 4000 km².

Cette thèse est divisée en trois chapitres. Le premier représente un article portant sur l'étude du massif granulitique de Blanský Les, unité à l'histoire structurale la plus complex de la région. Ce travail a été publié dans Mineralogy and Petrology journal (2006). Le second chapitre traite de l'évolution régionale de la zone Moldanubienne de Bohème du Sud. Les résultats obtenus sont comparés avec des études d'autres régions orogéniques ou avec des modèles numériques de collision continentale. L'article portant sur ce travail sera soumis au journal Tectonics en Juin 2007. La dernière partie de ma thèse est concentrée sur la caractérisation des mécanismes de déformation des granulites felsiques. Les résultats sont extrapolés pour obtenir des données sur le comportement rhéologique de la croûte inférieure varisque d'une part, et d'autre part sur le comportement des roches felsiques sous des conditions metamorphiques de HT et HP. L'article corespondant sera soumis au Journal of Metamorphic Geology en automne 2007.

Le Massif de Bohème représente la partie affleurante la plus à l'Est de l'orogène Varisque en Europe. De 380 à 300 Ma, le complexe subduction - collision provoque la formation d'une orogène d'environ 300 km de large, montrant une zonalité tectonique comparable à d'autres fragments de la chaîne varisque Européenne. Du NO au SE, l'orogène se dessine graduellement depuis les sediments paleozoiques Saxothuringien vers les roches de haut degré métamorphique Saxothuringiennes puis une zone de suture jusqu'à l'unité faiblement métamorphisé Teplá - Barrandienne. Plus au SE, les granitoïdes de type d'arc séparent la zone Teplá - Barrandienne de l'unité de racine orogénique Moldanubienne. Cette partie de l'orogène présente d'importants terrains anatexiques contenant des lentilles de roches de la croûte inférieure et roches

mantelliques. A l'Est, la microplaque Brunia est peu affectée par les différents phases de déformation liées à l'orogène Varisque.

La partie Moldanubienne étudiée a été déformé entre ~350-335 Ma, par une deformation pénétrative lié au raccourcissement NO-SE, puis entre ~330-310 Ma lié à une transpression NE-SO. Cette zone tes représentée un mélange de roches mantelliques, de croûte inféreure et moyenne, montrant des déformations polyphasées, qui ont nécéssité une combinaison de méthodes de recherche variée pour retracer son évolution. Nous nous sommes intéressés à la partie occidentale de la racine Moldanubienne pour révéler le comportement mécanique de la croûte profonde dans un contexte collisionnel. Nous soulignons aussi, les différents mécanismes d'exhumation de la croûte inférieure dans les niveaux structuraux supérieurs. La région d'étude concerne une surface de 130 par 30 km dans le massif de Bohème du Sud, approximativement le long de la ligne de reflexion sismique 9HR. Nous inteprétations reposent majoritairement sur l'évolution structurale observée sur le terrain. Les caractèristiques des différents objets structuraux telles que foliations, lineations et structures de petites échelles ont été généralisées et confrontées avec les cartes géologiques existantes pour obtenir les directions régionales des différentes fabriques orogéniques. Les données structurales de terrains sont supportées par l'étude microstructurale et la pétorologie disponible dans la littérature. Les fabriques ont seulement pu être extrapolées à 3-5 km de profondeur depuis les données structurales, mais les structrues plus profondes ont été caractérisiées grâce à la ligne de réflexion sismique qui traverse la majorité des unités. La conjonction de ces deux méhodes d'analyse nous permet de suggérer une architecture tectonique de l'échelle de la croûte elle-même. La modélisation 3D des anomalies gravitaires a été employée pour supporter les interpétations structurales et sismiques. Pour obtenir des contraintes chronologiques sur ce scénario d'évolution de la déformation, une compilation des données géochronologiques nous a permit de compiler environ 550 âges concernant le Massif de Bohème. L'ensemble de ces résulats se finalise par la proposition d'un modèle géotectonique à l'échelle du Massif de Bohème.

Le schéma structural adopté pour le Sud du domaine Moldanubien fait appel à 5 phases de déformation. Elles sont dominées par foliations inclinées vers le NO, associées au climax du métamorphisme amphibolique. En particulier, la foliation fortement inclinée S_3 et faiblement inclinée S_4. Ces deux structures indiquent un raccourcissement intense précédent un flux subhorizontal de roches partiellement fondues. Elles sont parallèles à la direction des marges de

Brunia et de la zone Saxothuringienne; leurs orientations peuvent être corrélées avec celles des fabriques subverticales et subhorizontales des foliations qui prévalent à l'est du domaine Moldanubien. A proximité des unités granulitiques, S_4 dessine une géométrie irrégulière qui s'adapte passivement aux courbes des corps granulitiques plus compétents.

Au SO, cette fabrique est retravaillée par une schistosité de crénulation avec des indicateurs cinématiques indiquant un régime transpressif dextre. Cette fabrique prouve l'existense d'un raccourcissement NE-SO qui a été initié à la limite SO de la zone Moldanubienne. La présence d'un bloc continental causant ce raccourcissement demeure hypothétique. Le magmatisme syntéctonique, l'anatexie et les déformations associés culminent à environ 320 Ma, à peu près 15 Ma après les déformations Moldanubiennes antérieures. De part l'orientation et l'âge différent de cet évènement, le système tectonique qui en est responsable doit être traité comme un épisode isolé survenant à la fin de la collision Varisque dans le Massif de Bohème.

Dans le centre de la région d'étude affleure plusieurs massifs rhéologiquement plus compétents, qui imposent des pertubations sur les fabriques décrites précedement. A l'intérieur de ces massifs, les anciennes structures Varisques ont été bien préservées, documentant une histoire exhumatoire en deux temps (D_2 et D_3) de ces roches de HP et HT. La modélisation gravitaire ainsi que les interprétations structurales indiquent que les massifs granulitiques ont une extension verticale de plusieurs kilomètres. De plus, la sismique réflexion renseigne sur l'existence d'une fabrique probable, à fort pendage, à travers toute l'épaisseur de la croûte sous les granulites. Cette caractéristique est interprétée comme une continuation possible du mélange dominé par les granulites affleurant à la surface. Cette région verticale de faible réflectivité pourrait alors être l' indice d'un chenal ascentionnel de granulites déformées.

La géométrie complexe de la fabrique S_3 du faciès amphibolitique dessine une structure resemblant à un pli d'échelle crustale, interprétée comme le résultat d'un plissement isopaque d'une lentille granulitique déjà exhumée en continuité cinématique avec la fabrique amphibolitique S_3.

Un large domaine de fabriques granulitiques affleurent dans le corps granulitique de Blanský Les. Des reliques d'une fabrique précoce S_1, caractérisé par un litage compositionnel sont préservés à de rares endroits dans la fabrique S_2 mylonitique. La fabrique S_2 nous permet de reconstruire les mécanismes d'exhumation précoces. En effet, le refroidissement occasionné a gelé ces fabriques rendant possible leur observation sur une surface continue de 8x2 km. La

fabrique S_2 est à 70° de la structure du facies amphibolitique dominante présente dans les granulites rétrogressés environnantes. La géométrie cylindrique de S_2 a été restaurée, et après dépliage, suggère que les granulites partiellement fondus de la croûte inférieure ont été incorporée dans les niveaux de croûte moyenne sous la forme d'extrusions plastiques syn-compressionnelles. Un tel mécanisme peut rendre compre de la présence de portions relativement petites (X000 km^3) de roches de HP HT à l'intérieur de roches issues de niveaux supérieurs dans les parties internes des orogènes. Une fois mise en place, les granulites sont déformés de façon cohérentes avec la croûte moyenne environnante.

La fabrique S_2 est orientée sub-perpendiculairement par rapport à la direction NE-SO de l'orogène, aisni que la plus jeune S_5. Les variations régionales observées des directions principales de déformation sont de même ordre que celles observées dans les orogènes récentes, comme dans les Alpes par exemple.

Sur les 850 affleurements étudiés dans le sud de la Bohême, les plus représentatifs ont été échantilonnés pour réaliser des observations pétrographiques. Dans le cas des granulites felsiques, l'étude pétrologique a été couplée avec l'analyse microstructurale des fabriques exhumatoires dans le but de définir les mécanismes de déformation et estimer leur rhéologie pendant l'exhumation. Les études détaillées des fabriques de facies granulitiques montrent des reliques du précurseur granulitique en divers affleurements. Ceci permit de décrir le processus de granulitisation et aida à contraindre l'histoire pré-granulitique des roches.

Afin de répondre aux questions précédentes, il est nécessaire de combiner plusieurs approches parmi lesquelles l'analyse des orientations cristallographiques préférentielles (LPO) à l'aide des méthodes de diffraction des électrons rétrodiffusés (EBSD) et "fore-scattered" (FSD) est la plus importante. La quantification des divers paramètres microstructuraux grâce à une digitalisation manuelle des lames minces s'est également avérée essentielle. Les processus chimiques liés à la recristallisation ont été étudiés par microscopie électronique à balayage couplée à un détecteur EDX en réalisant des cartes compositionnelles ainsi que des analyses ponctuelles des zones représentatives.

Les reliques des précurseurs des granulites sont de larges perthites pouvant atteindre 1,7 cm, elles-mêmes présentant de nombreuses inclusions de quartz, grenat et disthène et plus rarement de biotite, rutile, ilménite, zircon, monazite, apatite et sulfures de fer. Hormis les perthites, ces

granulites sont constituées d'une matrice à grain fin et de bandes de quartz rubanés. Les inclusions de grenat, biotite et parfois de disthène sont automorphes ce qui est incompatible avec des processus de déformation à l'état solide lors de leur croissance et de leur incorporation dans les perthites. De plus, les inclusions de quartz montrent des formes "en gouttes" ou automorphes caractéristiques d'une cristallisation à l'interface solide-liquide. Ces caractères indiquent que le protolithe des granulites felsiques était un orthogneiss grenu formé dans des conditions d'hypersolvus et présentant une association feldspath d'alcali – quartz – grenat – biotite - disthène.

Quelques perthites préservent d'excellents témoins de granulitisation dans leurs ombres de pression où elles recristallisent en une fine matrice granulitique de K-feldspath et de plagioclase. Cette matrice, protégée par les perthites, montre une orientation cristallographique préférentielle plus ou moins identique à celle de la perthite originelle indiquant une désintégration quasi-statique de celle-ci en une matrice granulitique fine et à granulométrie uniforme. Les images obtenues par diffraction des électrons rétrodiffusés (images BSE) indiquent un développement des nouveaux grains le long d'un net front de recristallisation qui progresse graduellement vers le grain de perthite intact. La recristallisation isochimique et quasi-statique des larges perthites a probablement été engendrée par les déséquilibres chimiques occasionnés par les changements de pression ainsi que par une faible déformation.

La phase de déformation D_2 induit un fluage de la matrice et entraîne le développement d'une foliation mylonitique pénétrative S_2. Dans la majorité des affleurements, la granulitisation a affecté la totalité des roches felsiques formant un réseau de couches molles interconnectées (IWL) contenant des quartz rubanés plus ou moins isolés.

L'analyse de cette microstructure révèle une déformation plastique intense du quartz tandis que la matrice à grain fin, qui est bien plus conséquente, montre seulement de faibles signes de déformation plastique. Ces caractéristiques microstructurales associées à la présence d'un liquide d'anatexie intergranulaire syntectonique impliquent un comportement fortement ductile approchant les caractères d'un flux pseudoplastique, probablement facilité par un mécanisme de glissement aux frontières de grains (GBS). Malgré la faible orientation préférentielle des grains de feldspath de la matrice, les obsrevations EBSD révèlent une forte orientation cristallographique préférentielle à la fois des K-feldspaths et des plagioclases, suggérant une importante contribution du mécanisme glissement par dislocation. La combinaison des

mécanismes de glissement par dislocation et de glissement aux frontières de grains accrue par la présence de liquides silicatés permet un transport rapide et efficace de portions relativement petites de croûte inférieure vers la surface à travers la racine orogénique.

Un épisode de déformation plus jeune est matérialisé par le développement de structures dans le faciès amphibolite dans la croûte moyenne. Après refroidissement et cristallisation du liquide d'anatexie le long des frontières de grains, les granulites ne se sont déformées que par un glissement par dislocation moins efficace, semblablement aux orthogneiss communs partiellement fondus où le liquide se sépare du solide dans des poches ou bandes. Un durcissement important des granulites rétrogradées indiqué par les microstructures a augmenté leur résistance et a permis un plissement actif des lentilles de granulite. Cela indique que les granulites se sont comportées comme des boudins fortement étirés au milieu de métasédiments moins rigides.

La inversion de rhéologie des feldpaths ainsi décrite, donc celle de la roche entière (affaiblissement dans des conditions de HT et de HP de croûte inférieure et durcissement dans la croûte moyenne) devrait changer les considérations rhéologiques et géotectoniques actuelles qui ne sont basées aujourd'hui que sur les lois de Byerlee et de Weertmann.